Weighing the spacetime along the line of sight using times of arrival of electromagnetic signals

Mikołaj Korzyński,[1,*] Jan Miśkiewicz,[1,2] and Julius Serbenta[1]

[1] *Center for Theoretical Physics, Polish Academy of Sciences, Al. Lotników 32/46, 02-668 Warsaw, Poland*
[2] *Faculty of Physics, University of Warsaw, ul. Pasteura 5, 02-093 Warsaw, Poland*

(Received 2 February 2021; accepted 6 June 2021; published 8 July 2021)

We present a new method of measuring the mass density along the line of sight, based on precise measurements of the variations of the times of arrival (TOAs) of electromagnetic signals propagating between two distant regions of spacetime. The TOA variations are measured between a number of slightly displaced pairs of points from the two regions. These variations are due to the nonrelativistic geometric effects (Rømer delays and finite distance effects) as well as the gravitational effects in the light propagation (gravitational ray bending and Shapiro delays). We show that from a sufficiently broad sample of TOA measurements we can determine two scalars quantifying the impact of the spacetime curvature on the light propagation, directly related to the first two moments of the mass density distribution along the line of sight. The values of the scalars are independent of the angular positions or the states of motion of the two clock ensembles we use for the measurement and free from any influence of masses off the line of sight. These properties can make the mass density measurements very robust. The downside of the method is the need for extremely precise signal timing.

DOI: 10.1103/PhysRevD.104.024026

I. INTRODUCTION

In this paper we develop a method of tomographic measurement of mass density of matter along the line of sight using variations of times of arrival (TOAs) of pulses of electromagnetic radiation between pairs of points from two small, distant regions connected by a null geodesic. The result may be seen as a continuation of the research program initiated in [1,2] on determining the spacetime geometry, or—more precisely—the spacetime curvature, directly from precise optical or astrometric measurements, but this time focusing on a different observable, namely the precise time when a sharp discontinuity of the electromagnetic field reaches a receiver.

The TOAs of electromagnetic signals are among the most important observables in general relativity. They have been studied in many fields of relativity and astronomy: in pulsar and binary pulsar timing [3–5], time-delay cosmography using strong lenses in cosmology [6,7], experiments with atomic clocks and clock ensembles in gravitational fields [8], relativistic geodesy [9], navigation on Earth [10,11] or measurements of Shapiro delays from massive bodies [12]. They also played an important role in the early days of special relativity as the main observable in the Einstein's radar method of time and distance measurements. The general problem of TOAs in a curved spacetime is rather difficult; it has been considered by Synge [13], and later by Teyssandier, Le Poncin-Lafitte and Linet [14–16].

In this work we propose a differential measurement in which we compare the TOAs between many pairs of distant of points, with the points contained in two fixed distant regions. The points in each region are displaced with respect to each other in both space and time. The measurement can be performed with the help of two ensembles (or groups) of comoving synchronized clocks, each located in one of the two distant regions. We assume that the clocks are equipped with transmitters and receivers of electromagnetic radiation and are able to emit pulses of radiation at prescribed moments. They can also measure precisely the moments of reception of signals emitted by other clocks, recognizing at the same time the origin of each received signal. The clocks within each ensemble are in free fall and at rest with respect to each other. We assume that they are positioned fairly close to each other and in a prescribed manner within the ensembles, while the ensembles themselves are located far apart (see Fig. 1).

Each of the two ensembles plays a different role in the measurement. The clocks in the emitters' ensemble emit signals in the form of pulses according to a fixed measurement protocol. Each signal should contain a time marker, defining the emission moment as sharply as possible, for example by the means of a discontinuity in a component of the electromagnetic field. The clocks in the receivers' group register the moments of arrival of the markers (see Fig. 1). We assume that the receivers can also

*korzynski@cft.edu.pl

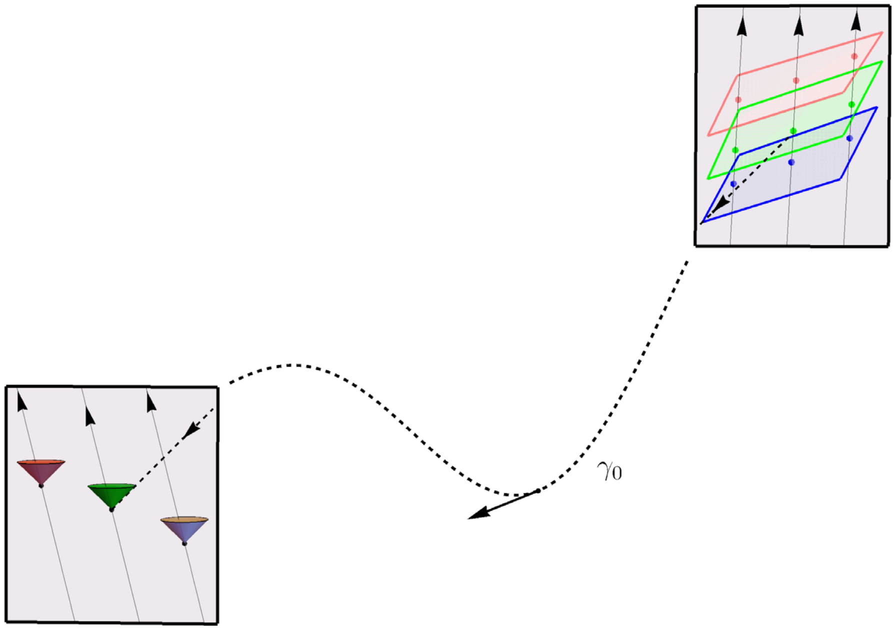

FIG. 1. The synchronized, comoving clocks in the emitters' ensemble (left) emit pulses of radiation in all directions at prescribed moments defined by their local time. The pulses travel then a long distance through the curved spacetime and finally reach the receivers' ensemble (right), where each of the synchronized and comoving clocks records the time of arrival of each signal. The regions of emission and reception are connected by the fiducial null geodesic γ_0.

recognize the origin of each signal, meaning the emitting clock and the moment of emission [17]. This way the system is able to record the TOAs between *all* emitter-receiver pairs and for various moments of emission. In this paper we provide a method of combining all these data and extracting information about the spacetime curvature and the matter content along the line of sight, assuming that we know precisely the placement and the motions of the emitters and receivers as measured in their respective local inertial frames.

The two ensembles resemble two clock-based gravitational compasses as discussed in [18–20]. Recall that the clock-based gravitational compass is a curvature-measuring device using differences in ticking rates of precise clocks. It generalizes the notion of the gravitational compass introduced by Szekeres [21] and developed also by other authors [22–25]. The setup we discuss may be also be considered a special case of an extended gravitational clock compass in the terminology of [18–20], consisting of two distinct groups of clocks. Unlike the former, it is only extended along a single null geodesic, and therefore it is only able to measure some of the curvature components. On the other hand, this extension is so large that we need to allow the curvature to vary along the way.

Direct measurements of the spacetime curvature in general relativity are usually quite challenging for a simple reason; with the exception of cosmology, black hole theory or strong gravitational lensing, the scale of the curvature is usually very large in comparison to all other time and length scales involved. Thus the curvature corrections to observables are usually tiny and need to be distinguished from many other effects. However, the measurement presented here is designed in such a way that potentially much larger contributions to the TOAs due to the kinematical effects (states of motion of the two ensembles), attitude effects (angular position or attitude of both ensembles with respect to each other or to the line of sight) and influence of nearby masses off the line of sight (Shapiro delays from nearby masses) cancel out completely. Effectively it is only the gravity of the mass density located along the null geodesic linking the two regions that contributes to the results. This implies a strong resistance of the measurement to perturbations by external masses or due to the effects of unknown velocities or misalignment of the two clock ensembles. This property makes the measurement very robust despite very small magnitude of the expected signal. Moreover, thanks to the advancements in atomic clock techniques, the time measurements are now among the most precise types of measurements possible today, and therefore the TOAs can in principle be measured with high precision.

The quantities determined by the measurement are the *distance slip* μ, introduced in Grasso *et al.* [1] and Korzyński and Villa [26], and a closely related quantity ν. Recall that the dimensionless scalar μ measures the difference between the parallax effects and the magnification between two points along a null geodesic, suitably averaged over all possible baseline orientations. In a flat spacetime the effect of the transverse displacement of the receiver on the apparent position of a distant luminous source (i.e., the trigonometric parallax) is identical to the effect of the same displacement of the source in the opposite direction, leading to $\mu = 0$. In a curved spacetime this is no longer the case, and, as a result, the two methods of distance measurement to a single body, by angular size and by parallax, may yield different numbers, resulting in nonvanishing μ. We showed in [1] that the measurement of μ is selectively sensitive to the curvature along the line of sight and that for short distances it is sensitive to an integral of a single component of the stress-energy tensor. The same applies to ν and therefore the method we present may be seen as a tricky differential measurement of the Shapiro delays, sensitive only to the signal originating from the mass density along the line of sight.

In the meantime, as an important side result, we develop further the bilocal approach to light propagation in the curved spacetime, introduced first in [1]. In this framework the TOAs, just like other observables, are expressed as functions of the curvature tensor along the line of sight, describing the influence of spacetime geometry on light propagation, as well as the momentary positions and motions of both sources and receivers, as described in their locally flat coordinates. The dependence of the TOAs on the spacetime geometry is clearly separated from the dependence on the momentary positions and motions of the clocks. We then consider the emitters and the receivers as contained in two distant, free-falling Einstein elevators. The direct influence of gravity is undetectable inside each elevator within the time scale of the experiment. However, light propagating over long distances from one elevator to the other does feel the impact of the curved spacetime and, as we show in this paper, this impact can be detected.

A. Geometric description and mathematical apparatus

The description of light propagation using bilocal operators is quite different from the more standard approach in which we use an approximation (for example post-Newtonian, post-Minkowskian or linearized gravity), to calculate the potentials or metric components from the mass distribution and then trace the perturbed null geodesics as well as the perturbed worldlines of the emitters and receivers of the pulses. In contrast, the bilocal approach works in any spacetime and does not require an explicit decomposition of the metric into a global flat background plus perturbations. It shares many features with the time transfer function formalism of Teyssandier, Le Poncin-Lafitte and Linet [14–16], including the use of Synge's world function, but it also differs in a number of important ways. Firstly, our formalism does not aim to be global; it provides expressions for the variations of the TOAs in the form of a Taylor expansion valid in the immediate neighbourhood of a given pair of points, rather than the exact or approximate value of the TOAs between any emitter-receiver pair in a given spacetime. Consequently, it does not need to make use of a global time coordinate as a reference.

Following [1], we proceed here by deriving a number of exact geometric relations between the spacetime geometry, the kinematical quantities describing the momentary positions and states of motion of the emitters and receivers in their local inertial frames, and the TOAs they measure. The whole framework is therefore formulated in a coordinate-independent, geometric way.

The dependence of the TOAs on the spacetime geometry enters only via two covariantly defined tensors and one bitensor encoding the impact of the spacetime on the wavefronts, just like in [1]. These linear operators are defined as functionals of the components of the Riemann curvature tensor along the line of sight, independently from any tetrads, frames or other structures. This is again in contrast to [14–16], where the dependence of TOAs on the spacetime geometry enters directly via the components of the metric expressed in a particular coordinate system, related to the post-Newtonian or post-Minkowskian approximation. As we will see, this last feature is crucial for deriving the key result of this paper, namely the method for extracting the bare curvature effects from the variations of the TOAs.

Since the definitions and the measurements of the observables in question require no external structures like global coordinate systems (for example the Solar System barycentric coordinates), large-scale nonrotating reference frames, Killing vectors etc., we avoid any problems of the astrometric data reduction in the data interpretation [27].

B. The basic idea of the measurement

We consider the exact moment of arrival of a signal sent from a point in the emitters' region $N_{\mathcal{E}}$ as measured by a clock performing the measurement in a local inertial frame in the receivers' region $N_{\mathcal{O}}$. We fix the receivers' reference frame by fixing their common four-velocity $u_{\mathcal{O}}^{\mu}$ and thus also the corresponding coordinate time. The TOA depends now on the spatial position and the moment of emission in $N_{\mathcal{E}}$ and the spatial position of the receiver in $N_{\mathcal{O}}$. We consider two reference points $\mathcal{E} \in N_{\mathcal{E}}$ and $\mathcal{O} \in N_{\mathcal{O}}$ such that a signal from $\mathcal{E}$ reaches $\mathcal{O}$. We can then describe the positions and the emission moment by the displacement vectors from $\mathcal{O}$ (three spatial components only) and $\mathcal{E}$ (four-dimensional spacetime vectors). We can then expand the TOA up to the next-to-leading, second order in the displacements. At the leading, linear order we just see the Rømer delays, i.e., the dependence of the TOAs on the position of the emitter and the receiver along the line of sight, and the frequency/time transfer effects (the redshift or blueshift of frequencies and difference between the receiver's proper time lapse and the observed emitter's time lapse), see Fig. 2, upper panel. These effects do not depend explicitly on the spacetime curvature and can be described using just special relativity (see Butkevich and Lindegren [28] for a discussion in the context of precise astrometry). However, as we will see, the quadratic term in the

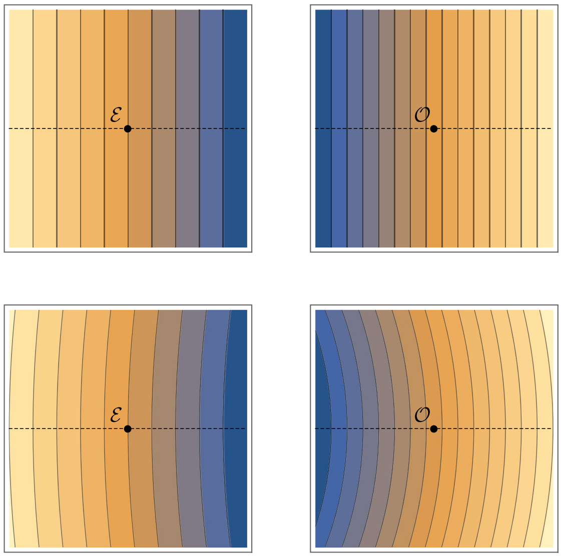

FIG. 2. Upper panel, left: The variations of the TOAs of light signals, as registered by the receiver in his or her proper time, plotted for a fixed observation point $\mathcal{O}$, but variable emission point. Blue colour denotes an earlier TOA, while yellow a later TOA. For sufficiently small displacements we see only the leading order, linear effects in displacements. Upper panel, right: the same TOAs, but for a fixed emission point $\mathcal{E}$ and variable observation points. Note that in both cases in the linear order we only see the dependence on the displacements along the line of sight (Rømer delays). Due to special relativistic effects the dependence on displacements does not need to be exactly the same on both ends. Lower panel, left: Again TOAs for a fixed observation point $\mathcal{O}$ and displaced emission points. For sufficiently large displacements we begin to see the quadratic order effects in displacements, in the form of transverse delays. Lower panel, right: The TOAs for a fixed emission point $\mathcal{O}$ and displaced observation points, together with the second order effects. In a general spacetime the magnitude of the second order effects may be different at the two endpoints.

displacements contains curvature corrections on top of the standard, distance-dependent effects present also in a flat spacetime (Fig. 2, lower panel). The idea is to recognize and evaluate these curvature corrections to the "flat" finite distance effects.

The quadratic term in question encodes the subleading, transverse effects in the TOA variations as well as the cross effects of displacements on both ends. They are usually much smaller than the linear effects and are responsible for, among other things, the curved shape of the light cones and the wave fronts. The TOAs depend also on the receivers' and emitters' rest frames via the standard special relativity effects, but we prove here that the two quantities we measure are Lorentz-invariant with respect to both the emitters' and receivers' frames.

The basic idea of the measurement has a simple geometric interpretation; the TOAs between two regions can be geometrically described by a subset of the product manifold $M \times M$ constructed from the spacetime M. We consider the locus of pairs of spacetime events which can be connected by a null geodesic. Under fairly mild assumptions this locus is (locally) an embedded hypersurface in $M \times M$ and we will call it the *local surface of communication* (LSC). Its shape in the vicinity of a given point $(\mathcal{O}, \mathcal{E})$ can be approximated by its second order tangent surface by the means of a Taylor series. The second order term in this approximation, related to the extrinsic curvature of the LSC as an embedded hypersurface in $M \times M$, contains spacetime curvature corrections and, as we show, can be related to the Riemann tensor along the line of sight. The measurement itself amounts to sampling the LSC over a large number of nearby emission/reception event pairs, with the help of clocks equipped with electromagnetic radiation transmitters and receivers. Note that by definition each emission-reception pair we register yields a point in $M \times M$ lying on the LSC. If the sampling is sufficiently broad, the shape of the LSC in the second order Taylor expansion can be recovered completely from the data and the extrinsic curvature tensor can be obtained componentwise. Finally, the two bilocal scalars μ and ν measuring the spacetime curvature are calculated from the extrinsic curvature and the first order term.

The local surface of communication is an important theoretical concept we introduce in this paper. It encodes the information about light propagation between two distant regions of the spacetime, very much like the bilocal geodesic operator discussed in Grasso *et al.* [1]. We will explore the relation between these two geometric objects and prove a number of results related to the geometry of the LSC.

We point out here that the TOAs of mechanical waves in elastic media and their variations have been studied extensively in seismology. In fact, the formalism developed in this paper may be also regarded as the general relativistic counterpart of the second order approximation for travel times in seismic ray theory [29–32].

C. Assumptions and limitations of the approach

We assume the validity of the geometric optics approximation throughout the work. This means that the electromagnetic wave's wavelength is assumed to be much smaller than all other length scales involved and the radiation intensity small enough so as not to produce any significant contribution to the stress-energy tensor. With these assumptions we can consider the electromagnetic radiation as propagating along null geodesics of a fixed metric [33,34]. Consequently, we can assume that a pulse of radiation originating from single emission event propagates along this event's future light cone.

The assumptions regarding the two distant regions are similar to those in [1]. We assume that both regions we consider are sufficiently small in comparison with the spacetime curvature scale that the light propagation between them can be approximated using the first order geodesic deviation equation. As we will see in this paper, this is equivalent to assuming that the Synge's world function can be approximated by its Taylor series truncated at the second order. In a more physical language, this means that we demand the curvature to be constant in the transverse directions across the long, thin cylinder connecting both regions. It follows that we need to assume the matter density and the tidal effects to be constant in the transverse directions as well.

We assume that each process of emission and reception of a signal happens at one single event and without instrumental delays. We also disregard any nongravitational effects of refraction or pulse dispersion due to the presence of a medium, for example ionized hydrogen, along the line of sight. This kind of medium produces additional frequency-dependent delays related to the electron column density along the line of sight [4].

D. Structure of the paper

The paper is organized as follows: In Sec. II we describe in detail the geometry of the problem, introduce the product manifold and discuss all types of coordinate systems we use in the rest of the paper. Then, in Sec. III, we introduce the mathematical machinery of the paper; we derive the relation between the shape of the local surface of communication and the spacetime curvature, first generally and then in the small curvature limit, and prove a number of general results regarding the geometry of the LSC. We then derive exact expressions for the TOA and finally discuss the inverse problem of reconstructing the shape of the local surface of communication from TOA measurements.

In Sec. IV we introduce the two scalar observables measuring the curvature corrections and prove their properties. Section V contains the derivation of the order-of-magnitude estimates of various TOA effects in terms of the characteristic scales of the problem. Additionally, we relate the two observables to the first two moments of the mass distribution along the line of sight. We also summarize the most important results of the first five sections. Section VI contains an example of the measurement protocol. We conclude the paper with a summary and conclusions. The Appendix contains the details and the derivations of more elaborate technical results of the paper.

E. Notation and conventions

In this work we use many different types of indices, related to various types of geometric objects and bases (tetrads), and running over different sets of integers. We will now summarize our index conventions.

The Greek indices $\mu, \nu, \ldots$ run from to 0 to 3 and denote geometric objects expressed in various coordinate bases. We borrow the notation from [35] for bilocal (or two-point) geometric objects, in which primed Greek indices $\mu', \nu', \ldots$ refer to the tangent space at the observation point $\mathcal{O}$, while the unprimed ones refer to the emission point $\mathcal{E}$. The Latin indices $i', j', k', \ldots$ and $i, j, k, \ldots$ run from 1 to 3, again referring to $\mathcal{O}$ and $\mathcal{E}$ respectively. They will be used for the spatial components of vectors and other objects. We also use indices with an overline $\bar{\mu}, \bar{\nu}, \ldots$ for geometric objects expressed in a parallel propagated tetrad along the fiducial null geodesic γ_0, independently of the point along γ_0. The Latin capitals, both with overline $(\bar{A}, \bar{B}, \ldots)$ or without $(A, B, \ldots$ or $A', B', \ldots)$, run from 1 to 2 and will be used for the transverse spatial components, orthogonal to the line of sight.

TABLE I. Most important acronyms used in the paper and the reference to the appropriate section, listed in alphabetical order.

Acronym	Meaning	Section
BGO	Bilocal geodesic operator	III A
COM	Center of mass	V A
LF	Locally flat (coordinates)	II D
LOS	Line of sight	II A
LSC	Local surface of communication	II C
ODE	Ordinary differential equation	III A
OLF	Orthonormal locally flat (coordinates)	II D
ON	Orthonormal	IV A
PLF	Parallel-propagated locally flat (coordinates)	II D
TOA	Time of arrival	I

Finally, we also introduce notation for eight-dimensional vectors in the direct sum of the tangent spaces at $\mathcal{O}$ and $\mathcal{E}$, i.e., in $T_{\mathcal{O}}M \oplus T_{\mathcal{E}}M$, as well as tensors on this space. The geometric objects themselves will be denoted by boldface capitals, i.e., $\mathbf{X}, \mathbf{Y}, \ldots$. Moreover, all index numbers in this case will be denoted by the boldface font; the indices run by convention from **0** to **7**. The first four components (i.e., **0–3**) will refer to the μ' components in $T_{\mathcal{O}}M$, while the latter four (**4–7**) to the μ components from $T_{\mathcal{E}}M$. We will also use the boldface latin letters $\mathbf{i}, \mathbf{j}, \ldots$ to denote the seven components ranging from **1** to **7**, i.e., omitting the **0** component.

For the sake of simplicity we will assume that $c = 1$ throughout the paper, i.e., we are using distance units to express time. In Table I we list the most important acronyms used in the paper.

II. GEOMETRICAL PRELIMINARIES

A. Geometric setup

The geometric setup is similar to that of [1] (see Fig. 3). Let M be the spacetime of dimension 4, equipped with a smooth metric g of signature $(-,+,+,+)$. We consider two points $\mathcal{O}$ and $\mathcal{E}$ such that an electromagnetic signal emitted at $\mathcal{E}$ can be received at $\mathcal{O}$. In other words, we assume that $\mathcal{O}$ lies on the future light cone centered at $\mathcal{E}$. In this case $\mathcal{O}$ and $\mathcal{E}$ can be connected by a null geodesic γ_0. We also consider two small regions $N_{\mathcal{O}} \subset M$ and $N_{\mathcal{E}} \subset M$ around points $\mathcal{O}$ and $\mathcal{E}$ respectively, extending in both space and time. Under the assumptions above we may expect that signals from other points (events) in $N_{\mathcal{E}}$ can be received at other points in $N_{\mathcal{O}}$.

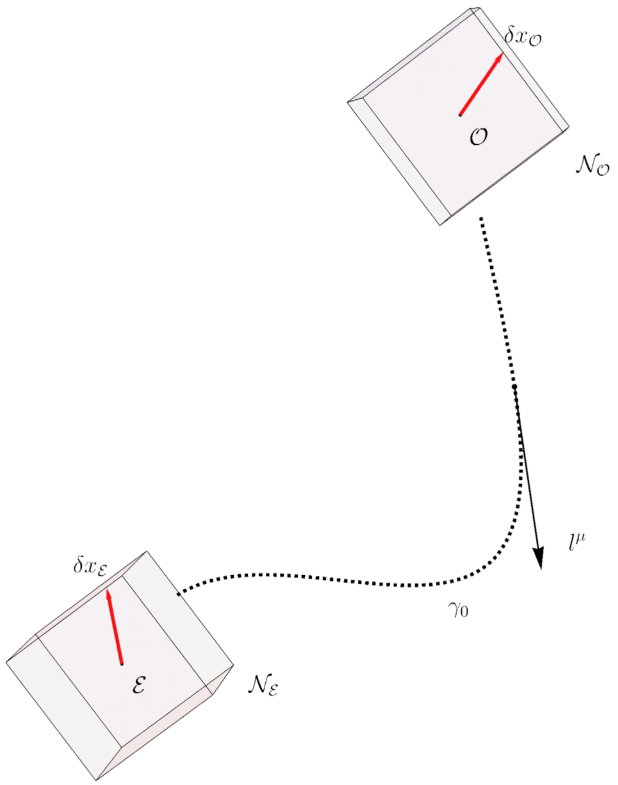

FIG. 3. Geometric setup of the paper, with two locally flat regions $N_{\mathcal{O}}$ and $N_{\mathcal{E}}$, connected by a null geodesic γ_0 passing through $\mathcal{O}$ and $\mathcal{E}$. The displacement vectors $\delta x_{\mathcal{O}}$ and $\delta x_{\mathcal{E}}$ identify points in both regions. The tangent vector to γ_0 is denoted by l^{μ}.

We assume that both $N_{\mathcal{E}}$ and $N_{\mathcal{O}}$ are sufficiently small to be effectively flat. Namely, if $\mathcal{R}$ denotes the spacetime curvature radius scale and L the size of both regions, then we assume that $L^2/\mathcal{R}^2$, a dimensionless quantity scaling the curvature corrections within both regions, is negligibly small. In this case we may simply identify points in $N_{\mathcal{O}}$ with vectors in the tangent space $T_{\mathcal{O}}M$ with the help of the exponential map and the spacetime metric g with the flat metric on the tangent space; the same construction works for $N_{\mathcal{E}}$. With this identification the points $\mathcal{O}$ and $\mathcal{E}$ will serve as reference for other points in $N_{\mathcal{O}}$ and $N_{\mathcal{E}}$ and vectors in $T_{\mathcal{O}}M$ and $T_{\mathcal{E}}M$, denoted $\delta x_{\mathcal{O}}$ and $\delta x_{\mathcal{E}}$, as displacement vectors representing points. The null geodesic γ_0 connecting $\mathcal{O}$ and $\mathcal{E}$ will be referred to as the *line of sight* (LOS) or the *fiducial null geodesic* and will be used as reference for other geodesics connecting points in $N_{\mathcal{O}}$ and $N_{\mathcal{E}}$. We assume that γ_0 is parametrized affinely by the parameter λ, although we make no assumptions regarding the normalization of this parametrization. In order to be consistent with [1,2] we will assume that the parametrization runs backward in time, i.e., from $\mathcal{O}$ to $\mathcal{E}$. The null tangent vector to γ_0 will be denoted by l.

In a general spacetime it is possible that more than one geodesic connects a pair of points from $N_{\mathcal{O}}$ and $N_{\mathcal{E}}$. In the context of geometrical optics this means that we may expect multiple imaging and, consequently, many TOAs of a single signal from a given event. The TOAs becomes then multivalued for a given receiver. For the sake of simplicity we will assume throughout this paper that both $N_{\mathcal{E}}$ and $N_{\mathcal{O}}$ lie in the normal convex neighbourhood of $\mathcal{E}$. Under this assumption the geodesics connecting such pairs are unique and no multiple TOAs are possible. This assumption also allows us to define a single-valued world function; an important object in this work.

We point out, however, that the results of this paper should also hold if multiple imaging is present, but $N_{\mathcal{O}}$ and $N_{\mathcal{E}}$ do not contain conjugate points, i.e., they are away from caustics, and they are both sufficiently small. In this case we simply need to limit the geodesics considered to those contained in a sufficiently narrow tube around a single connecting geodesic γ_0 [1], and this way limit our interest to a particular single image of the distant region $N_{\mathcal{E}}$ on the celestial sphere. However, in this paper we will not consider this situation in detail.

We assume that the light propagating between $\mathcal{E}$ and $\mathcal{O}$ is affected by the spacetime curvature, but this effect can be efficiently described in terms of the Riemann tensor along γ_0. In other words, the effects of higher derivatives of the curvature along the LOS are negligible. It follows that the behavior of geodesics connecting $N_{\mathcal{O}}$ and $N_{\mathcal{E}}$ can be very well approximated using the first order geodesic deviation equation (GDE). This is again true provided that $N_{\mathcal{O}}$ and $N_{\mathcal{E}}$ are small enough [1]. As we will see, this assumption has an important effect on the TOAs between the two regions. Namely, it means that we can approximate the variations of the TOAs using the second order Taylor expansion.

B. The product manifold

The geometric construction behind the direct curvature measurements from the TOA variations is much simpler to explain if we perform it at the level of the product manifold $M \times M$ instead of the spacetime M itself. Consider then the Cartesian product $M \times M$, consisting of pairs (p, q) of points in M. It is also a smooth manifold and its tangent vectors can be identified with *pairs* of vectors in M at two (usually distinct) points. Namely, for $\mathbf{X} \in T_{(p,q)}(M \times M)$ we have $\mathbf{X} \equiv (X_1, X_2)$, where $X_1 \in T_pM$ and $X_2 \in T_qM$. More formally, at every (p, q) we have a natural isomorphism $T_{(p,q)}(M \times M) \cong T_pM \oplus T_qM$ between the tangent space to the product manifold and a direct sum of the tangent spaces to the spacetime.

Moreover, $M \times M$ as a manifold can be equipped with a smooth metric tensor $\mathbf{h}$ constructed from g. There are many ways to define it, but we propose here the following one: for $\mathbf{X}, \mathbf{Y} \in T_pM \oplus T_qM$ we define $\mathbf{h}(\mathbf{X}, \mathbf{Y}) = g_p(X_1, Y_1) - g_q(X_2, Y_2)$, where $X_1, Y_1 \in T_pM$ and $X_2, Y_2 \in T_qM$ denote vectors from the decomposition of $\mathbf{X}$ and $\mathbf{Y}$ respectively, while g_p and g_q denote the spacetime metric g at p and q.

The reader may check that this metric is nondegenerate and of split signature (4,4), i.e., with equal number of positive and negative signs in the diagonal form.

The advantage of the product space construction is that now the bilocal scalars or tensors on M, defined for pairs of points, can be identified with strictly local functions or tensors in $M \times M$. Moreover, as we will see, the problem of TOA variations has a particularly simple and elegant geometric formulation in the language of the product manifold.

C. Local surface of communication

Consider now the neighbourhood of the point $(\mathcal{O}, \mathcal{E}) \in M \times M$, given by $N_{\mathcal{O}} \times N_{\mathcal{E}} \subset M \times M$. The signals propagating between both regions define the set $\Sigma \subset N_{\mathcal{O}} \times N_{\mathcal{E}}$ of pairs of points which can be connected by a null geodesics. Physically they correspond to pairs of points (x', x) such that the signal emitted from x can be received at x'. Note that by assumption we always have $(\mathcal{O}, \mathcal{E}) \in \Sigma$.

In a general situation Σ may have a complicated geometric structure; the wave fronts, which constitute simply the sections of Σ though surfaces $x^{\mu}_{\mathcal{E}} = \text{const}$, $x^{0'}_{\mathcal{O}} = \text{const}$, typically develop folds, cusps and other types of singularities [36,37]. However, in the absence of strong lensing we may expect it to form an embedded submanifold of codimension one passing through $(\mathcal{O}, \mathcal{E})$, at least locally within $N_{\mathcal{O}} \times N_{\mathcal{E}}$. We will therefore refer to Σ as the *local surface of communication* (LSC), the word "local" meaning simply that we restrict our considerations to a small neighborhood of $(\mathcal{O}, \mathcal{E})$.

The physical interpretations of Σ all follow from the fact that Σ governs the shapes of the past light cones centered at points in $N_{\mathcal{O}}$, as registered in $N_{\mathcal{E}}$, and the shapes of the future light cones centered at points in $N_{\mathcal{E}}$, as measured in $N_{\mathcal{O}}$. More precisely, the sections of Σ with the surfaces $x^{\mu'}_{\mathcal{O}} = \text{const}$ yield the past light cones in $N_{\mathcal{E}}$ with vertex at chosen $x^{\mu'}_{\mathcal{O}}$, while the sections with $x^{\mu}_{\mathcal{E}} = \text{const}$ give light cones in $N_{\mathcal{O}}$ with vertex at $x^{\mu}_{\mathcal{E}}$. The shapes of the light cones on the other hand govern the times of arrival as well as the shapes of the wavefronts. The latter means that it also controls the direction of light propagation. In Sec. III we will show that the shape of Σ near $(\mathcal{O}, \mathcal{E})$ is directly related to the spacetime curvature tensor along γ_0.

D. Coordinate systems and orthonormal tetrads

We will use a number of distinct types of coordinate systems thoughout the paper. We will list them below from the most general to the most specific.

The most general type is any coordinates in M covering both $N_{\mathcal{O}}$ and $N_{\mathcal{E}}$. However, we will more often use the *locally flat* (LF) coordinates, i.e., any coordinates covering $N_{\mathcal{O}}$ and $N_{\mathcal{E}}$ such that the Christoffel symbols vanish at $\mathcal{O}$ and $\mathcal{E}$,

$$\Gamma^{\mu}{}_{\nu\alpha}(\mathcal{E}) = \Gamma^{\mu'}{}_{\nu'\alpha'}(\mathcal{O}) = 0,$$

or, equivalently, that the first derivatives of the metric components vanish at $\mathcal{O}$ and $\mathcal{E}$. A special type of coordinates of this kind can be obtained from a pair of orthonormal tetrads, one in $T_{\mathcal{O}}M$ and the other in $T_{\mathcal{E}}M$. Namely, given two such orthonormal tetrads $(u_{\mathcal{O}}, e_i)$, $(u_{\mathcal{E}}, f_j)$, consistent with the spacetime orientation and with both $u_{\mathcal{O}}$ and $u_{\mathcal{E}}$ timelike and future pointing, we can introduce locally flat coordinates at $N_{\mathcal{O}}$ and $N_{\mathcal{E}}$ as a pair of Riemann normal coordinates defined by the two tetrads. We define the point $p \in N_{\mathcal{O}}$ corresponding to (sufficiently small) coordinates $(y^{\mu}) \in \mathbb{R}^4$ as $\exp(y^0 u_{\mathcal{O}} + y^i e_i)$, with exp denoting the exponential map at $\mathcal{O}$ (analogous construction works in $N_{\mathcal{E}}$). We will call such coordinates the *orthonormal locally flat* (OLF) coordinates.

Finally, given a single orthonormal tetrad (u, e_i) at $\mathcal{O}$, properly oriented with future pointing, timelike u, we can parallel propagate it along γ_0. This provides us with a parallel-propagated tetrad at every point along γ_0, useful for describing geometric objects along the line of sight, as well as a corresponding orthonormal tetrad at $\mathcal{E}$. Repeating the same construction of the Riemann normal coordinates yields *parallel-propagated locally flat* (PLF) coordinates covering $N_{\mathcal{O}}$ and $N_{\mathcal{E}}$ as a special case of OLF coordinates. For any of these coordinate systems we will use the corresponding coordinate tetrads at $T_{\mathcal{O}}M$ and $T_{\mathcal{E}}M$ for decomposing the tensors and the bitensors into components.

Given two pairs of tetrads used for defining the OLF coordinates, say $((u_{\mathcal{O}}, e_i), (u_{\mathcal{E}}, f_j))$ and $((\tilde{u}_{\mathcal{O}}, \tilde{e}_i), (\tilde{u}_{\mathcal{E}}, \tilde{f}_j))$, we can always transform the first pair into the second one by a pair of proper, orthochronal Lorentz transforms acting on the two tetrads. This way we see that the OLF coordinates are defined uniquely up to the action of a pair of special, orthochronal Lorentz groups. On the other hand, the PLF coordinates are defined uniquely up to the action of a single proper, orthochronal Lorentz group.

As a special type of oriented and time-oriented orthonormal tetrads along γ_0 we will consider the *adapted tetrads*, i.e., those for which the third spatial vector is aligned along the null tangent vector l^{μ}. For a tetrad (u, e_i) this simply means that $l^{\mu} = Q(-u^{\mu} + e_3^{\mu})$ for some tetrad-dependent $Q > 0$. Adapted tetrads will be denoted by (u, e_A, e_3) and we will call the two spatial vectors e_A^{μ}, orthogonal to l^{μ}, the *transverse vectors*, forming a Sachs basis [37]. Adapted tetrads can be transformed into other adapted tetrads by the elements of the stabilizer of the null direction of l^{μ}, a four-dimensional subgroup of the proper orthochronal Lorentz group defined by the condition $\Lambda^{\alpha}{}_{\beta} l^{\beta} = C l^{\alpha}$ for some $C > 0$, with $\Lambda^{\alpha}{}_{\beta}$ denoting the group element. Any oriented and time-oriented orthonormal tetrad can be transformed into an adapted tetrad by a spatial rotation aligning e_3^{μ} with the spatial projection of l^{μ}.

Let us stress here that we assume that each of our coordinate systems and tetrads is properly oriented and the tetrads are also time-oriented. This is an important restriction, as it makes the spatial volume three-form unique and well defined. We will make use of this fact in Sec. IV B.

Finally, any coordinate system (ξ^μ) covering $N_\mathcal{O}$ and $N_\mathcal{E}$ provides automatically a coordinate system $(\xi^\mu, \xi^{\mu'})$ on $N_\mathcal{O} \times N_\mathcal{E}$. Moreover, it is easy to see that any of the locally flat coordinates at $\mathcal{O}$ and $\mathcal{E}$, i.e., LF, OLF or PLF coordinates, produce this way a locally flat coordinate system at the point $(\mathcal{O}, \mathcal{E}) \in N_\mathcal{O} \times N_\mathcal{E}$ with respect to the metric $\mathbf{h}$.

III. THE CURVATURE TENSOR AND THE SHAPE OF THE LOCAL SURFACE OF COMMUNICATION

The goal of this section is to derive the first key result of this paper, i.e., the relation between the shape of the LSC and the Riemann tensor along the LOS. The derivation uses the Synge's world function for its intermediate steps and therefore we begin by a short review of its definition and properties.

The world function is a powerful tool for tracing geodesics between pairs of points [13,35] and determining which pairs of points can be connected by null geodesics [14–16]. It also helps to express the relations between geodesics in curved spacetime in a covariant way and to solve the geodesic deviation equations of the first and higher orders [38]. It has also found its applications in the problem of navigation in a curved spacetime using electromagnetic signals, as in the Global Positioning System (GPS) [10,39]. We will now briefly review its most important properties; for a more detailed treatment and full derivations see [13,35]. In this work we follow the notation and conventions of [35].

The world function σ is defined on pairs of points from M. Let $x' \in M$ be one point (called the *base point*) and $x \in M$ (the *field point*) be another one belonging to the normal convex neighbourhood of x'. In this case there is a unique, affine parametrized geodesic segment $\gamma(\lambda)$ through these two points. We define

$$\sigma(x, x') = \frac{\Delta\lambda}{2} \int_{\lambda_{x'}}^{\lambda_x} g_{\mu\nu} \frac{\mathrm{d}x^\mu}{\mathrm{d}\lambda} \frac{\mathrm{d}x^\nu}{\mathrm{d}\lambda} \mathrm{d}\lambda,$$

where the integration is performed along $\gamma(\lambda)$, λ_x is the value of the affine parameter λ corresponding to x, $\lambda_{x'}$ to x' and $\Delta\lambda = \lambda_x - \lambda_{x'}$ is the affine distance between the two endpoints.

The partial derivatives of σ with respect to the components x' and x, taken in any coordinate system, are proportional to the components of the tangent vectors to γ at x and x' with lowered indices,

$$\sigma_{,\nu} = \Delta\lambda \frac{\mathrm{d}x^\mu}{\mathrm{d}\lambda}\bigg|_{\lambda=\lambda_x} g_{\mu\nu} \tag{1}$$

$$\sigma_{,\nu'} = -\Delta\lambda \frac{\mathrm{d}x^{\mu'}}{\mathrm{d}\lambda}\bigg|_{\lambda=\lambda_{x'}} g_{\mu'\nu'}. \tag{2}$$

Here, following [35], the primed indices refer to the differentiation with respect to x' and the unprimed to x. Note that in any coordinates $\sigma_{,\nu} = \sigma_{;\nu}$ and $\sigma_{,\nu'} = \sigma_{;\nu'}$, because the covariant and the partial first derivatives of a two-point function always coincide. σ obeys also the identity $2\sigma = \sigma^{;\alpha}\sigma_{;\alpha} = \sigma^{;\alpha'}\sigma_{;\alpha'}$. Differentiating it covariantly with respect to x and x' yields the following relations:

$$\sigma_{,\nu'} = \sigma_{;\mu'\nu'}\sigma^{;\mu'} = \sigma_{;\mu\nu'}\sigma^{;\mu} \tag{3}$$

$$\sigma_{,\nu} = \sigma_{;\mu'\nu}\sigma^{;\mu'} = \sigma_{;\mu\nu}\sigma^{;\mu}. \tag{4}$$

Moreover, we always have $\sigma_{;\mu\nu} = \sigma_{;\nu\mu}$, $\sigma_{;\mu'\nu'} = \sigma_{;\nu'\mu'}$, $\sigma_{;\mu\nu'} = \sigma_{;\nu'\mu}$.

The applicability of the world function to the problem of signal propagation follows from the observation that $\sigma(x, x') = 0$ if and only if x and x' are linked by a null geodesic [16]. This means that the local surface of communication between the neighborhoods of x and x' may be identified with the zero level set of σ, i.e., $\Sigma = \{(p', q) \in U' \times U | \sigma(p', q) = 0\}$, where U and U' are sufficiently small neighborhoods of x and x'.

Our goal is to understand the TOAs and the shape of Σ in the neighborhood of $\mathcal{E}$ and $\mathcal{O}$. We will begin by considering the second order Taylor expansion of σ near this pair of points. Let $x_\mathcal{E}$ and $x_\mathcal{O}$ be the coordinates of the points $\mathcal{E}$ and $\mathcal{O}$ in a general coordinate system and let $\delta x_\mathcal{O}$ and $\delta x_\mathcal{E}$ be small displacements expressed in the same coordinates. As noted before, for points contained in $N_\mathcal{O}$ and $N_\mathcal{E}$ we may identify $\delta x_\mathcal{O}$ and $\delta x_\mathcal{E}$ with tangent vectors at $T_\mathcal{O}M$ and $T_\mathcal{E}M$. By convention $\mathcal{O}$ will play the role of the base point x', while $\mathcal{E}$ will be identified with the field point x. In this setup we have the following Taylor expansion,

$$\begin{aligned}
&\sigma(x_\mathcal{E} + \delta x_\mathcal{E}, x_\mathcal{O} + \delta x_\mathcal{O}) \\
&\quad = \sigma_{,\mu'}\delta x_\mathcal{O}^{\mu'} + \sigma_{,\mu}\delta x_\mathcal{E}^{\mu} + \frac{1}{2}\sigma_{,\mu'\nu'}\delta x_\mathcal{O}^{\mu'}\delta x_\mathcal{O}^{\nu'} + \sigma_{,\mu'\nu}\delta x_\mathcal{O}^{\mu'}\delta x_\mathcal{E}^{\nu} \\
&\qquad + \frac{1}{2}\sigma_{,\mu\nu}\delta x_\mathcal{E}^{\mu}\delta x_\mathcal{E}^{\nu} + O(\delta x^3),
\end{aligned}$$

the higher order terms being of the order of three and up in the displacements. Since $\sigma(x_\mathcal{E}, x_\mathcal{O}) = 0$ (recall that by assumption $\mathcal{E}$ and $\mathcal{O}$ are connected by the fiducial *null* geodesic γ_0) we have no free term in this expansion. The partial derivatives of σ are evaluated at $(x_\mathcal{E}, x_\mathcal{O})$. Now, while the formula in this form works in any coordinate system, in LF coordinates it takes a particularly useful form; namely, in this case we have $\sigma_{;\mu\nu} = \sigma_{,\mu\nu}$, $\sigma_{;\mu'\nu'} = \sigma_{,\mu\nu}$. On top of that, we always have $\sigma_{;\mu\nu'} = \sigma_{,\mu\nu'}$, $\sigma_{;\mu'\nu} = \sigma_{,\mu'\nu}$, $\sigma_{;\mu} = \sigma_{,\mu}$ and

$\sigma_{;\mu'} = \sigma_{,\mu'}$, so we can rewrite the Taylor expansion using the *covariant* second derivatives of bitensors only

$$\begin{aligned}\sigma(x_{\mathcal{E}} + \delta x_{\mathcal{E}}, x_{\mathcal{O}} + \delta x_{\mathcal{O}}) &= \sigma_{;\mu'}\delta x_{\mathcal{O}}^{\mu'} + \sigma_{;\mu}\delta x_{\mathcal{E}}^{\mu} + \frac{1}{2}\sigma_{;\mu'\nu'}\delta x_{\mathcal{O}}^{\mu'}\delta x_{\mathcal{O}}^{\nu'} + \sigma_{;\mu'\nu}\delta x_{\mathcal{O}}^{\mu'}\delta x_{\mathcal{E}}^{\nu} \\ &\quad + \frac{1}{2}\sigma_{;\mu\nu}\delta x_{\mathcal{E}}^{\mu}\delta x_{\mathcal{E}}^{\nu} + O(\delta x^3). \end{aligned} \tag{5}$$

Therefore, in LF coordinates the expansion contains only the covariant derivatives of σ, which turn out to have a special geometric meaning. We will explore this fact in the rest of this section.

Define now the 1×8 matrix

$$\mathbf{L} = -\frac{1}{\Delta\lambda}\begin{pmatrix} \sigma_{,\mu'} & \sigma_{,\mu} \end{pmatrix}, \tag{6}$$

which constitutes the matrix representation the rescaled gradient of σ as a function on $M \times M$ at $(\mathcal{O}, \mathcal{E})$, i.e., the linear mapping $\mathbf{L}\colon T_{\mathcal{O}}M \oplus T_{\mathcal{E}}M \to \mathbb{R}$. From the properties of the first derivatives of the world function (1)–(2) we can easily prove that it is in fact composed of the components of tangent vectors to γ, calculated with the parametrization λ at the two endpoints, and with lowered indices

$$\mathbf{L} = \begin{pmatrix} l_{\mathcal{O}\mu'} & -l_{\mathcal{E}\mu} \end{pmatrix}. \tag{7}$$

We also define the 8×8 matrix

$$\mathbf{U} = -\frac{1}{\Delta\lambda}\begin{pmatrix} \sigma_{;\mu'\nu'} & \sigma_{;\mu'\nu} \\ \sigma_{;\mu\nu'} & \sigma_{;\mu\nu} \end{pmatrix}, \tag{8}$$

i.e., the rescaled Hessian of σ. It is the matrix representation of a symmetric bilinear mapping $\mathbf{U}\colon (T_{\mathcal{O}}M \oplus T_{\mathcal{E}}M) \times (T_{\mathcal{O}}M \oplus T_{\mathcal{E}}M) \to \mathbb{R}$. As a matrix it decomposes naturally into four 4×4 matrices in the block decomposition

$$\mathbf{U} = \begin{pmatrix} U_{\mathcal{O}\mathcal{O}} & U_{\mathcal{O}\mathcal{E}} \\ U_{\mathcal{E}\mathcal{O}} & U_{\mathcal{E}\mathcal{E}} \end{pmatrix},$$

with $U_{\mathcal{O}\mathcal{O}\mu'\nu'}$ and $U_{\mathcal{E}\mathcal{E}\mu\nu}$ being tensors at $\mathcal{O}$ and $\mathcal{E}$ respectively and $U_{\mathcal{O}\mathcal{E}\mu'\nu}$ and $U_{\mathcal{E}\mathcal{O}\mu\nu'}$ being bitensors.

Define now the eight-dimensional vector in $T_{\mathcal{O}}M \oplus T_{\mathcal{E}}M$, composed of the two displacement vectors [40]

$$\mathbf{X} = \begin{pmatrix} \delta x_{\mathcal{O}}^{\mu'} \\ \delta x_{\mathcal{E}}^{\mu} \end{pmatrix}.$$

With these definitions and with the help of (5) we can rewrite the equation $\sigma(x', x) = 0$ for the surface of communication Σ in LF coordinates as an equation in $T_{\mathcal{O}}M \oplus T_{\mathcal{E}}M$,

$$\mathbf{L}(\mathbf{X}) + \frac{1}{2}\mathbf{U}(\mathbf{X}, \mathbf{X}) + O(\mathbf{X}^3) = 0. \tag{9}$$

If we neglect the third and higher order terms we obtain an equation of a seven-dimensional quadric in an eight-dimensional vector space. Equation (9) has no free term, which means that the quadric approximating Σ must pass through the origin $\mathbf{X} = 0$, i.e., point $(\mathcal{O}, \mathcal{E})$. This is again a consequence of our initial assumption that $\mathcal{O}$ and $\mathcal{E}$ can be linked by the fiducial *null* geodesic γ_0. The quadric Eq. (9) is not the normal form, but, as we show in Appendix A, can be transformed to the normal form.

We point out that in this approach $\mathbf{X}$, $\mathbf{L}$ and $\mathbf{U}$ can always be interpreted as eight-dimensional geometric objects, living on $M \times M$, and with the summation implied in the equations performed over all eight components of vectors in $T_{\mathcal{O}}M \oplus T_{\mathcal{E}}M$. However, we can also divide the components of $\mathbf{X}$ into the four components corresponding to $T_{\mathcal{O}}M$ and the four components corresponding $T_{\mathcal{E}}M$, and sum over them separately. This way the one-form $\mathbf{L}$ decomposes into two one-forms $l_{\mathcal{O}}$ and $l_{\mathcal{E}}$ as in (6) and the two-form $\mathbf{U}$ decomposes into four two-forms as in (8). While the first representation is more concise and simpler from the geometric point of view, the second one is more closely related to the spacetime itself and has therefore a more straightforward physical interpretation. In the rest of the paper we will freely switch between these two equivalent representations of equations and geometric objects.

A. Physical interpretation and algebraic properties of L and U

We will now briefly summarize the algebraic properties and the physical interpretation of the covector $\mathbf{L}$ and the quadratic form $\mathbf{U}$. We note first that both objects are given up to a common rescaling. Namely, the transformation $\mathbf{L} \to C \cdot \mathbf{L}$, $\mathbf{U} \to C \cdot \mathbf{U}$ with $C > 0$ amounts to an affine reparametrization of the fiducial null geodesic $\lambda \to C^{-1} \cdot \lambda$ and therefore leaves all physical quantities invariant. Therefore, the global scaling of both objects plays the role of a gauge degree of freedom [1,2].

$\mathbf{L}$ is always null with respect to the metric $\mathbf{h}$, i.e., $\mathbf{h}^{-1}(\mathbf{L}, \mathbf{L}) = 0$. Moreover, both of its constituent covectors are null with respect to the spacetime metric, i.e., $l_{\mathcal{O}}^{\mu'} l_{\mathcal{O}\mu'} = l_{\mathcal{E}}^{\mu} l_{\mathcal{E}\mu} = 0$. Since $l_{\mathcal{O}}^{\mu'}$ and $l_{\mathcal{E}}^{\mu}$ are the tangent vectors to the fiducial null geodesic γ_0 at $\mathcal{O}$ and $\mathcal{E}$, $\mathbf{L}$ describes the way events at and near $\mathcal{E}$ appear to an observer at $\mathcal{O}$. Namely, $l_{\mathcal{O}}^{\mu'}$ defines the apparent position in the sky of an object at $\mathcal{E}$, as it is registered by observers at $\mathcal{O}$ and, by extension, the approximate position of every light signal from $N_{\mathcal{E}}$ as seen by observers at $N_{\mathcal{O}}$ [1]. $l_{\mathcal{E}}^{\mu}$ on the other hand, is related to the viewing angle, i.e., the direction from which observers at $N_{\mathcal{O}}$ observe the events at $N_{\mathcal{E}}$. They are also both related to the redshift, or frequency transfer, between a frame defined by a normalized, future-pointing timelike vector $u^{\mu}_{\mathcal{E}}$ at $\mathcal{E}$ and a frame defined by another such vector at $u^{\mu'}_{\mathcal{O}}$, via the standard relation $1+z=\frac{u^{\mu}_{\mathcal{E}} l_{\mathcal{E}\mu}}{u^{\mu'}_{\mathcal{O}} l_{\mathcal{O}\mu'}}$ for the redshift z [1,16].

From the definition (8) it is straightforward to see that $\mathbf{U}$ is a symmetric matrix, i.e.,

$$\mathbf{U}^T = \mathbf{U}, \tag{10}$$

or, equivalently, that $U_{\mathcal{O}\mathcal{O}\alpha'\beta'} = U_{\mathcal{O}\mathcal{O}\beta'\alpha'}$, $U_{\mathcal{E}\mathcal{E}\alpha\beta} = U_{\mathcal{E}\mathcal{E}\beta\alpha}$, $U_{\mathcal{E}\mathcal{O}\alpha\beta'} = U_{\mathcal{O}\mathcal{E}\beta'\alpha}$. Additional algebraic relations between $\mathbf{U}$ and $\mathbf{L}$ follow from the properties for the world function (3)–(4). Combining them with (10) yields four relations between the submatrices of $\mathbf{U}$ and the tangent vectors $l_{\mathcal{O}}$, $l_{\mathcal{E}}$

$$U_{\mathcal{O}\mathcal{O}\alpha'\beta'} l^{\beta'}_{\mathcal{O}} = U_{\mathcal{O}\mathcal{O}\beta'\alpha'} l^{\beta'}_{\mathcal{O}} = -\frac{1}{\Delta\lambda} l_{\mathcal{O}\alpha'} \tag{11}$$

$$U_{\mathcal{E}\mathcal{O}\alpha\beta'} l^{\beta'}_{\mathcal{O}} = U_{\mathcal{O}\mathcal{E}\beta'\alpha} l^{\beta'}_{\mathcal{O}} = \frac{1}{\Delta\lambda} l_{\mathcal{E}\alpha} \tag{12}$$

$$U_{\mathcal{O}\mathcal{E}\alpha'\beta} l^{\beta}_{\mathcal{E}} = U_{\mathcal{E}\mathcal{O}\beta\alpha'} l^{\beta}_{\mathcal{E}} = \frac{1}{\Delta\lambda} l_{\mathcal{O}\alpha'} \tag{13}$$

$$U_{\mathcal{E}\mathcal{E}\alpha\beta} l^{\beta}_{\mathcal{E}} = U_{\mathcal{E}\mathcal{E}\beta\alpha} l^{\beta}_{\mathcal{E}} = -\frac{1}{\Delta\lambda} l_{\mathcal{E}\alpha}. \tag{14}$$

The bilocal operator $\mathbf{U}$ has a simple geometric interpretation; it relates the variations of the endpoints of a geodesic to the variations of the tangent vectors at the endpoints, calculated at linear order around γ_0. Let $\delta x^{\mu'}_{\mathcal{O}}$ and $\delta x^{\nu}_{\mathcal{E}}$ be the endpoints variations, expressed in general coordinates, and let $\delta l_{\mathcal{O}\mu'}$ and $\delta l_{\mathcal{E}\nu}$ be the variations of the components of the tangent vectors. We introduce the covariant variations $\Delta l_{\mathcal{O}\mu'} = \delta l_{\mathcal{O}\mu'} - \Gamma^{\nu'}{}_{\mu'\sigma'}(\mathcal{O}) l_{\mathcal{O}\nu'} \delta x^{\sigma'}_{\mathcal{O}}$ and $\Delta l_{\mathcal{E}\mu} = \delta l_{\mathcal{E}\mu} - \Gamma^{\nu}{}_{\mu\sigma}(\mathcal{E}) l_{\mathcal{E}\nu} \delta x^{\sigma}_{\mathcal{E}}$; with this notation we have

$$\Delta l_{\mathcal{O}\mu'} = U_{\mathcal{O}\mathcal{O}\mu'\nu'} \delta x^{\nu'}_{\mathcal{O}} + U_{\mathcal{O}\mathcal{E}\mu'\nu} \delta x^{\nu}_{\mathcal{E}} \tag{15}$$

$$-\Delta l_{\mathcal{E}\mu} = U_{\mathcal{E}\mathcal{O}\mu\nu'} \delta x^{\nu'}_{\mathcal{O}} + U_{\mathcal{E}\mathcal{E}\mu\nu} \delta x^{\nu}_{\mathcal{E}}, \tag{16}$$

(see Appendix B for the proof).

In Appendix A we prove a couple of simple algebraic results regarding $\mathbf{U}$ and we will briefly summarize them here. $\mathbf{U}$ as a symmetric, bilinear form is always degenerate in one direction. Namely, we define the vector via $\mathbf{L}^\sharp = \begin{pmatrix} l^{\mu'}_{\mathcal{O}} & l^{\mu}_{\mathcal{E}} \end{pmatrix}$, i.e., as the upper-index version of the covector $\mathbf{L}$. Then we have $\mathbf{U}(\mathbf{L}^\sharp, \cdot) = 0$.

In a flat spacetime $\mathbf{U}$ turns out to degenerate in as many as four linearly independent directions. This degeneracy is actually related to the translational invariance of the Minkowski spacetime; the condition for two points to be connected by a null geodesic does not depend on their absolute position, but rather in their relative positions. Thus the four components of the absolute position drop out from the condition (9). The invariant signature of $\mathbf{U}$ in a flat spacetime reads actually (1,3,4), i.e., one minus sign, four plus signs and four zeros. In the small curvature limit, when the light propagation is only slightly perturbed by curvature corrections (see Sec. III B), the three zeros may turn into any other signs. In the general case, however, the signature of $\mathbf{U}$ is only subject to the degeneracy condition in the direction of $\mathbf{L}^\sharp$, as we have mentioned above.

The basic principle of the measurement we discuss in this paper in based on the fact that $\mathbf{U}$ can be expressed as a functional of the curvature tensor along the LOS. The relation we present here is indirect; $\mathbf{U}$ is related by a nonlinear transform to another geometrical object describing the propagation of light between $N_{\mathcal{O}}$ and $N_{\mathcal{E}}$, the bilocal geodesic operator, which in turn is related to the curvature as a solution of a simple ordinary differential equation (ODE). We will explain this point in detail.

Recall first the bilocal geodesic operator (BGO) $\mathbf{W}\colon T_{\mathcal{O}}M \oplus T_{\mathcal{O}}M \to T_{\mathcal{E}}M \oplus T_{\mathcal{E}}M$, relating the perturbed initial data for a geodesic near $\mathcal{O}$ to the perturbed final data near $\mathcal{E}$, discussed extensively in [1]. In the context of null geodesics it may be seen as a general relativistic generalization of the ray bundle transfer matrix from nonrelativistic optics [41]. $\mathbf{W}$ can represented by four bitensors

$$\mathbf{W} = \begin{pmatrix} W_{XX}{}^{\mu}{}_{\nu'} & W_{XL}{}^{\mu}{}_{\nu'} \\ W_{LX}{}^{\mu}{}_{\nu'} & W_{LL}{}^{\mu}{}_{\nu'} \end{pmatrix},$$

each mapping vectors from $T_{\mathcal{O}}M$ to $T_{\mathcal{E}}M$. By definition it links the displacement and the direction deviation vectors of a perturbed geodesic (not necessary null) at $\lambda = \lambda_{\mathcal{O}}$ to the displacement and the direction deviation vectors at $\lambda = \lambda_{\mathcal{E}}$, at the linear order

$$\delta x^{\mu}_{\mathcal{E}} = W_{XX}{}^{\mu}{}_{\nu'} \delta x^{\nu'}_{\mathcal{O}} + W_{XL}{}^{\mu}{}_{\nu'} \Delta l^{\nu'}_{\mathcal{O}} \tag{17}$$

$$\Delta l^{\mu}_{\mathcal{E}} = W_{LX}{}^{\mu}{}_{\nu'} \delta x^{\nu'}_{\mathcal{O}} + W_{LL}{}^{\mu}{}_{\nu'} \Delta l^{\nu'}_{\mathcal{O}}, \tag{18}$$

with $\Delta l^{\mu'}_{\mathcal{O}} = \delta l^{\mu'}_{\mathcal{O}} + \Gamma^{\mu'}{}_{\nu'\sigma'}(\mathcal{O}) l^{\nu'}_{\mathcal{O}} \delta x^{\sigma'}_{\mathcal{O}}$ and $\Delta l^{\mu}_{\mathcal{E}} = \delta l^{\mu}_{\mathcal{E}} + \Gamma^{\mu}{}_{\nu\sigma}(\mathcal{E}) l^{\nu}_{\mathcal{E}} \delta x^{\sigma}_{\mathcal{E}}$. The equations above constitute the relativistic counterpart of the decomposition of the ray bundle transfer matrix into the $ABCD$ blocks in the nonrelativistic optics [41].

One can now show that $\mathbf{U}$ between $\mathcal{O}$ and $\mathcal{E}$ is related to $\mathbf{W}$ between the same pair of points by a nonlinear matrix transform, derived in Appendix C. In the block matrix form with indices suppressed it reads

$$\mathbf{U} = \begin{pmatrix} -g_{\mathcal{O}} W_{XL}^{-1} W_{XX} & g_{\mathcal{O}} W_{XL}^{-1} \\ g_{\mathcal{E}}(W_{LL} W_{XL}^{-1} W_{XX} - W_{LX}) & -g_{\mathcal{E}} W_{LL} W_{XL}^{-1} \end{pmatrix}. \tag{19}$$

Here g stands for the lower-index metric tensor in the coordinate frame, taken at $\mathcal{O}$ or $\mathcal{E}$. It lowers the first index in each submatrix, consistently with the definition of $\mathbf{U}$ above. The transformation (19) works in any coordinate system and any tetrads. Moreover, since $U_{\mathcal{E}\mathcal{O}} = U_{\mathcal{O}\mathcal{E}}^T$ there is actually no need to evaluate the complicated, lower-left expression for $U_{\mathcal{E}\mathcal{O}}$, it is enough to evaluate the upper-right one for $U_{\mathcal{O}\mathcal{E}}$ and transpose. Note that the transformation works as long as W_{XL} is invertible. With this assumption we can also derive the inverse transform

$$\mathbf{W} = \begin{pmatrix} -U_{\mathcal{O}\mathcal{E}}^{-1}U_{\mathcal{O}\mathcal{O}} & U_{\mathcal{O}\mathcal{E}}^{-1}g_{\mathcal{O}} \\ g_{\mathcal{E}}^{-1}(U_{\mathcal{E}\mathcal{E}}U_{\mathcal{O}\mathcal{E}}^{-1}U_{\mathcal{O}\mathcal{O}} - U_{\mathcal{E}\mathcal{O}}) & -g_{\mathcal{E}}^{-1}U_{\mathcal{E}\mathcal{E}}U_{\mathcal{O}\mathcal{E}}^{-1}g_{\mathcal{O}} \end{pmatrix}, \tag{20}$$

with g^{-1} denoting the upper-index metric. We may therefore regard $\mathbf{U}$ and $\mathbf{W}$ as two equivalent methods of encoding the geometric information about the behavior of perturbed geodesics passing near the two endpoints $\mathcal{E}$ and $\mathcal{O}$. $\mathbf{W}$ corresponds to the initial value problem, parametrized by the initial data $(\delta x_{\mathcal{O}}^{\mu'}, \Delta l_{\mathcal{O}}^{\mu'})$ according to (17)–(18), while $\mathbf{U}$ governs the boundary problem parametrized by $(\delta x_{\mathcal{O}}^{\mu'}, \delta x_{\mathcal{E}}^{\mu})$ via (15)–(16).

The relation between the pair of matrices W_{XX}, W_{XL}, known as Jacobi propagators [38,42,43], and the second derivatives of the world function, proportional to $\mathbf{U}$, is an old result dating back to Dixon [43] (see also [38]). It has found its applications in the study of equations of motions of massive objects [35]. Here we have presented this relation in a complete form, including all four constituent bitensors of $\mathbf{W}$, and applied it in the context of geometric optics and perturbed light rays.

The relation of $\mathbf{W}$ to the curvature is best described in a parallel propagated tetrad along γ_0 and the corresponding PLF coordinates. In this case $\mathbf{W}$ is simply the resolvent matrix of the first order geodesic deviation equation (GDE) with $\lambda = \lambda_{\mathcal{O}}$ as the initial data point [1,41]. Namely, for a solution $\xi(\lambda)$ of the GDE in a parallel propagated tetrad

$$\ddot{\xi}^{\bar{\mu}}(\lambda) - R^{\bar{\mu}}{}_{\bar{\alpha}\bar{\beta}\bar{\nu}}(\lambda)l^{\bar{\alpha}}l^{\bar{\beta}}\xi^{\bar{\nu}}(\lambda) = 0.$$

With the initial data $\xi(\lambda_{\mathcal{O}})^{\bar{\mu}} = \delta x_{\mathcal{O}}^{\bar{\mu}}$, $\dot{\xi}(\lambda_{\mathcal{O}})^{\bar{\mu}} = \Delta l_{\mathcal{O}}^{\bar{\mu}}$ we have the following relation:

$$\begin{pmatrix} \xi^{\bar{\mu}}(\lambda) \\ \dot{\xi}^{\bar{\nu}}(\lambda) \end{pmatrix} = \mathbf{W}(\lambda)\begin{pmatrix} \delta x_{\mathcal{O}}^{\bar{\mu}} \\ \Delta l_{\mathcal{O}}^{\bar{\nu}} \end{pmatrix},$$

with $\mathbf{W}(\lambda)$ expressed as an 8×8 matrix in the parallel-propagated tetrad. Therefore, we can obtain $\mathbf{W}$ between $\mathcal{O}$ and $\mathcal{E}$ as a solution of the resolvent matrix ODE in the parallel-propagated tetrad, with the value taken at $\lambda = \lambda_{\mathcal{E}}$. This ODE and the initial condition read

$$\dot{\mathbf{W}}(\lambda) = \left(\begin{pmatrix} 0 & I_4 \\ 0 & 0 \end{pmatrix} + \begin{pmatrix} 0 & 0 \\ R_{ll}(\lambda) & 0 \end{pmatrix}\right)\mathbf{W}(\lambda) \tag{21}$$

$$\mathbf{W}(\lambda_{\mathcal{O}}) = I_8, \tag{22}$$

where I_n is the n-dimensional unit matrix and $R_{ll}(\lambda)$ is the optical tidal matrix $R^{\bar{\mu}}{}_{\bar{\alpha}\bar{\beta}\bar{\nu}}(\lambda)l^{\bar{\alpha}}l^{\bar{\beta}}$ in the parallel propagated frame. Note that the equations above are formally identical to the equations for the time evolution operator in quantum mechanics, with λ playing the role of the time and with the Hamiltonian consisting of a λ-independent "free evolution" term and the λ-dependent perturbation given by appropriate components of the Riemann tensor. The "free Hamiltonian" fully governs $\mathbf{W}$ (and thus also $\mathbf{U}$) in a flat spacetime and it is therefore responsible for the finite-distance optical effects mentioned in Sec. I B. The second term on the other hand generates the curvature corrections present in nonflat spacetimes. This way we obtain a formal separation of the optical effects into the finite-distance effects, present also in the Minkowski space, and the "pure" curvature effects.

B. Small curvature limit

In the absence of strong lensing we may expect the curvature terms appearing in (21) to be small in comparison to the rest. In Sec. V we will make this statement more precise by deriving more precise estimates, but here we simply assume that we may treat the curvature terms as small corrections superimposed on top of the finite distance terms. The standard procedure in this case is to apply the perturbative expansion in powers of the Riemann tensor [44–46]. We will follow this approach and truncate the expansion at the first order, effectively linearizing the dependence on the curvature in all relations above.

The details of the calculations are laid out in the Appendix. First, the derivation of $\mathbf{W}$ at first order from (21) is described in Appendix D, and then the linearization of (19) around a "flat" solution, leading to the analogous expansion in powers of curvature for $\mathbf{U}$, is described in Appendix E. As expected, the final expression for $\mathbf{U}$ contains a finite distance term and a curvature correction. In a parallel transported tetrad and PLF coordinates it reads

$$\mathbf{U} = \mathbf{U}^{(0)} + \mathbf{U}^{(1)} \tag{23}$$

with

$$\mathbf{U}^{(0)} = \frac{1}{\Delta\lambda}\begin{pmatrix} -\eta_{\bar{\mu}\bar{\nu}} & \eta_{\bar{\mu}\bar{\nu}} \\ \eta_{\bar{\mu}\bar{\nu}} & -\eta_{\bar{\mu}\bar{\nu}} \end{pmatrix}, \tag{24}$$

and

$$\mathbf{U}^{(1)} = -\int_{\lambda_{\mathcal{O}}}^{\lambda_{\mathcal{E}}} \left(\begin{array}{c|c} R_{\bar{\mu}\bar{\alpha}\bar{\beta}\bar{\nu}}(\lambda) l^{\bar{\alpha}} l^{\bar{\beta}} \frac{(\lambda_{\mathcal{E}}-\lambda)^2}{\Delta\lambda^2} & R_{\bar{\mu}\bar{\alpha}\bar{\beta}\bar{\nu}}(\lambda) l^{\bar{\alpha}} l^{\bar{\beta}} \frac{(\lambda-\lambda_{\mathcal{O}})(\lambda_{\mathcal{E}}-\lambda)}{\Delta\lambda^2} \\ \hline R_{\bar{\mu}\bar{\alpha}\bar{\beta}\bar{\nu}}(\lambda) l^{\bar{\alpha}} l^{\bar{\beta}} \frac{(\lambda-\lambda_{\mathcal{O}})(\lambda_{\mathcal{E}}-\lambda)}{\Delta\lambda^2} & R_{\bar{\mu}\bar{\alpha}\bar{\beta}\bar{\nu}}(\lambda) l^{\bar{\alpha}} l^{\bar{\beta}} \frac{(\lambda-\lambda_{\mathcal{O}})^2}{\Delta\lambda^2} \end{array} \right) \mathrm{d}\lambda. \tag{25}$$

The leading order term $\mathbf{U}^{(0)}$ gives the finite distance effects, inversely proportional to the affine distance $\Delta\lambda$ between $\mathcal{E}$ and $\mathcal{O}$, while $\mathbf{U}^{(1)}$ governs the leading order curvature corrections, proportional to the integrals of the optical tidal tensor with kernels of the form of second order polynomials in the affine parameter λ.

C. Times of arrival of signals

We now use the results derived above to approximate the shape of Σ in LF coordinates near $(\mathcal{O}, \mathcal{E})$ by its second order tangent. This approximation automatically yields an approximation for the TOAs of pulsed electromagnetic signals between displaced points.

We begin by solving perturbatively (9) near $\mathbf{X} = 0$, treating $\mathbf{U}$ as small. Formally we write $\mathbf{X} = \mathbf{X}_{(0)} + \mathbf{X}_{(1)}$ and obtain the relations

$$\mathbf{L}(\mathbf{X}_{(0)}) = 0, \tag{26}$$

$$\mathbf{L}(\mathbf{X}_{(1)}) = -\frac{1}{2}\mathbf{U}(\mathbf{X}_{(0)}, \mathbf{X}_{(0)}). \tag{27}$$

At the leading, linear order we simply obtain the equation of the tangent space to Σ, given by $\mathbf{L}(\mathbf{X}_{(0)}) = 0$. Expressed back in the spacetime notation this is equivalent to the condition for the time of arrival of the form

$$l_{\mathcal{O}\mu'} \delta x_{\mathcal{O}}^{\mu'} = l_{\mathcal{E}\mu} \delta x_{\mathcal{E}}^{\mu}$$

in LF coordinates. This condition is covariant, i.e., it maintains the same form in any coordinate system. Its physical significance has been discussed in [1], where it is called the *flat lightcones approximation* (FLA). The FLA takes into account the effects of the delays along the LOS (or Rømer delays), the frequency shift between the rest frames of the emitters and the receivers (of whatever physical origin), but not the transverse delay effects. In order to evaluate them we need to go to the subleading, quadratic order, given by (27).

Note that from (26) the leading term $\mathbf{X}_{(0)}$ is orthogonal to the normal vector $\mathbf{L}$, or $\mathbf{X}_{(0)} \in \mathbf{L}^{\perp}$, where $\mathbf{L}^{\perp}$ denotes the seven-dimensional normal subspace to $\mathbf{L}$. Therefore, (27) depends effectively only on the operator $\mathbf{U}$ restricted to the subspace $\mathbf{L}^{\perp}$. We will denote this restriction as $\mathbf{U}^{\perp} = \mathbf{U}|_{\mathbf{L}^{\perp}}$; the equations now take the form of

$$\mathbf{L}(\mathbf{X}_{(0)}) = 0 \tag{28}$$

$$\mathbf{L}(\mathbf{X}_{(1)}) = -\frac{1}{2}\mathbf{U}^{\perp}(\mathbf{X}_{(0)}, \mathbf{X}_{(0)}). \tag{29}$$

In order to describe the TOA conditions in detail we introduce an OLF coordinate system, constructed from a pair of tetrads $(u_{\mathcal{O}}, e_i)$, $(u_{\mathcal{E}}, f_j)$. $u_{\mathcal{O}}$ is chosen here to be aligned with the four-velocities of the receivers, $u_{\mathcal{E}}$ with the four-velocities of the emitters, while the remaining spacelike vectors are so far arbitrary. The rest of the equations in this section are expressed in these coordinates. We introduce the (tetrad-dependent) gauge condition

$$l_{\mathcal{O}0'} \equiv \mathbf{L_0} = 1, \tag{30}$$

which fixes the normalization of $\mathbf{L}$ and $\mathbf{U}$.

In our measurement the time of arrival $\delta x_{\mathcal{O}}^{0'}$ plays a different role than other components of $\mathbf{X}$. Namely, we may treat the spatial positions of the receivers $\delta x_{\mathcal{O}}^{i'}$, the spatial positions of the emitters $\delta x_{\mathcal{E}}^{i}$ and the moments of emission $\delta x_{\mathcal{E}}^{0}$ as controlled by the experimentator. The time of arrival of the signals on the other hand is an uncontrolled, measured quantity. Therefore in the subsequent analysis we will treat $\delta x_{\mathcal{O}}^{0'}$ as a function of the other seven components, which in turn play the role of the independent variables

$$\mathbf{X^0} \equiv \delta x_{\mathcal{O}}^{0'} \equiv \tau(\delta x_{\mathcal{O}}^{i'}, \delta x_{\mathcal{E}}^{\mu}) \equiv \tau(\mathbf{X^a}),$$

with index $\mathbf{a}$ running from $\mathbf{1}$ to $\mathbf{7}$. The functional dependence is defined implicitly by Eq. (9), or, more generally, by the vanishing condition for the world function $0 = \sigma(x_{\mathcal{E}}^{\mu} + \delta x_{\mathcal{E}}^{\mu}, x_{\mathcal{O}}^{0'} + \tau(\delta x_{\mathcal{O}}^{i'}, \delta x_{\mathcal{E}}^{\mu}), x_{\mathcal{O}}^{i'} + \delta x_{\mathcal{O}}^{i'})$. This way we represent Σ locally as a graph of a function $\mathbf{X^0} = \tau(\mathbf{X^a})$ in $T_{\mathcal{O}}M \oplus T_{\mathcal{E}}M$. In the following calculations we will expand $\tau(\mathbf{X^a})$ in terms of the other seven components $\mathbf{X^a}$ up to the second order, consistently with the expansions (28)–(29) and (9). The expansion can be obtained directly from (9)

$$\mathbf{X^0} = -\mathbf{L_a}\mathbf{X^a} - \frac{1}{2}\mathbf{Q_{ab}}\mathbf{X^a}\mathbf{X^b} + O((\mathbf{X^a})^3), \tag{31}$$

with $\mathbf{Q_{ab}}$ being a symmetric square matrix of dimension seven given by

$$\mathbf{Q_{ab}} = \mathbf{U_{ab}} - 2\mathbf{U_{0(a}}\mathbf{L_{b)}} + \mathbf{U_{00}}\mathbf{L_a}\mathbf{L_b}.$$

Higher order terms on the right hand side are of the order of $O((\mathbf{X^a})^3)$ and will be neglected from now on. Returning to the standard notation on M this can be written as

$$\delta x^{0'}_{\mathcal{O}} = -l_{\mathcal{O}i'}\delta x^{i'}_{\mathcal{O}} + l_{\mathcal{E}\mu}\delta x^{\mu}_{\mathcal{E}} - \frac{1}{2}(Q_{\mathcal{O}\mathcal{O}i'j'}\delta x^{i'}_{\mathcal{O}}\delta x^{j'}_{\mathcal{O}} + 2Q_{\mathcal{O}\mathcal{E}i'\mu}\delta x^{i'}_{\mathcal{O}}\delta x^{\mu}_{\mathcal{E}} + Q_{\mathcal{O}\mathcal{O}\mu\nu}\delta x^{\mu}_{\mathcal{E}}\delta x^{\nu}_{\mathcal{E}}), \tag{32}$$

with $Q_{\mathcal{O}\mathcal{O}i'j'}$, $Q_{\mathcal{E}\mathcal{E}\mu\nu}$, $Q_{\mathcal{O}\mathcal{E}i'\mu}$ being the submatrices of $\mathbf{Q_{ab}}$,

$$Q_{\mathcal{O}\mathcal{O}i'j'} = U_{\mathcal{O}\mathcal{O}i'j'} - 2U_{\mathcal{O}\mathcal{O}0'(i'}l_{\mathcal{O}j')} + U_{\mathcal{O}\mathcal{O}0'0'}l_{\mathcal{O}i'}l_{\mathcal{O}j'} \tag{33}$$

$$Q_{\mathcal{E}\mathcal{E}\mu\nu} = U_{\mathcal{E}\mathcal{E}\mu\nu} - 2U_{\mathcal{O}\mathcal{E}0'(\mu}l_{\mathcal{E}\nu)} + U_{\mathcal{O}\mathcal{O}0'0'}l_{\mathcal{E}\mu}l_{\mathcal{E}\nu} \tag{34}$$

$$Q_{\mathcal{O}\mathcal{E}i'\mu} = U_{\mathcal{O}\mathcal{E}i'\mu} - U_{\mathcal{O}\mathcal{E}0'\mu}l_{\mathcal{O}i'} - U_{\mathcal{O}\mathcal{O}0'i'}l_{\mathcal{E}\mu} + U_{\mathcal{O}\mathcal{O}0'0'}l_{\mathcal{O}i'}l_{\mathcal{E}\mu}. \tag{35}$$

Taken together they form $\mathbf{Q_{ab}}$ according to

$$\mathbf{Q_{ab}} = \left(\begin{array}{c|c} Q_{\mathcal{O}\mathcal{O}} & Q_{\mathcal{O}\mathcal{E}} \\ \hline Q_{\mathcal{E}\mathcal{O}} & Q_{\mathcal{E}\mathcal{E}} \end{array}\right), \tag{36}$$

(note that the submatrices here are of unequal shape and size and that $Q_{\mathcal{E}\mathcal{O}} = Q^T_{\mathcal{O}\mathcal{E}}$). In the terminology of [14,15], Eq. (32) provides the Taylor expansion (up to a constant) for the reception time transfer function $\mathcal{T}_r$ expressed in locally flat coordinates at $\mathcal{O}$ and $\mathcal{E}$.

The seven-dimensional subvectors $\mathbf{X^a}$ contain now the degrees of freedom under control of the experimentator, i.e., the positions of emitters and receivers with respect to their local inertial frames, plus the moment of emission in the emitter's frame. Together with $\mathbf{X^0}$ they form an eight-dimensional vector in $T_{\mathcal{O}}M \oplus T_{\mathcal{E}}M$. The matrix $\mathbf{Q}$ has a simple algebraic interpretation as a method to express $\mathbf{U}^{\perp}$ using the components $\mathbf{a} = \mathbf{1}, \ldots \mathbf{7}$. Namely, let $E_{\boldsymbol{\mu}}$ denote the eight basis vectors $(u_{\mathcal{O}}, e_i, u_{\mathcal{E}}, f_j)$ in $T_{\mathcal{O}}M \oplus T_{\mathcal{E}}M$. Then we have

$$\mathbf{Q_{ab}} = \mathbf{U}(E_{\mathbf{a}} - \mathbf{L_a}E_{\mathbf{0}}, E_{\mathbf{b}} - \mathbf{L_b}E_{\mathbf{0}}).$$

Since the combinations $E_{\mathbf{a}} - \mathbf{L_a}E_{\mathbf{0}}$ are all orthogonal to $\mathbf{L}$, the components above can be calculated from $\mathbf{U}^{\perp}$ only.

D. Geometry of the LSC

We can obtain a deeper geometric insight into the problem if we consider Σ as a surface embedded isometrically in $(M \times M, \mathbf{h})$, (see Fig. 4). The reader may check that, in this interpretation, $\mathbf{L}$ is simply the normal covector to Σ at $(\mathcal{O}, \mathcal{E})$, while $\mathbf{U}^{\perp}$ can be identified with its covariant derivative in the tangent directions, i.e., the extrinsic curvature (or the second fundamental form), of Σ at $(\mathcal{O}, \mathcal{E})$. The vector $\mathbf{L}$ is null with respect to the metric $\mathbf{h}$ and therefore cannot be normalized; both $\mathbf{L}$ and $\mathbf{U}^{\perp}$ are thus given only up to rescalings, unless we fix them with a condition of type (30). In this picture the fundamental Eqs. (31) and (32) for the TOAs may be interpreted as resulting simply from approximating Σ by its second order tangent, defined by the null normal and extrinsic curvature, in locally flat coordinates in $M \times M$. In particular, $\mathbf{Q_{ab}}$ represents in this case the extrinsic curvature at $(\mathcal{O}, \mathcal{E})$ expressed in the coordinate system on Σ given by the seven components $\mathbf{X^a}$ restricted to Σ (see Fig. 4).

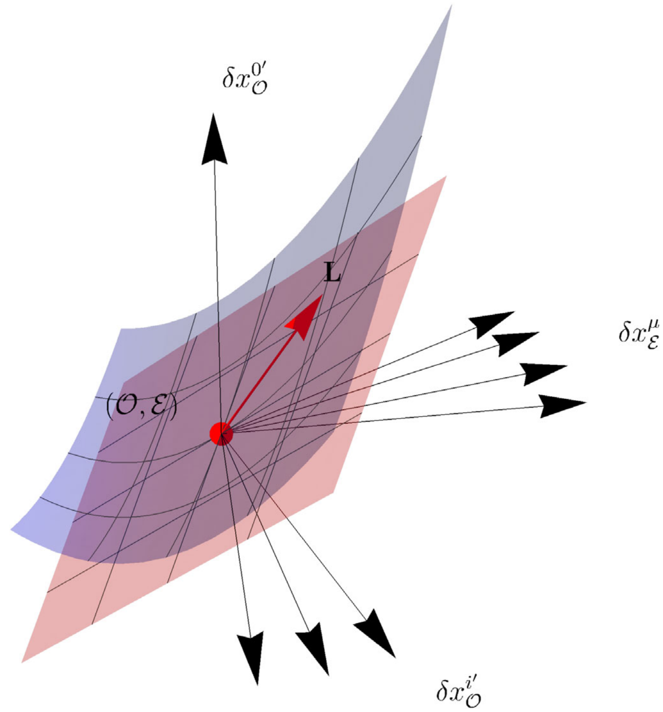

FIG. 4. Approximating of Σ by its first and second order tangents hypersurfaces in $M \times M$. The first order tangent is parametrized just by the normal vector $\mathbf{L}$. The second order tangent requires also the extrinsic curvature $\mathbf{Q}$. The surface may be then represented by the graph with $\delta x^{0'}_{\mathcal{O}}$ as the dependent variable.

We will now list a few algebraic properties of $\mathbf{U}^{\perp}$, or the extrinsic curvature tensor, proved in Appendix A. Independently of the spacetime geometry, $\mathbf{U}^{\perp}$ is always degenerate in two directions, spanned by the vectors $\mathbf{K}_{\mathcal{O}} = (\, l^{\mu'}_{\mathcal{O}} \quad 0\,)$ and $\mathbf{K}_{\mathcal{E}} = (\,0 \quad l^{\mu}_{\mathcal{E}}\,)$, namely we have $\mathbf{U}^{\perp}(\mathbf{K}_{\mathcal{O}}, \cdot) = \mathbf{U}^{\perp}(\mathbf{K}_{\mathcal{E}}, \cdot) = 0$. In a flat spacetime $\mathbf{U}^{\perp}$ is in fact degenerate in five directions and has the signature of (0,2,5), i.e., no pluses, two minuses and five zeros. In the small curvature limit three of the zeros may change into other signs.

E. The inverse problem: L and $\mathbf{U}^{\perp}$ from the measurements of TOAs

Equations (31) and (32) provide also a method for the inverse problem, i.e., the problem of determining the components of $\mathbf{L}$ and $\mathbf{Q}$ from the TOA measurements. As our input dataset we may consider a finite sample of pairs of events connected by null geodesics. Assume thus that we have obtained by direct measurements a sample of pairs of points $\delta x^{\mu}_{\mathcal{E}(i)}$, $\delta x^{\mu'}_{\mathcal{O}(i)}$, $i = 1, \ldots, n$, in $N_{\mathcal{E}}$ and $N_{\mathcal{O}}$, such that signals from the former event reach the latter. The pairs form a set of eight-vectors $\mathbf{X}_{(i)}$. We can now write down Eq. (31) for each $\mathbf{X}_{(i)}$, expressed in a system of OLF coordinates, and treat the resulting system of n equations as a linear system for the components of $\mathbf{L}$ and $\mathbf{Q}$, with the components of $\mathbf{X}_{(i)}$ now considered known. Since the number of independent coordinates of $\mathbf{L}$ and $\mathbf{Q}$, subject to (30), is $7 + 28 = 35$, and since the problem is linear, we expect that with at least 35 independent measurements we may determine this way all components of $\mathbf{L}$ and $\mathbf{Q}$.[47]

Geometrically this procedure is equivalent to determining the shape of the LSC Σ in the second order Taylor approximation by probing it at a finite number of points near the origin. In this approximation Σ must be a quadric passing through the origin, therefore its shape near the origin is parametrized by 35 numbers. The inverse problem becomes then the question of finding a unique quadric of type (32) through a set of known points in dimension eight.

Note that the feasibility of this procedure crucially depends on the linear independence of the resulting equations for $\mathbf{Q_{ab}}$ and $\mathbf{L_a}$. This obviously imposes additional restrictions on the choice of the points over which we probe the TOAs. The detailed analysis of these restrictions is an algebraic geometry problem in dimension eight and it is beyond the scope of this article. We just note here that the independence condition for the equations is equivalent to a nondegeneracy condition for a 35×35 matrix; namely, the determinant made of the components and products of components of the seven-vectors $\mathbf{X}^{\mathbf{a}}_{(i)}$ should not vanish. We may therefore expect the independence to hold generically, i.e., always except a measure-zero set of degenerate configurations of sampling points. However, in this paper we do not attempt to provide a rigorous proof; in Sec. VI we simply present a particular choice of sampling points (i.e., a choice of the spatial positions of the emitters and the times of emission as well as the spatial positions of the receivers) for which we may prove that the inverse problem can always be solved. Nevertheless, many other sampling strategies should be possible here.

We also note here that the reconstruction of $\mathbf{U}$, defining the shape of the LSC via the quadric equation (9), from the TOA measurements near $\mathcal{O}$ and $\mathcal{E}$ is not complete. As long as the approximation (31) is valid, only the components of $\mathbf{U}^{\perp}$ can be reconstructed, while the rest is hidden in the unobservable, higher order effects in $\mathbf{X}^{\mathbf{a}}$. However, as we will see in the next section, this is not really a problem, because $\mathbf{U}^{\perp}$ contains all the information about the matter density along the line of sight we need.

IV. TWO SCALAR QUANTITIES MEASURING THE CURVATURE IMPRINT

The operator $\mathbf{U}^{\perp}$ consists of the finite distance part and much smaller curvature corrections. In order to evaluate the curvature imprint we need to find a way to measure the latter independently of the former. It should preferably be done in a covariant, tetrad-independent manner. In this section we present two functions of $\mathbf{U}^{\perp}$ and $\mathbf{L}$ which measure the curvature impact in a tetrad-invariant way.

Let $(u_{\mathcal{O}}, f_A, f_3)$ and $(u_{\mathcal{E}}, g_A, g_3)$ be a pair of adapted tetrads at $\mathcal{O}$ and $\mathcal{E}$ respectively. In the previous papers [1,26] we have introduced the distance slip, i.e., a scalar, dimensionless quantity, defined as

$$\mu = 1 - \frac{\det \Pi^{A'}{}_{B'}}{\det M^{A'}{}_{B}}.$$

Here $\Pi^{A'}{}_{B'}$ is the parallax matrix, describing the linear relation between the perpendicular displacement of the observer $\delta x^{B'}_{\mathcal{O}}$ and the apparent displacement of the image $\delta\theta^{A'} = (u^{\mu'}_{\mathcal{O}} l_{\mathcal{O}\mu'})^{-1} \Delta l^{A'}_{\mathcal{O}}$ of an object at $\mathcal{E}$ on the observer's celestial sphere, expressed in radians

$$\delta\theta^{A'} = -\Pi^{A'}{}_{B'} \delta x^{B'}_{\mathcal{O}}.$$

$M^{A'}{}_{B}$ on the other hand is the magnification matrix, relating the perpendicular displacement of the emitter $\delta x^{B}_{\mathcal{E}}$ to the apparent displacement of the image $\delta\theta^{A'}$ at linear order

$$\delta\theta^{A'} = M^{A'}{}_{B} \delta x^{B}_{\mathcal{E}}.$$

μ measures the spacetime curvature along the LOS by comparing two methods of distance determination to a single object; by parallax and by the angular size. It vanishes in a flat spacetime, or whenever the Riemann tensor along the LOS vanishes [1,26]. From (15) we can prove that this quantity can be calculated directly from $\mathbf{U}$ via the ratio of the determinants of its two transverse submatrices

$$\mu = 1 - \frac{\det U_{\mathcal{O}\mathcal{O}A'B'}}{\det U_{\mathcal{O}\mathcal{E}A'B}} = 1 - \frac{\det U_{\mathcal{O}\mathcal{O}}{}^{A'}{}_{B'}}{\det U_{\mathcal{O}\mathcal{E}}{}^{A'}{}_{B}}. \tag{37}$$

We can also define its counterpart with the roles of $\mathcal{O}$ and $\mathcal{E}$ reversed

$$\nu = 1 - \frac{\det U_{\mathcal{E}\mathcal{E}AB}}{\det U_{\mathcal{O}\mathcal{E}A'B}}. \tag{38}$$

It is also a dimensionless scalar and its physical interpretation is similar to that of μ; it measures the difference of the variations of the viewing angle with respect to displacements at $\mathcal{O}$ and at $\mathcal{E}$, and $\nu = 0$ in a flat spacetime. Both quantities are insensitive to the rescalings of $\mathbf{U}$ and $\mathbf{L}$ mentioned in Sec. III A.

The definitions of μ and ν between events $\mathcal{O}$ and $\mathcal{E}$ can be reformulated in terms of the cross-sectional area of infinitesimal bundles of null geodesics along γ_0 (see [37] for the definition of the infinitesimal bundles of rays). Namely, we have

$$\mu = 1 - \frac{\mathcal{A}_{\mathcal{E}}}{\mathcal{A}_{\mathcal{O}}}, \tag{39}$$

where $\mathcal{A}_{\mathcal{E}}$ and $\mathcal{A}_{\mathcal{O}}$ denote the signed cross-sectional areas of a bundle of rays parallel at $\mathcal{O}$, measured at $\mathcal{E}$ and $\mathcal{O}$ respectively. Without any curvature the bundle of rays remains parallel all along γ_0 and the cross-sectional area is constant. On the other hand, the focusing or defocusing due to the Weyl or Ricci tensors will lead to the variations of the area along γ_0 and thus to nonvanishing μ. An analogous formula for ν reads

$$\nu = 1 - \frac{\tilde{\mathcal{A}}_{\mathcal{O}}}{\tilde{\mathcal{A}}_{\mathcal{E}}}, \tag{40}$$

where the infinitesimal bundle of rays is assumed to be parallel at $\mathcal{E}$ instead of $\mathcal{O}$ and $\tilde{\mathcal{A}}$ denotes its cross-sectional area.

The language of bundles of null geodesics and its evolution along a null geodesic is probably more familiar to most relativists than the bilocal formulation (see, for example, Perlick [37] for a review) so we present this formulation in Appendix G. As a side result we also derive alternative expressions for μ and ν in terms of ODEs involving the shear and expansion of an appropriate bundle.

A. Independence from the adapted tetrads

While the definitions above require introducing two adapted tetrads at $\mathcal{O}$ and $\mathcal{E}$, both these quantities are in fact independent of the choice of these tetrads. More formally, the expressions (37) and (38) define two functions of the components of $\mathbf{U}$ expressed in adapted tetrads: $\mu \equiv \mu(U_{\mathcal{O}\mathcal{O}A'B'}, U_{\mathcal{O}\mathcal{E}A'B})$, $\nu \equiv \nu(U_{\mathcal{E}\mathcal{E}A'B'}, U_{\mathcal{O}\mathcal{E}A'B})$. On the other hand, we may also regard them as functions of the "abstract", tetrad-independent linear mappings $\mathbf{U}$, $\mathbf{L}$, and a pair of adapted orthonormal (ON) tetrads $(u_{\mathcal{O}}, f_A, f_3)$, $(u_{\mathcal{E}}, g_A, g_3)$ in which we have expressed their components,

$$\mu \equiv \mu(\mathbf{U}, \mathbf{L}, (u_{\mathcal{O}}, f_A, f_3), (u_{\mathcal{E}}, g_A, g_3)) \tag{41}$$

$$\nu \equiv \nu(\mathbf{U}, \mathbf{L}, (u_{\mathcal{O}}, f_A, f_3), (u_{\mathcal{E}}, g_A, g_3)). \tag{42}$$

In Appendix F we show explicitly that for any other pair of adapted ON tetrads $(\tilde{u}_{\mathcal{O}}, \tilde{f}_A, \tilde{f}_3)$ and $(\tilde{u}_{\mathcal{E}}, \tilde{g}_A, \tilde{g}_3)$ the values of both μ and ν are the same. We do it by showing that the transverse submatrices of $U_{\mathcal{O}\mathcal{O}}$, $U_{\mathcal{O}\mathcal{E}}$ and $U_{\mathcal{E}\mathcal{E}}$ transform very simply under the change of the adapted ON tetrads, i.e., via two-dimensional rotations of the transverse components. These transformations do not affect the values of the determinants in (37) and (38). This way we prove that μ and ν are adapted tetrad-independent functions of the geometric objects $\mathbf{U}$ and $\mathbf{L}$ only,

$$\mu \equiv \mu(\mathbf{U}, \mathbf{L}) \tag{43}$$

$$\nu \equiv \nu(\mathbf{U}, \mathbf{L}). \tag{44}$$

B. Extracting μ and ν from Q

We have defined μ and ν as a function of $\mathbf{L}$ and $\mathbf{U}$. However, we can show that it is only the components of $\mathbf{U}^{\perp}$ which contribute, i.e.,

$$\mu \equiv \mu(\mathbf{U}^{\perp}, \mathbf{L}) \tag{45}$$

$$\nu \equiv \nu(\mathbf{U}^{\perp}, \mathbf{L}). \tag{46}$$

Define first the four transverse eight-vectors labeled by $\mathcal{O}$, $\mathcal{E}$ and $A = 1, 2$

$$\mathbf{Z}_{\mathcal{O}A} = \begin{pmatrix} f_A^{\mu'} \\ 0 \end{pmatrix}$$
$$\mathbf{Z}_{\mathcal{E}A} = \begin{pmatrix} 0 \\ g_A^{\mu} \end{pmatrix}.$$

The reader may check that all four are orthogonal to $\mathbf{L}$. Now, we have obviously $U_{\mathcal{O}\mathcal{O}AB} = \mathbf{U}(\mathbf{Z}_{\mathcal{O}A}, \mathbf{Z}_{\mathcal{O}B})$, $U_{\mathcal{E}\mathcal{O}AB} = \mathbf{U}(\mathbf{Z}_{\mathcal{E}A}, \mathbf{Z}_{\mathcal{O}B})$, $U_{\mathcal{E}\mathcal{E}AB} = \mathbf{U}(\mathbf{Z}_{\mathcal{E}A}, \mathbf{Z}_{\mathcal{E}B})$. But since all transverse eight-vectors are orthogonal to $\mathbf{L}$, we simply have $U_{\mathcal{O}\mathcal{O}AB} = \mathbf{U}^{\perp}(\mathbf{Z}_{\mathcal{O}A}, \mathbf{Z}_{\mathcal{O}B})$, $U_{\mathcal{E}\mathcal{O}AB} = \mathbf{U}^{\perp}(\mathbf{Z}_{\mathcal{E}A}, \mathbf{Z}_{\mathcal{O}B})$, $U_{\mathcal{E}\mathcal{E}AB} = \mathbf{U}^{\perp}(\mathbf{Z}_{\mathcal{E}A}, \mathbf{Z}_{\mathcal{E}B})$, i.e., we only need $\mathbf{U}^{\perp}$ to calculate them. It follows that we can calculate μ and ν via (37) and (38) just from $\mathbf{U}^{\perp}$. This in turn means that it should be possible to express both scalars by the components of $\mathbf{Q_{ab}}$ expressed in a pair of adapted tetrads.

During the measurement we cannot expect the spatial vectors of the tetrads we use for defining the positions and directions to be aligned precisely along the line of sight. Therefore, we need to relax the requirement for the ON tetrads to be adapted. We will simply assume that after the measurement we are given $\mathbf{Q_{ab}}$ in an *arbitrary* pair of ON (and properly oriented) tetrads $(u_{\mathcal{O}}, e_i)$ and $(u_{\mathcal{E}}, f_j)$. Note that after the measurement of the components of $\mathbf{L}$ we can simply rotate both tetrads to make $e_3^{\mu'}$ and f_3^{μ} aligned with $l_{\mathcal{O}}^{\mu'}$ and $l_{\mathcal{E}}^{\mu}$ and later work in a pair of adapted tetrads. The reader may check that in this case the transverse components of $U_{\mathcal{O}\mathcal{O}}$ and $U_{\mathcal{O}\mathcal{E}}$ and $U_{\mathcal{E}\mathcal{E}}$ coincide with the corresponding components of $Q_{\mathcal{O}\mathcal{O}}$, $Q_{\mathcal{O}\mathcal{E}}$, $Q_{\mathcal{E}\mathcal{E}}$ [see Eqs. (33)–(34)] so we can directly substitute $Q_{\mathcal{O}\mathcal{O}A'B'}$, $Q_{\mathcal{O}\mathcal{E}A'B}$ and $Q_{\mathcal{E}\mathcal{E}AB}$ to (37)–(38). However, the tetrad adjustment can be avoided if we introduce more general, rotationally invariant definitions of μ, ν.

Given the decomposition of $\mathbf{Q_{ab}}$ in not necessarily adapted $(u_{\mathcal{O}}, e_i)$, $(u_{\mathcal{E}}, f_j)$ we define

$$\mu = 1 - \frac{Q_{\mathcal{O}\mathcal{O}i'j'}Q_{\mathcal{O}\mathcal{O}k'l'}\epsilon_{\mathcal{O}}^{i'k'}\epsilon_{\mathcal{O}}^{j'l'}}{Q_{\mathcal{O}\mathcal{E}i'j}Q_{\mathcal{O}\mathcal{E}k'l}\epsilon_{\mathcal{O}}^{i'k'}\epsilon_{\mathcal{E}}^{jl}} \tag{47}$$

$$\nu = 1 - \frac{Q_{\mathcal{E}\mathcal{E}ij}Q_{\mathcal{E}\mathcal{E}kl}\epsilon_{\mathcal{E}}^{ik}\epsilon_{\mathcal{E}}^{jl}}{Q_{\mathcal{O}\mathcal{E}i'j}Q_{\mathcal{O}\mathcal{E}k'l}\epsilon_{\mathcal{O}}^{i'k'}\epsilon_{\mathcal{E}}^{jl}}, \tag{48}$$

with the two antisymmetric, spatial two tensors

$$\epsilon_{\mathcal{O}}^{i'j'} = \frac{1}{l_{\mathcal{O}0'}}\varepsilon_{\mathcal{O}}^{i'j'k'}l_{\mathcal{O}k'} \tag{49}$$

$$\epsilon_{\mathcal{E}}^{ij} = \frac{1}{l_{\mathcal{E}0}}\varepsilon_{\mathcal{E}}^{ijk}l_{\mathcal{E}k}. \tag{50}$$

$\varepsilon_{\mathcal{O}}^{i'j'k'}$ and $\varepsilon_{\mathcal{E}}^{ijk}$ denote here the standard, totally antisymmetric spatial three-tensors, with $\varepsilon_{\mathcal{O}}^{1'2'3'} = \varepsilon_{\mathcal{E}}^{123} = 1$, i.e., the SO(3)-invariant, upper-index spatial volume forms. The expressions on the right hand sides of (47)–(48) are obviously SO(3) invariant in both $N_{\mathcal{E}}$ and $N_{\mathcal{O}}$, and thus they are insensitive to spatial rotations of the tetrads at $\mathcal{O}$ and $\mathcal{E}$. Thus they can also be applied with nonadapted ON tetrads. On the other hand, if we do align the vectors f_3 and g_3 with $l_{\mathcal{O}}$ and $l_{\mathcal{E}}$ respectively, this way both tetrads are adapted, then

$$\epsilon_{\mathcal{O}}^{i'j'} = \begin{cases} 1 & \text{for } i' = 1', j' = 2' \\ -1 & \text{for } i' = 2', j' = 1' \\ 0 & \text{otherwise} \end{cases}$$

$$\epsilon_{\mathcal{E}}^{ij} = \begin{cases} 1 & \text{for } i = 1, j = 2 \\ -1 & \text{for } i = 2, j = 1. \\ 0 & \text{otherwise.} \end{cases}$$

It is now easy to see that in Eqs. (47)–(48), expressed in adapted tetrads, the contractions of $Q_{\mathcal{O}\mathcal{O}}$, $Q_{\mathcal{O}\mathcal{E}}$ and $Q_{\mathcal{E}\mathcal{E}}$ with $\epsilon_{\mathcal{O}}^{i'j'}$ and $\epsilon_{\mathcal{E}}^{ij}$ automatically yield their transverse subdeterminants. These are in turn equal to the corresponding transverse subdeterminants of $U_{\mathcal{O}\mathcal{O}}$, $U_{\mathcal{O}\mathcal{E}}$ and $U_{\mathcal{E}\mathcal{E}}$ because of (33)–(35). Therefore, in a pair of adapted ON tetrads we have (47) equal to (37) and (48) equal to (38).

Summarizing, we have proved that both definitions (47)–(48) and (37)–(38) are equivalent, but the Eqs. (47)–(48) can be used with *any* pair of ON, oriented and time-oriented tetrads at $\mathcal{O}$ and $\mathcal{E}$. In other words, (47)–(48) are fully invariant with respect to proper, orthochronal Lorentz transforms on both geodesic endpoints.

1. Remarks

In a similar way we may introduce fully Lorentz-invariant versions of (37) and (38)

$$\mu = 1 - \frac{U_{\mathcal{O}\mathcal{O}i'j'}U_{\mathcal{O}\mathcal{O}k'l'}\epsilon_{\mathcal{O}}^{i'k'}\epsilon_{\mathcal{O}}^{j'l'}}{U_{\mathcal{O}\mathcal{E}i'j}U_{\mathcal{O}\mathcal{E}k'l}\epsilon_{\mathcal{O}}^{i'k'}\epsilon_{\mathcal{E}}^{jl}} \tag{51}$$

$$\nu = 1 - \frac{U_{\mathcal{E}\mathcal{E}ij}U_{\mathcal{E}\mathcal{E}kl}\epsilon_{\mathcal{E}}^{ik}\epsilon_{\mathcal{E}}^{jl}}{U_{\mathcal{O}\mathcal{E}i'j}U_{\mathcal{O}\mathcal{E}k'l}\epsilon_{\mathcal{O}}^{i'k'}\epsilon_{\mathcal{E}}^{jl}}. \tag{52}$$

Here both scalars are formally expressed as functions of $\mathbf{U}^{\perp}$ and $\mathbf{L}$ as well as a pair of properly oriented ON tetrads,

$$\mu \equiv \mu(\mathbf{U}^{\perp}, \mathbf{L}, (u_{\mathcal{O}}, e_i), (u_{\mathcal{E}}, f_i)) \tag{53}$$

$$\nu \equiv \nu(\mathbf{U}^{\perp}, \mathbf{L}, (u_{\mathcal{O}}, e_i), (u_{\mathcal{E}}, f_i)), \tag{54}$$

with the tetrad dependence effectively spurious, as in (45)–(46).

C. μ and ν and the stress-energy tensor

From (25), (37) and (38) respectively we can show that in the leading order of the expansion in the curvature

$$\mu = 8\pi G \int_{\lambda_{\mathcal{O}}}^{\lambda_{\mathcal{E}}} T_{ll}(\lambda)(\lambda_{\mathcal{E}} - \lambda)\mathrm{d}\lambda + O(\mathrm{Riem}^2) \tag{55}$$

$$\nu = 8\pi G \int_{\lambda_{\mathcal{O}}}^{\lambda_{\mathcal{E}}} T_{ll}(\lambda)(\lambda - \lambda_{\mathcal{O}})\mathrm{d}\lambda + O(\mathrm{Riem}^2), \tag{56}$$

where $T_{ll}(\lambda) \equiv T_{\mu\nu}l^{\mu}l^{\nu}$. Thus both μ and ν effectively depend on a single component of the stress-energy tensor out of the whole Riemann tensor. Equations (55)–(56) are most conveniently derived in a parallel-transported adapted tetrad $(\hat{u}, \hat{e}_A, \hat{e}_3)$, although note that both equations are in fact covariant and therefore valid in all possible tetrads or coordinates. Since the equation for μ has already been derived in [1], we present in detail the derivation of Eq. (56) for ν.

From (24) and (25) we get the first two terms of expansion of the transverse components of $U_{\mathcal{E}\mathcal{E}}$ and $U_{\mathcal{O}\mathcal{E}}$ in the powers of the Riemann tensor

$$U_{\mathcal{E}\mathcal{E}\bar{A}\bar{B}} = -\Delta\lambda^{-1}\delta_{\bar{A}\bar{B}} - \int_{\lambda_{\mathcal{O}}}^{\lambda_{\mathcal{E}}} R_{\bar{A}\bar{\mu}\bar{\nu}\bar{B}}(\lambda)l^{\bar{\mu}}l^{\bar{\nu}}\frac{(\lambda - \lambda_{\mathcal{O}})^2}{\Delta\lambda^2}\mathrm{d}\lambda + O(\mathrm{Riem}^2)$$

$$U_{\mathcal{O}\mathcal{E}\bar{A}\bar{B}} = \Delta\lambda^{-1}\delta_{\bar{A}\bar{B}} - \int_{\lambda_{\mathcal{O}}}^{\lambda_{\mathcal{E}}} R_{\bar{A}\bar{\mu}\bar{\nu}\bar{B}}(\lambda)l^{\bar{\mu}}l^{\bar{\nu}}\frac{(\lambda_{\mathcal{E}} - \lambda)(\lambda - \lambda_{\mathcal{O}})}{\Delta\lambda^2}\mathrm{d}\lambda + O(\mathrm{Riem}^2).$$

From this we get the expansion of the determinants

$$\det U_{\mathcal{E}\mathcal{E}\bar{A}\bar{B}} = \Delta\lambda^{-2} + \Delta\lambda^{-1}\int_{\lambda_{\mathcal{O}}}^{\lambda_{\mathcal{E}}} R^{\bar{A}}{}_{\bar{\mu}\bar{\nu}\bar{A}}(\lambda) l^{\bar{\mu}} l^{\bar{\nu}} \frac{(\lambda-\lambda_{\mathcal{O}})^2}{\Delta\lambda^2}\,\mathrm{d}\lambda + O(\mathrm{Riem}^2)$$
$$\det U_{\mathcal{O}\mathcal{E}\bar{A}\bar{B}} = \Delta\lambda^{-2} - \Delta\lambda^{-1}\int_{\lambda_{\mathcal{O}}}^{\lambda_{\mathcal{E}}} R^{\bar{A}}{}_{\bar{\mu}\bar{\nu}\bar{A}}(\lambda) l^{\bar{\mu}} l^{\bar{\nu}} \frac{(\lambda_{\mathcal{E}}-\lambda)(\lambda-\lambda_{\mathcal{O}})}{\Delta\lambda^2}\,\mathrm{d}\lambda + O(\mathrm{Riem}^2).$$

In the next step we simplify the integrands. Note that for a null vector $l^{\bar{\mu}}$ the contraction of the Riemann over the two transverse indices is equal to the full contraction over the whole space [1], i.e., $R^{\bar{A}}{}_{\bar{\mu}\bar{\nu}\bar{A}} l^{\bar{\mu}} l^{\bar{\nu}} = R^{\bar{\alpha}}{}_{\bar{\mu}\bar{\nu}\bar{\alpha}} l^{\bar{\mu}} l^{\bar{\nu}} = -R_{\bar{\mu}\bar{\nu}} l^{\bar{\mu}} l^{\bar{\nu}}$. Moreover, from the Einstein equations

$$R_{\mu\nu} - \frac{1}{2} R g_{\mu\nu} = 8\pi G T_{\mu\nu} - \Lambda g_{\mu\nu},$$

it is easy to show that $R_{\bar{\mu}\bar{\nu}} l^{\bar{\mu}} l^{\bar{\nu}} = 8\pi G T_{\bar{\mu}\bar{\nu}} l^{\bar{\mu}} l^{\bar{\nu}}$, i.e., only the matter stress-energy tensor contributes to both integrals, while the cosmological constant drops out, thus

$$\det U_{\mathcal{E}\mathcal{E}\bar{A}\bar{B}} = \Delta\lambda^{-2} - \Delta\lambda^{-1} 8\pi G\int_{\lambda_{\mathcal{O}}}^{\lambda_{\mathcal{E}}} T_{ll}(\lambda) \frac{(\lambda-\lambda_{\mathcal{O}})^2}{\Delta\lambda^2}\,\mathrm{d}\lambda + O(\mathrm{Riem}^2)$$
$$\det U_{\mathcal{O}\mathcal{E}\bar{A}\bar{B}} = \Delta\lambda^{-2} + \Delta\lambda^{-1} 8\pi G\int_{\lambda_{\mathcal{O}}}^{\lambda_{\mathcal{E}}} T_{ll}(\lambda) \frac{(\lambda_{\mathcal{E}}-\lambda)(\lambda-\lambda_{\mathcal{O}})}{\Delta\lambda^2}\,\mathrm{d}\lambda + O(\mathrm{Riem}^2),$$

From this and (38) we get the expansion of ν in the form of

$$\nu = \Delta\lambda 8\pi G\int_{\lambda_{\mathcal{O}}}^{\lambda_{\mathcal{E}}} T_{ll}(\lambda)\left(\frac{(\lambda-\lambda_{\mathcal{O}})^2}{\Delta\lambda^2} + \frac{(\lambda_{\mathcal{E}}-\lambda)(\lambda-\lambda_{\mathcal{O}})}{\Delta\lambda^2}\right)\mathrm{d}\lambda + O(\mathrm{Riem}^2). \tag{57}$$

Simplifying the integrand we obtain (56). Equation (55) for μ can be derived the same way from the analogous expansion of $U_{\mathcal{O}\mathcal{O}\bar{A}\bar{B}}$ in the powers of $R^{\mu}{}_{\nu\alpha\beta}$. However, note that there is also a short-cut reasoning leading directly from (56) to (55); since ν is simply the same quantity as μ, but with the role of the geodesic endpoints $\mathcal{O}$ and $\mathcal{E}$ reversed, we can simply obtain (55) from (56) by consistently swapping the $\mathcal{O}$ and $\mathcal{E}$ subscripts on the right hand side.

We also point out that the expansions (55)–(56) in the curvature contain no free term. It follows that $\mu = \nu = 0$ in the absence of curvature.

V. EXPANSION IN SMALL PARAMETERS

We will now compare the magnitude of various terms in Eq. (9) governing the TOAs in a typical astrophysical situation. We assume that the curvature tensor is of the scale of $\mathcal{R}^{-2}$, where $\mathcal{R}$ is the curvature radius scale and $\mathbf{X}$ is of the order of the size of $N_{\mathcal{O}}$ and $N_{\mathcal{E}}$, denoted by L. For simplicity we pick the affine parameter λ normalized in the receivers' frame, i.e., $l_{\mathcal{O}\mu} u^{\mu}_{\mathcal{O}} = 1$. In this case we can also assume that $\lambda_{\mathcal{O}} = 0$ and $\lambda_{\mathcal{E}} = D$, where D is the affine distance from $\mathcal{O}$ to $\mathcal{E}$ in the receivers' frame.

We introduce the dimensionless counterparts of the objects appearing in (9), (24) and (25), denoted by tilde

$$\lambda = D\tilde{\lambda} \tag{58}$$

$$\mathbf{X} = L\tilde{\mathbf{X}} \tag{59}$$

$$\mathbf{L} = \tilde{\mathbf{L}} \tag{60}$$

$$l^{\bar{\mu}} = \tilde{l}^{\bar{\mu}} \tag{61}$$

$$R^{\bar{\mu}}{}_{\bar{\nu}\bar{\alpha}\bar{\beta}} = \mathcal{R}^{-2}\tilde{R}^{\bar{\mu}}{}_{\bar{\nu}\bar{\alpha}\bar{\beta}}. \tag{62}$$

Then (9) can be recast in the following form:

$$0 = L\tilde{\mathbf{L}}(\tilde{\mathbf{X}}) + \frac{1}{2}\left(\frac{L^2}{D}\right)\tilde{\mathbf{U}}^{(0)}(\tilde{\mathbf{X}},\tilde{\mathbf{X}}) + \frac{1}{2}\left(\frac{DL^2}{\mathcal{R}^2}\right)\tilde{\mathbf{U}}^{(1)}(\tilde{\mathbf{X}},\tilde{\mathbf{X}}), \tag{63}$$

with the dimensionless expansion for $\mathbf{U}$ given by

$$\tilde{\mathbf{U}}^{(0)} = D\mathbf{U}^{(0)} = \begin{pmatrix} -\eta_{\bar{\mu}\bar{\nu}} & \eta_{\bar{\mu}\bar{\nu}} \\ \eta_{\bar{\mu}\bar{\nu}} & -\eta_{\bar{\mu}\bar{\nu}} \end{pmatrix} \tag{64}$$

$$\tilde{\mathbf{U}}^{(1)} = \frac{\mathcal{R}^2}{D}\mathbf{U}^{(1)} = \int_0^1 \mathrm{d}\tilde{\lambda}\tilde{R}^{\bar{\mu}}{}_{\bar{\nu}\bar{\alpha}\bar{\beta}}(\tilde{r})l^{\bar{\nu}}l^{\bar{\alpha}}P(\tilde{\lambda}), \tag{65}$$

where $P(\tilde{\lambda})$ denotes the appropriate second order polynomials for each submatrix [see Eq. (25)]. Dividing the resulting equation by L we obtain

$$0=\tilde{\mathbf{L}}(\tilde{\mathbf{X}})+\frac{1}{2}\left(\frac{L}{D}\right)\tilde{\mathbf{U}}^{(0)}(\tilde{\mathbf{X}},\tilde{\mathbf{X}})+\frac{1}{2}\left(\frac{L}{D}\right)\left(\frac{D}{\mathcal{R}}\right)^2\tilde{\mathbf{U}}^{(1)}(\tilde{\mathbf{X}},\tilde{\mathbf{X}}). \tag{66}$$

In this form the hierarchy between the three terms is evident. Assuming $L \ll D \ll \mathcal{R}$ (physically realistic case) we see that the first term, responsible for the LOS effects, is $O(1)$ and thus dominating over the other two. The finite distance corrections term, responsible for the "flat" transverse effects in TOAs, scales like the ratio of the size L of the regions $N_{\mathcal{O}}$, $N_{\mathcal{E}}$ and their mutual distance D. Finally, the curvature term is a small correction upon the finite distance term, smaller again by the factor $D^2/\mathcal{R}^2$. We also see that the curvature correction grows with the distance D between the two regions. This is expected, as the signals pick up more and more curvature corrections as they propagate through the curved spacetime. The second term, on the other hand, decreases as D grows.

We may now solve (66) for $\tilde{\mathbf{X}}^0$, as in Sec. III C, this time treating L/D and $D^2/\mathcal{R}^2$ as legitimate small parameters. We get the dimensionless version of Eq. (31)

$$\begin{aligned}\tilde{\mathbf{X}}^{\mathbf{0}} = &-\tilde{\mathbf{L}}_{\mathbf{a}}\tilde{\mathbf{X}}^{\mathbf{a}} - \left(\frac{L}{D}\right)\frac{1}{2}(\tilde{\mathbf{U}}^{(0)}_{\mathbf{ab}} - 2\tilde{\mathbf{U}}^{(0)}_{\mathbf{0(a}}\tilde{\mathbf{L}}_{\mathbf{b})} + \tilde{\mathbf{U}}^{(0)}_{\mathbf{00}}\tilde{\mathbf{L}}_{\mathbf{a}}\tilde{\mathbf{L}}_{\mathbf{b}})\tilde{\mathbf{X}}^{\mathbf{a}}\tilde{\mathbf{X}}^{\mathbf{b}}\\ &- \left(\frac{L}{D}\right)\left(\frac{D}{\mathcal{R}}\right)^2\frac{1}{2}(\tilde{\mathbf{U}}^{(1)}_{\mathbf{ab}} - 2\tilde{\mathbf{U}}^{(1)}_{\mathbf{0(a}}\tilde{\mathbf{L}}_{\mathcal{R}\,\mathbf{b})} + \tilde{\mathbf{U}}^{(1)}_{\mathbf{00}}\tilde{\mathbf{L}}_{\mathbf{a}}\tilde{\mathbf{L}}_{\mathbf{b}})\tilde{\mathbf{X}}^{\mathbf{a}}\tilde{\mathbf{X}}^{\mathbf{b}} + \text{h.o.t.},\end{aligned} \tag{67}$$

where the higher order terms (h.o.t.) include, among other things, terms with higher powers of the small parameters, i.e., $O((\frac{L}{D})^2)$, $O((\frac{D}{\mathcal{R}})^3)$ or their products, which arise when we solve (66) for $\tilde{\mathbf{X}}^{\mathbf{0}}$. Note that if the curvature corrections are sufficiently small while L is large enough it may happen that $(\frac{L}{D})^2$ is comparable or larger than $(\frac{L}{D})(\frac{D}{\mathcal{R}})^2$. In this case we may need to include the second or even higher power terms in $\frac{L}{D}$ in Eq. (67) and in the data analysis. They are of third and higher order in $\tilde{\mathbf{X}}$, i.e., of the form $(\frac{L}{D})^2 Q^{(3)}_{\mathbf{abc}}\tilde{\mathbf{X}}^{\mathbf{a}}\tilde{\mathbf{X}}^{\mathbf{b}}\tilde{\mathbf{X}}^{\mathbf{c}}$ etc. Their presence complicates the inverse problem and thus also the measurement μ and ν, but the general idea should still remain applicable; with sufficiently many sampling points $\tilde{\mathbf{X}}^{\mathbf{a}}_{(i)}$ over which we measure the TOAs we should be able to obtain exactly also the third or higher order terms in $\tilde{\mathbf{X}}^{\mathbf{a}}$ in the Taylor expansion (67), since the third order tangent surface is also parametrized by a finite number of parameters.

We will not discuss here the inverse problem with a longer Taylor expansions in detail. Let us just note that the number of additional unknown coefficients to be determined in the process is not as large as one might think at first. As an example, note that the term $Q^{(3)}_{\mathbf{abc}}$ represents the higher order corrections to the TOA in a *flat* spacetime, with no curvature corrections. Thus we may expect that this term, just like the one arising from $\mathbf{U}^{(0)}$, has a fairly simple, universal form in a parallel propagated, adapted ON tetrad, as in Eq. (24). In a generic situation this term can be parametrized by L/D and six numbers relating the orthonormal tetrads on $\mathcal{O}$ and $\mathcal{E}$ we use (this follows from the Lorentz invariance of a flat spacetime). This means that the effective number of new, free parameters we need to include with a third order Taylor expansion is at most seven.

A. Particular case: weak field limit with nonrelativistic dust

Consider a spacetime filled with a static or very slowly varying dust distribution, i.e., $T_{00} = \rho(x^i)$, T_{0i} and T_{ij} negligible. We assume that the weak field limit of GR holds, i.e., $g_{\mu\nu} = \eta_{\mu\nu} + h_{\mu\nu}$ with $h_{\mu\nu}$ small. Let the receivers' frame $u^\mu_{\mathcal{O}}$ coincide fairly precisely with the rest frame of the dust. As before, let λ denote the affine distance along γ_0 normalized with respect to $u^\mu_{\mathcal{O}}$.

Note that in this case we have $\mu, \nu = O(h)$. It follows that in the leading order in the metric perturbation $h_{\mu\nu}$ we may approximate γ_0 in the integration by an unperturbed geodesic (i.e., a null straight line in $\eta_{\mu\nu}$) and the affine parameter by the radial coordinate r centered at $\mathcal{O}$; corrections to μ and ν will be at most $O(h^2)$. The integrals (55) and (56) take now the form of

$$\mu = 8\pi G\int_0^D \rho(r)(D-r)\mathrm{d}r + \text{h.o.t.} \tag{68}$$

$$\nu = 8\pi G\int_0^D \rho(r)r\mathrm{d}r + \text{h.o.t.}, \tag{69}$$

with the integration performed over a straight radial line. The higher order terms are either $O(h^2)$ or $O(\beta\cdot h)$, where $\beta = v/c$ is the relative velocity of the receivers and the dust, and we consider them negligible.

The dimensionless parameters μ and ν are not the most convenient tool to describe the mass distribution between $\mathcal{O}$ and $\mathcal{E}$, but with the help of the equations above they can be transformed into quantities with a more clear physical interpretation. We first note that their sum gives the integral of $\rho(r)$, or the zeroth moment of the mass distribution along the LOS

$$\mu + \nu = 8\pi G D \int_0^D \rho(r)\mathrm{d}r,$$

providing this way the true tomography of the matter distribution $\rho(x^i)$, unlike μ or ν themselves, which provide density integrals with linear kernels. It also follows that this sum can be translated directly into the average matter density along LOS, defined by

$$\langle\rho\rangle = \frac{1}{D}\int_0^D \rho(r)\mathrm{d}r.$$

Namely, we have the relation

$$\langle\rho\rangle = \frac{\mu+\nu}{8\pi G D^2}. \tag{70}$$

On top of that, μ and ν contain the information about the first moment of the mass distribution along the LOS, related to the position of its center of mass (COM). Namely, consider the dimensionless parameter α_{CM}

$$\alpha_{\mathrm{CM}} = \frac{\int_0^D \rho(r)\frac{r}{D}\mathrm{d}r}{\int_0^D \rho(r)\mathrm{d}r}.$$

It determines the position of the COM along γ_0; α_{CM} is equal to 0 for a mass distribution centered at $\mathcal{O}$, 1 for a mass distribution centered at $\mathcal{E}$ and $\frac{1}{2}$ if it has its COM at the midpoint. One can now prove using (68)–(69) that

$$\alpha_{\mathrm{CM}} = \frac{\nu}{\mu+\nu}. \tag{71}$$

Equations (70) and (71) show how to relate μ, ν and the distance D between $\mathcal{E}$ and $\mathcal{O}$ to physically more interesting quantities; the directional average of the mass distribution and the COM of this distribution.

Note that while Eq. (70) requires formally the normalized affine distance D between $\mathcal{O}$ and $\mathcal{E}$, we may use instead the angular diameter distance D_{ang} or the parallax distance D_{par} in the receivers' frame which is much simpler to measure in the astronomical context. These distance measures differ at most by $O(h)$, so in the leading order they lead to the same value of $\langle\rho\rangle$.

B. Estimating the signal from a small background matter density

We will now estimate the additional TOA variations caused by a small mass density along the LOS in the weak field approximation. This estimate may also serve as an indicator of the minimal precision of pulse timing required for detection of the mass density. We consider here a simplified scenario in which the spacetime is filled with a tiny, constant background mass density $\rho(x) \equiv \rho$ of pressureless matter. We perform the measurement of μ and ν along the line of sight between the two groups of clocks of size L and separated by the distance of D. The idea is now to estimate the contribution coming from the constant stress-energy tensor $T_{00} = \rho$, $T_{0i} = T_{ij} = 0$ to the TOAs in the form of (31) or, equivalently, of (67), ignoring the Weyl or the cosmological constant terms since their contributions will cancel out anyway.

Since the stress-energy tensor $T_{\mu\nu}$ is of the order of ρ, its contribution to the Ricci tensor is $R_{\mu\nu} \sim 8\pi G\rho$. This in turn corresponds to the curvature radius $\mathcal{R}^2 = (8\pi G\rho)^{-1}$ in the terminology of Sec. V. It follows now from (67) that the pressureless matter contribution to the dimensionless TOA $\tilde{\mathbf{X}}^{\mathbf{0}}$, contained in the third term on the right-hand side, is of the order of $(\frac{L}{D})(\frac{D}{\mathcal{R}})^2 = (\frac{L}{D})4\pi G\rho D^2 = 4\pi G\rho DL$. Returning to the dimensional TOA $\mathbf{X}^{\mathbf{0}} = L\tilde{\mathbf{X}}^{\mathbf{0}}$ we obtain the estimate $\mathbf{X}^{\mathbf{0}} \sim 4\pi G\rho DL^2$ for the TOA variations induced by the mass density along the LOS. For comparison we include here the analogous estimate for the finite distance variations, which are of the order of L^2/D.

This estimate can be also reformulated as a simple rule of thumb for the TOA variations. Namely, note that $4\pi\rho DL^2$ is simply the total mass M_{tot} contained in a thin 3D cylinder of radius L and height D, connecting $N_{\mathcal{O}}$ and $N_{\mathcal{E}}$ along the spatial dimensions. With this interpretation $4\pi G\rho DL^2$ is simply the half of the Schwarzschild radius corresponding to M_{tot}. The result may therefore be rephrased as follows: the TOA variations caused by the matter along the LOS, expressed in units of length, are of the order of the Schwarzschild radius of the total mass contained in a spatial cylinder connecting $N_{\mathcal{O}}$ and $N_{\mathcal{E}}$ whose radius L is equal to the physical size of each of the two clock systems. Note also that the same number may serve as an estimate of the precision of time measurements required to detect the mass density background of the order of ρ.

C. Summary of the results

We will pause here to give a short summary of the most important results of Secs. II–V.

1. Local variations of the TOAs in the vicinity of two points $\mathcal{E}$ and $\mathcal{O}$ can be expanded in a Taylor series consisting of the leading order, linear effects and the quadratic effects in the displacements [see Eq. (9) or (31)]. The linear effects involve the line of sight delays (Rømer delays) as well as the frequency shifts

and are governed by the components of the eight-vector $\mathbf{L}$. The quadratic effects involve, among other things, the transverse variations and are governed by the quadratic form $\mathbf{U}^{\perp}$. They consist of the finite distance effects, present also in flat spacetimes and are related to the distance between the endpoints, as well as the curvature effects which are usually much smaller and superimposed on the former. This approach to the TOA variations has a neat geometric interpretation of approximating the LSC $\Sigma \in M \times M$ by its second order tangent at $(\mathcal{O}, \mathcal{E})$, defined by the normal vector $\mathbf{L}$ and the extrinsic curvature $\mathbf{U}^{\perp}$.

2. $\mathbf{U}^{\perp}$ can be expressed as a functional of the Riemann tensor along the LOS, via an ODE in a parallel-transported tetrad [Eqs. (19), (21)]. It can therefore be used to measure the curvature impact on the propagation of signals.
3. The linear and quadratic order effects are effectively parametrized by a finite set of numbers, i.e., the independent components of $\mathbf{L}$ and $\mathbf{U}^{\perp}$, expressed in a chosen pair of locally flat, orthonormal coordinates. By sampling the TOAs over a sufficient number of evenly distributed points we can determine all of these components and thus reconstruct the shape of the LSC.
4. In order to quantify the curvature effects we have defined two scalar, dimensionless functions μ and ν of the components of $\mathbf{L}$ and $\mathbf{U}^{\perp}$ [see Eqs. (33)–(35) and (47)–(48)]. They are both selectively sensitive to the curvature corrections present in $\mathbf{U}^{\perp}$ and insensitive to the finite distance effects, i.e., they both vanish identically in a flat spacetime. Moreover, both quantities are invariant with respect to the proper orthochronous Lorentz transformations of the coordinates on both endpoints (see Appendix F).
5. For short distances, at the leading order expansion in the curvature tensor, both μ and ν depend only on integrals of the stress-energy tensor [Eqs. (55)–(56)], with the contributions from the Weyl tensor (tidal forces) and the cosmological constant vanishing identically.
6. Lorentz invariance implies the insensitivity of the measurement to the states of motion and the angular positions (or attitudes) of the two clock ensembles; after the measurements we may perform the calculations in the internal ON tetrads of the ensembles, recover the components of $\mathbf{L}$ and $\mathbf{U}^{\perp}$ in these tetrads and calculate the two invariants μ and ν. Their invariance under passive Lorentz transforms of the coordinates implies thus the invariance with respect to active Lorentz boosts and spatial rotations of the ensembles. On the other hand, the independence from the Weyl tensor implies the insensitivity of the measurement to the influence of masses off the LOS.
7. The values of μ and ν can be finally related to the zeroth and first moment of the mass density distribution along the LOS [Eqs. (70) and (71)], yielding a directional, tomographic measurement of the mass distribution $\rho(x^i)$.

VI. AN EXAMPLE OF THE MEASUREMENT PROTOCOL

As a proof of concept, we will now present a particular method of measurement of μ and ν with the help of two ensembles of clocks capable of exchanging electromagnetic signals. We stress that this is not the only possible measurement protocol based on the geometric principles introduced in this paper. The setup we present is in fact rather wasteful when it comes to resources; it is neither optimal with respect to the number of clocks involved, nor with respect the total number of measurements performed, since, as we will see, only ≈10% of measured TOAs are finally used in the data processing stage. However, the peculiar geometry of both ensembles we consider here allows for a fairly straightforward reconstruction of the components of $\mathbf{L}$ and $\mathbf{Q}$ from the TOAs.

Assume we have at our disposal two sets of clocks, 13 receivers $(O_1, \ldots, O_{13})$ in $N_{\mathcal{O}}$ and 13 emitters $(E_1, \ldots, E_{13})$ in $N_{\mathcal{E}}$. The clocks within each group are in free fall, comoving and synchronized, i.e., all clocks in one group give the same readings along the simultaneity hypersurfaces of their rest frames, respectively $u_{\mathcal{O}}$ or $u_{\mathcal{E}}$. The readings of the clocks will be denoted by $t_{\mathcal{O}}$ and $t_{\mathcal{E}}$. The relative motion of the two groups may be arbitrary and is considered uncontrolled by the experimentator.

Let L define the size of each group. We position 13 emitters and 13 receivers according to Table II, see also Fig. 5. Their positions are measured with respect to two OLF coordinate systems at $N_{\mathcal{O}}$ and $N_{\mathcal{E}}$ respectively, constructed from two orthonormal, oriented tetrads, $(u_{\mathcal{O}}, e_i)$ at $\mathcal{O}$ and $(u_{\mathcal{E}}, f_i)$ and $\mathcal{E}$. Therefore, the attitude of both groups of clocks with respect to each other, with respect to the line of sight, or with respect to any other external reference frame, is also arbitrary and will be treated as an uncontrolled variable.

TABLE II. Arrangement of both the emitters and the receivers described in their local spatial coordinates.

1	(0,0,0)	8	$(L, L, 0)$
2	$(L, 0, 0)$	9	$(-L, -L, 0)$
3	$(-L, 0, 0)$	10	$(L, 0, L)$
4	$(0, L, 0)$	11	$(-L, 0, -L)$
5	$(0, -L, 0)$	12	$(0, L, L)$
6	$(0, 0, L)$	13	$(0, -L, -L)$
7	$(0, 0, -L)$	...	...

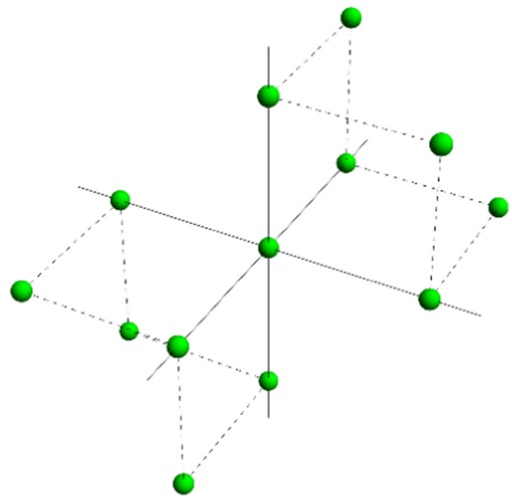

FIG. 5. Arrangement of the emitters and the receivers within their respective groups, given in their locally flat, comoving frame. We present here the receivers. The three solid lines are the X, Y, and Z axes. O_1 is the central receiver, O_2–O_7 are positioned pairwise at the opposite sides at the three axes at the distance of L from the center. O_8–O_{13} lie on the three normal planes of the axes.

All emitters now send time- and source-stamped signals at three equally spaced moments in time, corresponding to the readings $t_{\mathcal{E}} - L$, $t_{\mathcal{E}}$, and $t_{\mathcal{E}} + L$. All signals are then received by all 13 receivers, their origins are recognized and their precise TOAs with respect to the receivers' time $t_{\mathcal{O}}$ are recorded. This yields $13 \times 13 \times 3 = 507$ measurements of TOAs between precisely localized pairs of events. After the measurement we extract the signal from the data using the procedure sketched below, effectively using only 57 of them.

In the first step we use the emission time $t_{\mathcal{E}}$ of the second group of signals and the TOA $t_{\mathcal{O}}$, the second signal sent from the central emitter E_1 and registered by the central receiver O_1, to define the respective offsets for all time measurements by the emitters and the receivers. By subtracting these offsets from all readings we obtain the time coordinates $\delta x^0_{\mathcal{E}}$ and $\delta x^{0'}_{\mathcal{O}}$ respectively from the times registered by the clocks in each group, with the reference points $\mathcal{E}, \mathcal{O}$ defined by the emission and the reception of the second signal by the central clocks of the ensembles. This way we define also the fiducial null geodesic γ_0 through these points.

We now pick a set of 56 other times of arrival which we will further use to determine $\mathbf{L}$ and $\mathbf{Q}$. As we have seen in Sec III C, the TOAs are associated to seven-dimensional subvectors defining the event of emission in $N_{\mathcal{E}}$ and the spatial position of the receivers $N_{\mathcal{O}}$. Therefore the subvectors consisting of those components may be used for indexing the individual TOA measurements. We now need to define a set V of subvectors we will use for the measurement. We first take the TOAs related to the following 14 subvectors $\mathbf{H^a}$ with only one nonvanishing component,

$$\mathbf{H}^{\mathbf{a}}_{k+} = \begin{cases} 0 & \text{for } \mathbf{a} \neq k \\ L & \text{for } \mathbf{a} = k \end{cases}$$

$$\mathbf{H}^{\mathbf{a}}_{k-} = \begin{cases} 0 & \text{for } \mathbf{a} \neq k \\ -L & \text{for } \mathbf{a} = k \end{cases}.$$

They correspond to the second signal emitted by E_1 at $\mathcal{E}$ and received by the receivers O_2–O_7, the second signals emitted by E_2–E_7 and received by O_1 and the first and third signals emitted by E_1 and received by O_1. We also define 42 subvectors with two nonvanishing components,

$$\mathbf{H}^{\mathbf{a}}_{k+,l+} = \begin{cases} 0 & \text{for } \mathbf{a} \neq k \quad \text{and} \quad \mathbf{a} \neq l \\ L & \text{for } \mathbf{a} = k \quad \text{or} \quad \mathbf{a} = l \end{cases}$$

$$\mathbf{H}^{\mathbf{a}}_{k-,l-} = \begin{cases} 0 & \text{for } \mathbf{a} \neq k \quad \text{and} \quad \mathbf{a} \neq l \\ -L & \text{for } \mathbf{a} = k \quad \text{or} \quad \mathbf{a} = l \end{cases}.$$

We assume here that $k \neq l$ and for the sake of unique indexing we follow the convention that $k < l$ in the subscripts when describing them. The subvectors correspond to the second signal from E_1 received by O_8–O_{13}, the second signals from E_8–E_{13} received by O_1, some of the second signals form O_2–O_7 received by E_2–E_7, some of the first and third signals from E_2–E_7 received by O_1, and the first and third signals from E_1 received by some of the receivers O_2–O_7.

These subvectors, taken together with the measured TOA of the signal $\tau(\mathbf{H}^{\mathbf{a}}_{*})$, constitute the full eight-dimensional vectors $\mathbf{H}_{*} \in T_{\mathcal{O}}M \oplus T_{\mathcal{E}}M$, i.e.,

$$\mathbf{H}_{*} = \begin{pmatrix} \tau(\mathbf{H}^{\mathbf{a}}_{*}) \\ \mathbf{H}^{\mathbf{a}}_{*} \end{pmatrix}$$

or, equivalently, $\mathbf{H}^{\mathbf{0}}_{*} = \tau(\mathbf{H}^{\mathbf{a}}_{*})$, with $*$ denoting any of the subscripts for vectors in V, as defined above.

The set V contains $2 \times 7 + 21 \times 2 = 56$ subvectors and this is the number of TOAs we will use. It turns out that with this particular placement of the emitters and receivers it is possible to obtain exact expressions for the components of $\mathbf{L}$ and $\mathbf{Q}$ in the pair of ON tetrads $(u_{\mathcal{O}}, e_i)$ and $(u_{\mathcal{E}}, f_j)$ from the TOAs. We first note that the set V is centrally symmetric with respect to the origin. Namely, for every $\mathbf{H^a} \in V$ we also have $-\mathbf{H^a} \in V$, i.e., all sub-vectors from V can be arranged in pairs related by a point reflection through 0 [48]. Indeed, we have $-\mathbf{H}^{\mathbf{a}}_{\mathbf{k}+} = \mathbf{H}^{\mathbf{a}}_{\mathbf{k}-}$ and $-\mathbf{H}^{\mathbf{a}}_{\mathbf{k}+,\mathbf{l}+} = \mathbf{H}^{\mathbf{a}}_{\mathbf{k}-,\mathbf{l}-}$. This feature is important, because it simplifies greatly the problem of solving the system (31) separately for the components of $\mathbf{L}$ and $\mathbf{Q}$. Note that the linear and quadratic terms in (31) [or equivalently in (32)] differ in the way they behave when we flip the signs of all components of the subvector $\mathbf{X^a}$: $\mathbf{L_a X^a} = -\mathbf{L_a}(-\mathbf{X^a})$, but $\mathbf{Q_{ab} X^a X^b} = \mathbf{Q_{ab}}(-\mathbf{X^a})(-\mathbf{X^b})$.

The idea now is to make a direct use of this fact in order to decouple the equations governing the linear and quadratic terms.

We calculate from (31) the difference between the TOAs for the opposite subvectors $\mathbf{H}^{\mathbf{a}}_{\mathbf{k}+}$ and $-\mathbf{H}^{\mathbf{a}}_{\mathbf{k}+} = \mathbf{H}^{\mathbf{a}}_{\mathbf{k}-}$,

$$\frac{1}{2}(\tau(\mathbf{H}^{\mathbf{a}}_{k+}) - \tau(\mathbf{H}^{\mathbf{a}}_{k-})) = -\mathbf{L}_{\mathbf{a}}\mathbf{H}^{\mathbf{a}}_{k+} = -L\mathbf{L}_{\mathbf{k}}.$$

Thus we have obtained an exact expression for the components of $\mathbf{L}_{\mathbf{a}}$

$$\mathbf{L}_{\mathbf{k}} = -\frac{L^{-1}}{2}(\tau(\mathbf{H}^{\mathbf{a}}_{k+}) - \tau(\mathbf{H}^{\mathbf{a}}_{k-})), \tag{72}$$

with $\mathbf{k} = \mathbf{1}\ldots\mathbf{7}$ (recall that the missing component $\mathbf{L}_{\mathbf{0}}$ is equal to 1 due to the gauge condition (30) we have imposed in order to fix the normalization of $\mathbf{L}$ and $\mathbf{U}$).

We then calculate in the same way the average of the TOAs for the opposite subvectors

$$\frac{1}{2}(\tau(\mathbf{H}^{\mathbf{a}}_{k+}) + \tau(\mathbf{H}^{\mathbf{a}}_{k-})) = -\frac{1}{2}\mathbf{Q}_{\mathbf{ab}}\mathbf{H}^{\mathbf{a}}_{k,+}\mathbf{H}^{\mathbf{b}}_{k,+} = -\frac{L^2}{2}\mathbf{Q}_{\mathbf{kk}},$$

obtaining the relation

$$\mathbf{Q}_{\mathbf{kk}} = -L^{-2}(\tau(\mathbf{H}^{\mathbf{a}}_{k+}) + \tau(\mathbf{H}^{\mathbf{a}}_{k-})). \tag{73}$$

Finally we obtain the mixed terms $\mathbf{Q}_{\mathbf{kl}}$ with the help of the polarization identity

$$\mathbf{Q}(\mathbf{A}, \mathbf{B}) = \frac{1}{2}(\mathbf{Q}(\mathbf{A}+\mathbf{B}, \mathbf{A}+\mathbf{B}) - \mathbf{Q}(\mathbf{A}, \mathbf{A}) - \mathbf{Q}(\mathbf{B}, \mathbf{B}))$$

applied to $\mathbf{A}^{\mathbf{a}} = \mathbf{H}^{\mathbf{a}}_{k+}$ and $\mathbf{B}^{\mathbf{a}} = \mathbf{H}^{\mathbf{a}}_{l+}$ with $k < l$,

$$\begin{aligned}\mathbf{Q}_{\mathbf{kl}} &= L^{-2}\mathbf{Q}_{\mathbf{ab}}\mathbf{H}^{\mathbf{a}}_{k+}\mathbf{H}^{\mathbf{b}}_{l+} \\ &= \frac{L^{-2}}{2}(\mathbf{Q}_{\mathbf{ab}}\mathbf{H}^{\mathbf{a}}_{k+,l+}\mathbf{H}^{\mathbf{b}}_{k+,\quad l+} - \mathbf{Q}_{\mathbf{ab}}\mathbf{H}^{\mathbf{a}}_{k+}\mathbf{H}^{\mathbf{b}}_{k+} \\ &\quad - \mathbf{Q}_{\mathbf{ab}}\mathbf{H}^{\mathbf{a}}_{l+}\mathbf{H}^{\mathbf{b}}_{l+}).\end{aligned}$$

The three quadratic terms in the brackets can then be related to the appropriate averages of the TOAs for pairs of opposite subvectors, just like before. We obtain finally

$$\begin{aligned}\mathbf{Q}_{\mathbf{kl}} = \frac{L^{-2}}{2}(&-\tau(\mathbf{H}_{k+,l+}) - \tau(\mathbf{H}_{k-,l-}) + \tau(\mathbf{H}_{k+}) \\ &+ \tau(\mathbf{H}_{k-}) + \tau(\mathbf{H}_{l+}) + \tau(\mathbf{H}_{l-})).\end{aligned} \tag{74}$$

We have thus presented exact relations between the components of $\mathbf{L}$ and $\mathbf{Q}$ in the two internal ON tetrads and combinations of TOAs between chosen receiver-emitter pairs, proving this way the feasibility of recovering completely both objects from TOAs.

After that we divide $\mathbf{L} = (1 \quad \mathbf{L}_{\mathbf{a}})$ into $l_{\mathcal{O}\mu'}$ and $l_{\mathcal{O}\nu}$ according to (6) and $\mathbf{Q}$ into $Q_{\mathcal{O}\mathcal{O}i'j'}$, $Q_{\mathcal{O}\mathcal{E}i'\mu}$, $Q_{\mathcal{E}\mathcal{E}\mu\nu}$ according to (36). In the final step we apply relations (47)–(50) in order to obtain μ and ν.

VII. SUMMARY AND CONCLUSIONS

We have provided a method of measuring the integrated curvature along the line of sight by measuring the variations of times of arrival of electromagnetic signals between two regions in spacetime. In particular, we have demonstrated how it is possible to extract the two first moments of the mass density distribution along the line of sight. However, the method may require modifications when applied to real life physical situations or astronomical observations.

A. Alternative setups and protocols

The protocol described in Sec. VI can be modified in many ways. In particular, there is no need to place the clocks exactly according to Table II, or to send the signals precisely at the moments we have prescribed there. The clock placement and the emission moments can in principle be arbitrary (the only restriction being the nondegeneracy in the sense defined in Sec. III E), as long as they are all precisely measured within each ensemble. In particular, small deviations from the shape defined in Table II should not affect the measurement, provided that we take them into account while solving the inverse problem from Sec. III E via Eq. (32).

In a broader context, note that it is also possible to drop the assumptions of the clocks being comoving within each group; at least as long as we are able to translate each clock's proper time to locally flat coordinates. This is because the solution of the inverse problem requires only the coordinates of all emission and reception events as input, not the details of the motions of each individual clock we use. Therefore, given sufficiently precise local tracking of clocks within each group, we can in principle perform the measurement in a purely passive mode, with no attempts to steer or place the clocks in any way in each ensemble. Even small, uncontrolled forces (drag, radiation pressure, tidal forces) acting on the clocks can be in principle taken into account in this case.

Precise tracking and motion measurements of this kind can be achieved if each ensemble of clocks can also work as a clock compass, i.e., a device capable of determining the local inertial frame and measuring motions with respect to it by the exchanging of electromagnetic signals between clocks. An example of such device, based on clock frequency comparisons has been presented in Neumann *et al.* [18], Puetzfeld *et al.* [19], and Obukhov and Puetzfeld [49]. Therefore, two distant clock compasses, each additionally capable of clock tracking and long-range communication, can in principle probe the mass density distribution along their connecting line. More precise discussion of this kind of setup warrants a separate publication.

B. Dark matter within the Solar System

Two ensembles of clocks within the Solar System could in principle detect or provide upper bounds for the tiny background matter density within the Solar System, including the dark matter. The insensitivity of this method to the tidal perturbations by all bodies of the Solar System and the details of the motion of the clock ensembles makes it particularly attractive in this setting. However, as we will see, the measurement requires enormous precision of pulse timing and huge distances in order to be competitive with precise tracking of the Solar System bodies over long periods [50].

Using the results of Sec. V B we may estimate the minimal mass contained within the connecting cylinder such setup could detect. Assuming the timing precision of 10 ns for a single measurement, comparable to the timing precision of the Global Navigation Satellite Systems like GPS, or to the precision of the millisecond pulsar timing [51], we get the Schwarzschild radius of 3 m. This is a large value, corresponding to the mass of 2×10^{27} kg, close to the Jupiter mass. Assuming the dark matter mass density bounds of $\rho_{\mathrm{DM}} < 10^{-19}\ \mathrm{g\,cm^{-3}}$, taken from Pitjev and Pitjeva [50], we would need the connecting cylinder volume of at least $10^{10}\ \mathrm{AU}^3$, far exceeding the size of the Solar System. We see that without a significant improvement of the timing precision it seems unfeasible to achieve bounds comparable to [50] with two clock ensembles.

C. Binary pulsars as sources

Instead of using artificial sources of signals we may consider natural ones, provided by binary pulsars or the double pulsar [4]. In this case the orbital motion of the pulsars provides a natural sampling of the TOAs over the emitters' region, while the Earth's orbital motion provides the sampling over the receivers' region. The receiver-source distance is also larger by many orders of magnitude than what could be achieved with artificial sources, so we may expect a much larger integrated mass along the line of sight, and therefore also a significantly larger signal to measure.

Since we do not have independent measurements of the distances or orbital elements in the binary pulsar system, but rather we infer them from various relativistic effects via precise pulsar timing [52], the method of measurement would have to be modified. The effects of propagation of signals through the curved spacetime between the binary pulsar and the Solar System, including the effects of μ, $\nu \neq 0$, would need to be included into an extended model of the TOAs of the pulses, with a global fit of the observed data performed over all unknown parameters [51]. The feasibility of curvature measurements of this kind will be discussed in another publication.

ACKNOWLEDGMENTS

The work was supported by the National Science Centre, Poland (NCN) via the SONATA BIS program, Grant No. 2016/22/E/ST9/00578 for the project *"Local relativistic perturbative framework in hydrodynamics and general relativity and its application to cosmology"*.

APPENDIX A: NORMAL FORM OF THE QUADRIC EQUATION AND THE SHAPE OF THE LSC

We begin by absorbing the linear term in the quadric Eq. (9). Define the vector $\mathbf{Y} \in T_{\mathcal{O}}M \oplus T_{\mathcal{E}}M$ by $\mathbf{Y} = (0 \quad \Delta\lambda \cdot l_{\mathcal{E}}^{\mu})$. From (11)–(14) we have $\mathbf{U}(\mathbf{Y}, \cdot) = \mathbf{L}$ and $\mathbf{U}(\mathbf{Y}, \mathbf{Y}) = 0$. It follows that (9) is equivalent to

$$\mathbf{U}(\mathbf{Z}, \mathbf{Z}) = 0, \tag{A1}$$

where the new variable $\mathbf{Z}$ is defined as $\mathbf{Z} = \mathbf{X} + \mathbf{Y}$. Note that this equation still contains no free term.

In the second step we need to diagonalize $\mathbf{U}$ in order to determine its invariant signature. It is easy to show that, irrespective of the spacetime geometry, the quadratic form $\mathbf{U}$ must be degenerate in at least one direction. Define the vector $\mathbf{L}^{\sharp} \in T_{\mathcal{O}}M \oplus T_{\mathcal{E}}M$ as the vector obtained by raising the index of $\mathbf{L}$ with the help of the inverse metric $\mathbf{h}^{-1}$, i.e., $\mathbf{L}^{\sharp} = (l_{\mathcal{O}}^{\mu'} \quad l_{\mathcal{E}}^{\mu})$. This vector corresponds to a simultaneous displacement of both endpoints along γ_0, generated by the same infinitesimal variation of the affine parameter. Now, using again relations (11)–(14), we can show that $\mathbf{U}(\mathbf{L}^{\sharp}, \cdot) = 0$.

The shape of the quadric depends on the signature of the form $\mathbf{U}$. However, apart from the single degenerate direction we have pointed out above, it is impossible to determine the signature without further assumptions regarding the Riemann tensor along the LOS. We can, however, calculate the signature in a flat spacetime and then use this result to gain some insight into the small curvature limit case as defined in Sec. III B.

Let M be the Minkowski space in the standard coordinates (x^{μ}) and let $x_{\mathcal{O}}^{\mu}$ and $x_{\mathcal{E}}^{\mu}$ be two points connected by a null line γ_0, given by $x^{\mu}(\lambda) = x_{\mathcal{O}}^{\mu} + (\lambda - \lambda_{\mathcal{O}}) l^{\mu}$. The tangent vector l^{μ} satisfies $l^{\mu} = \Delta\lambda^{-1}(x_{\mathcal{E}}^{\mu} - x_{\mathcal{O}}^{\mu})$ and is null by assumption.

The world function of the Minkowski spacetime reads [13]

$$\sigma(x^{\mu}, x'^{\nu}) = \frac{1}{2}\eta_{\mu\nu}(x^{\mu} - x'^{\mu})(x^{\nu} - x'^{\nu}).$$

From (6) and (8) we have

$$\mathbf{U} = \frac{1}{\Delta\lambda}\begin{pmatrix} -\eta_{\mu\nu} & \eta_{\mu\nu} \\ \eta_{\mu\nu} & -\eta_{\mu\nu} \end{pmatrix}$$
$$\mathbf{L} = \begin{pmatrix} l_\mu & -l_\mu \end{pmatrix} \tag{A2}$$

for the null geodesic γ_0 between $x^\mu_\mathcal{O}$ and $x^\mu_\mathcal{E}$ [53].

The reduction of the quadric Eq. (9) to the normal form, together with the diagonalization of $\mathbf{U}$, is fairly simple in the flat case. We first introduce the vector $\xi^\mu = \delta x^\mu_\mathcal{E} + \Delta\lambda l^\mu - \delta x^\mu_\mathcal{O}$. It is equal to the position of one displaced point with respect to the other, i.e., $\xi^\mu = x^\mu_\mathcal{E} + \delta x^\mu_\mathcal{E} - x^\mu_\mathcal{O} - \delta x^\mu_\mathcal{O}$. We then express (9) in the new variables $(\xi^\mu, \delta x^\mu_\mathcal{O})$ instead of the components of $\mathbf{X}$. The quadric equation then takes a very simple form

$$-\frac{1}{\Delta\lambda}\eta_{\mu\nu}\xi^\mu\xi^\nu = 0, \tag{A3}$$

with all $\delta x^\mu_\mathcal{O}$ terms dropping out. This is, up to the prefactor, the standard condition for the two displaced points to be connected by a null vector. It is valid for any pair of points, not only for small displacements of the two points around the geodesic endpoints, which means that in the Minkowski space the quadric (9) is not an approximation, but rather it is the exact, "global" surface of communication. Note that in this form the quadric equation contains no linear terms and that it is also diagonal with respect to the new pair of variables, which means that we have achieved the normal form.

Thus the LSC in the Minkowski space turns out to be a highly degenerate quadric, with four degenerate directions corresponding to $\delta x^\mu_\mathcal{O}$. The reason of the four-fold degeneracy is the translational invariance of the Minkowski space, or, more precisely, the fact that the shape of a light cone does not depend on the position of its vertex. A pair of points $x^\mu_\mathcal{E} + \delta x^\mu_\mathcal{E}$ and $x^\mu_\mathcal{O} + \delta x^\mu_\mathcal{O}$ lies on the LSC if and only if the former is located on the light cone with its vertex located at the latter. Due to the light cone shape invariance the light cone equation depends only on the *relative* position vector ξ^μ of first endpoint with respect to the vertex, with no dependence on the absolute position of the vertex encoded in $\delta x^\mu_\mathcal{O}$.

It follows from (A3) that the signature of $\mathbf{U}$ in the Minkowski space is (1,3,4), i.e., one plus sign, three minus signs, four zeros [54]. Moreover, a small perturbation of the quadratic form $\mathbf{U}$ of the type (25) (i.e., the small curvature limit) cannot alter the first four signs, but it can affect the zeros even at linear order. As we have seen, one zero must always remain in the signature, but it is easy to show that the three other zeros can be turned into any other sign by a curvature perturbation. The resulting change of shape of the quadric approximating the LSC is precisely the curvature effect our measurement is sensitive to. Summarizing, the invariant signature of the quadratic form in the small curvature limit contains at least one plus, at least three minuses and at least one zero, but otherwise depends on the spacetime geometry.

1. Remark

We can extend these results to the quadratic form $\mathbf{U}^\perp$ defined on the seven-dimensional subspace $\mathbf{L}^\perp$, see Sec. III C. Since it is equal to the extrinsic curvature of the LSC, we study this way the local shape of the LSC.

The vector $\mathbf{L}^\sharp$ lies in the subspace $\mathbf{L}^\perp$, so from the results of Sec. III C we see that $\mathbf{L}^\sharp$ defines also a degenerate direction for $\mathbf{U}^\perp$, and thus also for the extrinsic curvature of the LSC. However, it is easy to show that $\mathbf{U}^\perp$ must always be degenerate in two different directions. Define two vectors $\mathbf{K}_\mathcal{O}, \mathbf{K}_\mathcal{E} \in T_\mathcal{O}M \oplus T_\mathcal{E}M$ via $\mathbf{K}_\mathcal{O} = \begin{pmatrix} l^{\mu'}_\mathcal{O} & 0 \end{pmatrix}$ and $\mathbf{K}_\mathcal{E} = \begin{pmatrix} 0 & l^\mu_\mathcal{E} \end{pmatrix}$. Both lie in the subspace $\mathbf{L}^\perp$ and it is easy to see from (11)–(14) that $\mathbf{U}(\mathbf{K}_\mathcal{E}, \cdot) = -\mathbf{U}(\mathbf{K}_\mathcal{O}, \cdot) = \frac{1}{\Delta\lambda}\mathbf{L}$. It follows that $\mathbf{U}^\perp$, defined as the restriction of $\mathbf{U}$ to the subspace $\mathbf{L}^\perp$, satisfies $\mathbf{U}^\perp(\mathbf{K}_\mathcal{E}, \cdot) = \mathbf{U}^\perp(\mathbf{K}_\mathcal{O}, \cdot) = 0$, so $\mathbf{U}^\perp$ is degenerate in the directions of both vectors.

In analogy with $\mathbf{U}$ we also consider the flat case and the small curvature limit as special cases. In a flat spacetime we may diagonalize $\mathbf{U}^\perp$ by the same substitution we have used for $\mathbf{U}$; we introduce again ξ^μ and $\delta x^\mu_\mathcal{O}$ as the new variables. The orthogonality condition $\mathbf{L}(\mathbf{X}) = 0$ defining $\mathbf{L}^\perp$ becomes simply $l_\mu \xi^\mu = 0$, with no restrictions on $\delta x^\mu_\mathcal{O}$. It follows that we can decompose ξ^μ according to

$$\xi^\mu = \xi^A e^\mu_A + \xi^l l^\mu, \tag{A4}$$

where the two spatial vectors e^μ_A, $A = 1, 2$, constitute an orthonormal basis of the transverse subspace orthogonal to l^μ. It is straightforward to show then that

$$\mathbf{U}^\perp(\mathbf{X}, \mathbf{X}) = -\frac{1}{\Delta\lambda}\xi^A\xi^B\delta_{AB}. \tag{A5}$$

Thus the extrinsic curvature is degenerate in five directions and negative in the two transverse directions of ξ^μ, so the overall signature reads (0,2,5). In the small curvature limit the two minus signs are stable against linear perturbations and two zeros are protected because of the identities proved above. Therefore up to three zeros out of five may turn into other signs due to linear curvature perturbations.

APPENDIX B: U AND THE VARIATIONS OF THE TANGENT VECTORS AT $\lambda_\mathcal{O}$ AND $\lambda_\mathcal{E}$

Let $t^{\mu'}_\mathcal{O}(x, x')$ and $t^\mu_\mathcal{E}(x, x')$ denote the tangent vectors to a geodesic passing through x and x', and parametrized so that $\lambda - \lambda' = \Delta\lambda$ for a fixed $\Delta\lambda$. The vectors can be related to the derivatives of the world function via

$$t_{\mathcal{O}\mu'}(x, x') = -\frac{1}{\Delta\lambda}\sigma_{,\mu'} \tag{B1}$$

$$t_{\mathcal{E}\mu}(x,x') = \frac{1}{\Delta\lambda}\sigma_{,\mu} \tag{B2}$$

(see [35]). We consider now a LF coordinate system, i.e., we have $\Gamma^{\mu'}{}_{\nu'\alpha'}(\mathcal{O}) = \Gamma^{\mu}{}_{\nu\alpha}(\mathcal{E}) = 0$. In these coordinates we calculate from (B1)–(B2) the linear variation of the components of the tangent vectors under the variation of the geodesic endpoints, calculated around the fiducial geodesic corresponding with $x = \mathcal{E}$, $x' = \mathcal{O}$. It takes the form of

$$\delta t_{\mathcal{O}\mu'} = -\frac{1}{\Delta\lambda}(\sigma_{,\mu'\nu'}\delta x^{\nu'}_{\mathcal{O}} + \sigma_{,\mu'\nu}\delta x^{\nu}_{\mathcal{E}}) \tag{B3}$$

$$\delta t_{\mathcal{E}\mu} = \frac{1}{\Delta\lambda}(\sigma_{,\mu\nu'}\delta x^{\nu'}_{\mathcal{O}} + \sigma_{,\mu\nu}\delta x^{\nu}_{\mathcal{E}}), \tag{B4}$$

with the partial derivatives of $\sigma(x,x')$ taken at $(\mathcal{E},\mathcal{O})$. But in the LF coordinates the standard second derivatives of σ coincide with the covariant ones, i.e., $\sigma_{;\mu\nu} = \sigma_{,\mu\nu}$, $\sigma_{;\mu'\nu'} = \sigma_{,\mu'\nu'}$, $\sigma_{;\mu'\nu} = \sigma_{,\mu'\nu}$, $\sigma_{;\mu\nu'} = \sigma_{,\mu\nu'}$. Also, in these coordinates the coordinate-wise variations of $t_{\mathcal{O}\mu'}$ and $t_{\mathcal{E}\mu}$ can be identified with the covariant direction variations, i.e., $\Delta l_{\mathcal{O}\mu'} = \delta t_{\mathcal{O}\mu'}$ and $\Delta l_{\mathcal{E}\mu} = \delta t_{\mathcal{E}\mu}$. In this case by comparing (B3)–(B4) with the definition of $\mathbf{U}$ (8) we get (15)–(16).

APPENDIX C: TRANSFORMATIONS BETWEEN W AND U IN THE GENERAL CASE

By comparing (17)–(18) to (15)–(16) we see that the transformation between $\mathbf{W}$ and $\mathbf{U}$ corresponds to passing from the initial value problem for the GDE, with the initial data for the perturbed geodesic given by the pair $(\delta x^{\mu'}_{\mathcal{O}}, \Delta l^{\nu'}_{\mathcal{E}})$, to the boundary problem, with the displacement vectors at both ends $(\delta x^{\mu'}_{\mathcal{O}}, \delta x^{\nu}_{\mathcal{E}})$ defining the boundary values. Now, in a linear system of ODEs passing from one problem to the other is a fairly straightforward algebraic problem we will solve below.

We transform the relation (17)–(18) in order to express $\Delta l^{\mu'}_{\mathcal{O}}$ and $\Delta l^{\nu}_{\mathcal{E}}$ by $\delta x^{\mu'}_{\mathcal{O}}$ and $\delta x^{\mu}_{\mathcal{E}}$; by left-multiplying both sides of (17) with W^{-1}_{XL} we obtain $\Delta l^{\mu'}_{\mathcal{O}}$, which we subsequently insert into (18) to get $\Delta l^{\nu}_{\mathcal{E}}$. After collecting the like terms and a small rearrangement we get

$$\Delta l^{\mu'}_{\mathcal{O}} = -(W^{-1}_{XL})^{\mu'}{}_{\nu} W_{XX}{}^{\nu}{}_{\sigma'}\delta x^{\sigma'}_{\mathcal{O}} + (W^{-1}_{XL})^{\mu'}{}_{\nu}\delta x^{\nu}_{\mathcal{O}} \tag{C1}$$

$$\begin{aligned}\Delta l^{\mu}_{\mathcal{E}} = {} & (-W_{LL}{}^{\mu}{}_{\nu'}(W^{-1}_{XL})^{\nu'}{}_{\kappa} W_{XX}{}^{\kappa}{}_{\sigma'} + W_{LX}{}^{\mu}{}_{\sigma'})\delta x^{\sigma'}_{\mathcal{O}} \\ & + W_{LL}{}^{\mu}{}_{\nu'}(W^{-1}_{XL})^{\nu'}{}_{\sigma}\delta x^{\sigma}_{\mathcal{E}}.\end{aligned} \tag{C2}$$

In the next step we need to lower the indices in both equations using $g_{\mu\nu}$ at $\mathcal{O}$ in the first equation and $g_{\mu\nu}$ at $\mathcal{E}$ in the second one. By comparing (15)–(16) with the result we obtain immediately the nonlinear relation (19).

The inverse relation can be derived similarly—we may re-express $\delta x^{\mu}_{\mathcal{E}}$ and $\Delta l^{\mu}_{\mathcal{E}}$ in (19) with $\delta x^{\mu'}_{\mathcal{O}}$ and $\Delta l^{\mu'}_{\mathcal{O}}$

$$\delta x^{\mu}_{\mathcal{E}} = -(U^{-1}_{\mathcal{O}\mathcal{E}})^{\mu\alpha'} U_{\mathcal{O}\mathcal{O}\alpha'\nu'}\delta x^{\nu'}_{\mathcal{O}} + (U^{-1}_{\mathcal{O}\mathcal{E}})^{\mu\alpha'} g_{\alpha'\nu'}\Delta l^{\nu'}_{\mathcal{O}} \tag{C3}$$

$$\begin{aligned}\Delta l^{\mu}_{\mathcal{E}} = {} & g^{\mu\sigma}(U_{\mathcal{E}\mathcal{E}\sigma\omega}(U^{-1}_{\mathcal{O}\mathcal{E}})^{\omega\alpha'} U_{\mathcal{O}\mathcal{O}\alpha'\nu'} - U_{\mathcal{E}\mathcal{O}\sigma\nu'})\delta x^{\nu'}_{\mathcal{O}} \\ & - g^{\mu\sigma} U_{\mathcal{E}\mathcal{E}\sigma\omega}(U^{-1}_{\mathcal{O}\mathcal{E}})^{\omega\gamma'} g_{\gamma'\nu'}\Delta l^{\nu'}_{\mathcal{O}}.\end{aligned} \tag{C4}$$

By comparing (17)–(18) with (C3)–(C4) we obtain the inverse relation (20).

APPENDIX D: MAPPING W UP TO THE LINEAR ORDER IN CURVATURE

In this Appendix we derive the formulas for zeroth and first order of $\mathbf{W}$, expressed in terms of curvature integrals along the null geodesic. This has already been done for timelike geodesics [46] and for null geodesic in the transverse subspace [44,45,55], albeit using different terminology and notation. For the sake of completeness we present a derivation in our framework.

Bilocal operators (W_{XX}, W_{XL}, etc.), constituting the 4×4 submatrices of the matrix $\mathbf{W}$, are solutions to the nonhomogeneous ODE (21) defined along the null geodesic between the emitter and observer. From this ODE we get system of differential equations

$$\begin{cases} \dot{W}_{XX} = W_{LX} \\ \dot{W}_{XL} = W_{LL} \\ \dot{W}_{LX} = R_{ll}W_{XX} \\ \dot{W}_{LL} = R_{ll}W_{XL}, \end{cases}$$

with initial conditions,

$$\begin{cases} W_{XX}(\lambda_{\mathcal{O}}) = I_4 \\ W_{XL}(\lambda_{\mathcal{O}}) = 0 \\ W_{LX}(\lambda_{\mathcal{O}}) = 0 \\ W_{LL}(\lambda_{\mathcal{O}}) = I_4. \end{cases}$$

We may also rewrite this, by substituting relevant matrices, as system of second-order equations,

$$\ddot{W}_{XX} = R_{ll}W_{XX} \tag{D1a}$$

$$\ddot{W}_{XL} = R_{ll}W_{XL} \tag{D1b}$$

$$W_{LX} = \dot{W}_{XX} \tag{D1c}$$

$$W_{LL} = \dot{W}_{XL}, \tag{D1d}$$

with initial conditions

$$W_{XX}(\lambda_{\mathcal{O}}) = I_4 \tag{D2a}$$

$$W_{XL}(\lambda_{\mathcal{O}}) = 0 \tag{D2b}$$

$$W_{LX}(\lambda_{\mathcal{O}}) = 0 \tag{D2c}$$

$$W_{LL}(\lambda_{\mathcal{O}}) = I_4 \tag{D2d}$$

The second-order equations (D1a) and (D1b) for W_{XX} and W_{XL}, together with the initial data (D2), form two autonomous matrix ODEs. Once we solve them we can obtain W_{LX} and W_{LL} by subsequent differentiation of W_{XX} and W_{XL}, see Eqs. (D1c) and (D1d). This system of ODEs has been presented in [1] and we will use it here to derive the perturbative expansion.

In zeroth order the solution of this system is the following:

$$W^{(0)\bar{\mu}}_{XX\ \ \bar{\nu}} = \delta^{\bar{\mu}}{}_{\bar{\nu}} \tag{D3a}$$

$$W^{(0)\bar{\mu}}_{XL\ \ \bar{\nu}} = (\lambda - \lambda_{\mathcal{O}})\delta^{\bar{\mu}}{}_{\bar{\nu}} \tag{D3b}$$

$$W^{(0)\bar{\mu}}_{LX\ \ \bar{\nu}} = 0 \tag{D3c}$$

$$W^{(0)\bar{\mu}}_{LL\ \ \bar{\nu}} = \delta^{\bar{\mu}}{}_{\bar{\nu}}. \tag{D3d}$$

In order to evaluate the first order we insert solutions (D3) into relevant equations (D1) containing the curvature factor and integrate with respect to the affine parameter. For W_{XX} we have

$$W^{(1)\bar{\mu}}_{XX\ \ \bar{\nu}} = \int_{\lambda_{\mathcal{O}}}^{\lambda_{\mathcal{E}}} d\lambda \int_{\lambda_{\mathcal{O}}}^{\lambda} R^{\bar{\mu}}{}_{\bar{\alpha}\bar{\beta}\bar{\nu}}(\lambda')l^{\bar{\alpha}}l^{\bar{\beta}}\mathrm{d}\lambda'.$$

and W_{LX}, as its derivative

$$W^{(1)\bar{\mu}}_{LX\ \ \bar{\nu}} = \int_{\lambda_{\mathcal{O}}}^{\lambda_{\mathcal{E}}} R^{\bar{\mu}}{}_{\bar{\alpha}\bar{\beta}\bar{\nu}}(\lambda)l^{\bar{\alpha}}l^{\bar{\beta}}\mathrm{d}\lambda.$$

Performing the same procedure for W_{XL} and W_{LL}, we get full first order $\mathbf{W}$

$$\begin{aligned}
W^{(1)\bar{\mu}}_{XX\ \ \bar{\nu}} &= \int_{\lambda_{\mathcal{O}}}^{\lambda_{\mathcal{E}}} \mathrm{d}\lambda \int_{\lambda_{\mathcal{O}}}^{\lambda} R^{\bar{\mu}}{}_{\bar{\alpha}\bar{\beta}\bar{\nu}}(\lambda')l^{\bar{\alpha}}l^{\bar{\beta}}\mathrm{d}\lambda',\\
W^{(1)\bar{\mu}}_{XL\ \ \bar{\nu}} &= \int_{\lambda_{\mathcal{O}}}^{\lambda_{\mathcal{E}}} \mathrm{d}\lambda \int_{\lambda_{\mathcal{O}}}^{\lambda} R^{\bar{\mu}}{}_{\bar{\alpha}\bar{\beta}\bar{\nu}}(\lambda')l^{\bar{\alpha}}l^{\bar{\beta}}(\lambda' - \lambda_{\mathcal{O}})\mathrm{d}\lambda',\\
W^{(1)\bar{\mu}}_{LX\ \ \bar{\nu}} &= \int_{\lambda_{\mathcal{O}}}^{\lambda_{\mathcal{E}}} R^{\bar{\mu}}{}_{\bar{\alpha}\bar{\beta}\bar{\nu}}(\lambda)l^{\bar{\alpha}}l^{\bar{\beta}}\mathrm{d}\lambda,\\
W^{(1)\bar{\mu}}_{LL\ \ \bar{\nu}} &= \int_{\lambda_{\mathcal{O}}}^{\lambda_{\mathcal{E}}} R^{\bar{\mu}}{}_{\bar{\alpha}\bar{\beta}\bar{\nu}}(\lambda)l^{\bar{\alpha}}l^{\bar{\beta}}(\lambda - \lambda_{\mathcal{O}})\mathrm{d}\lambda.
\end{aligned}$$

In order to simplify the formulas for $\mathbf{W}^{(1)}$, we can rewrite them via integration by parts as integrals with the kernel centered at $\lambda_{\mathcal{O}}$. For W_{XX} we have

$$\begin{aligned}
W^{(1)\bar{\mu}}_{XX\ \ \bar{\nu}} &= \int_{\lambda_{\mathcal{O}}}^{\lambda_{\mathcal{E}}} \mathrm{d}\lambda \int_{\lambda_{\mathcal{O}}}^{\lambda} R^{\bar{\mu}}{}_{\bar{\alpha}\bar{\beta}\bar{\nu}}(\lambda')l^{\bar{\alpha}}l^{\bar{\beta}}\mathrm{d}\lambda'\\
&= \int_{\lambda_{\mathcal{O}}}^{\lambda_{\mathcal{E}}} R^{\bar{\mu}}{}_{\bar{\alpha}\bar{\beta}\bar{\nu}}(\lambda)l^{\bar{\alpha}}l^{\bar{\beta}}(\lambda_{\mathcal{E}} - \lambda)\mathrm{d}\lambda,
\end{aligned}$$

where 1 is integrated to $\lambda - \lambda_{\mathcal{O}}$ and $\int_{\lambda_{\mathcal{O}}}^{\lambda} R^{\bar{\mu}}{}_{\bar{\alpha}\bar{\beta}\bar{\nu}}(\lambda')l^{\bar{\alpha}}l^{\bar{\beta}}d\lambda'$ is differentiated to $R^{\bar{\mu}}{}_{\bar{\alpha}\bar{\beta}\bar{\nu}}(\lambda)l^{\bar{\alpha}}l^{\bar{\beta}}$. Applying the same to other operators we also get

$$W^{(1)\bar{\mu}}_{XL\ \ \bar{\nu}} = \int_{\lambda_{\mathcal{O}}}^{\lambda_{\mathcal{E}}} R^{\bar{\mu}}{}_{\bar{\alpha}\bar{\beta}\bar{\nu}}(\lambda)l^{\bar{\alpha}}l^{\bar{\beta}}(\lambda_{\mathcal{E}} - \lambda)(\lambda - \lambda_{\mathcal{O}})\mathrm{d}\lambda, \tag{D4a}$$

$$W^{(1)\bar{\mu}}_{LX\ \ \bar{\nu}} = \int_{\lambda_{\mathcal{O}}}^{\lambda_{\mathcal{E}}} R^{\bar{\mu}}{}_{\bar{\alpha}\bar{\beta}\bar{\nu}}(\lambda)l^{\bar{\alpha}}l^{\bar{\beta}}\mathrm{d}\lambda, \tag{D4b}$$

$$W^{(1)\bar{\mu}}_{LL\ \ \bar{\nu}} = \int_{\lambda_{\mathcal{O}}}^{\lambda_{\mathcal{E}}} R^{\bar{\mu}}{}_{\bar{\alpha}\bar{\beta}\bar{\nu}}(\lambda)l^{\bar{\alpha}}l^{\bar{\beta}}(\lambda - \lambda_{\mathcal{O}})\mathrm{d}\lambda. \tag{D4c}$$

Finally, in order to make the formulas look more compact, we may rewrite $\mathbf{W}^{(0)}$ and $\mathbf{W}^{(1)}$ in the form of 8×8 matrices:

$$\mathbf{W}^{(0)} = \left(\begin{array}{c|c} I_4 & \Delta\lambda \cdot I_4 \\ \hline 0 & I_4 \end{array}\right) \tag{D5}$$

$$\mathbf{W}^{(1)} = \int_{\lambda_{\mathcal{O}}}^{\lambda_{\mathcal{E}}} \left(\begin{array}{c|c} R^{\bar{\mu}}{}_{\bar{\alpha}\bar{\beta}\bar{\nu}}(\lambda)l^{\bar{\alpha}}l^{\bar{\beta}}(\lambda_{\mathcal{E}} - \lambda) & R^{\bar{\mu}}{}_{\bar{\alpha}\bar{\beta}\bar{\nu}}(\lambda)l^{\bar{\alpha}}l^{\bar{\beta}}(\lambda_{\mathcal{E}} - \lambda)(\lambda - \lambda_{\mathcal{O}}) \\ \hline R^{\bar{\mu}}{}_{\bar{\alpha}\bar{\beta}\bar{\nu}}(\lambda)l^{\bar{\alpha}}l^{\bar{\beta}} & R^{\bar{\mu}}{}_{\bar{\alpha}\bar{\beta}\bar{\nu}}(\lambda)l^{\bar{\alpha}}l^{\bar{\beta}}(\lambda - \lambda_{\mathcal{O}}) \end{array}\right)\mathrm{d}\lambda, \tag{D6}$$

where $\Delta\lambda = \lambda_{\mathcal{E}} - \lambda_{\mathcal{O}}$. This result is consistent with Eq, (46) from Gallo and Moreschi [44] and equations (2.1)–(2.3) from Flanagan *et al.* [46].

APPENDIX E: MAPPING U UP TO THE LINEAR ORDER IN CURVATURE

We are working in a parallel propagated tetrad, so the metric tensor satisfies $\eta_{\bar\mu\bar\nu} = \mathrm{diag}(-1,1,1,1) = \eta^{\bar\mu\bar\nu}$. $\mathbf{U}$ and $\mathbf{W}$ are related between each other with a nonlinear transformation (19). Obviously the derivation of $\mathbf{U}^{(0)}$ and $\mathbf{U}^{(1)}$ requires evaluating W_{XL}^{-1}. Assuming that terms quadratic in curvature are small we have

$$W_{XL}^{-1\,(0)} = (W_{XL}^{(0)})^{-1},$$
$$W_{XL}^{-1\,(1)} = -(W_{XL}^{(0)})^{-1} W_{XL}^{(1)} (W_{XL}^{(0)})^{-1}.$$

Substituting (3) and (5) we get

$$(W_{XL}^{-1\,(0)})^{\bar\mu}{}_{\bar\nu} = \frac{1}{\Delta\lambda}\delta^{\bar\mu}{}_{\bar\nu}$$
$$(W_{XL}^{-1\,(1)})^{\bar\mu}{}_{\bar\nu} = -\frac{1}{\Delta\lambda^2}\int_{\lambda_\mathcal{O}}^{\lambda_\mathcal{E}} R^{\bar\mu}{}_{\bar\alpha\bar\beta\bar\nu}(\lambda) l^{\bar\alpha} l^{\bar\beta} (\lambda_\mathcal{E}-\lambda)(\lambda-\lambda_\mathcal{O})\mathrm{d}\lambda.$$

In order to find $\mathbf{U}^{(0)}$ we may use the relation (19) between $\mathbf{U}$ and $\mathbf{W}$ at zeroth order,

$$U_{\mathcal{O}\mathcal{O}}^{(0)} = -\eta W_{XL}^{-1\,(0)} W_{XX}^{(0)} = -\frac{\eta}{\Delta\lambda} I_4 \tag{E1a}$$

$$U_{\mathcal{O}\mathcal{E}}^{(0)} = \eta W_{XL}^{-1\,(0)} = \frac{\eta}{\Delta\lambda} I_4 \tag{E1b}$$

$$U_{\mathcal{E}\mathcal{O}}^{(0)} = U_{\mathcal{O}\mathcal{E}}^{(0)\,T} = \frac{\eta^T}{\Delta\lambda} I_4 \tag{E1c}$$

$$U_{\mathcal{E}\mathcal{E}}^{(0)} = -\eta W_{LL}^{(0)} W_{XL}^{-1\,(0)} = -\frac{\eta}{\Delta\lambda} I_4, \tag{E1d}$$

η denoting the metric. The linear order term $\mathbf{U}^{(1)}$ requires linearizing the relation (19) around $\mathbf{W}^{(0)}$. We assume

$$\mathbf{U} = \mathbf{U}^{(0)} + \mathbf{U}^{(1)}.$$

We will expand every bilocal operator contained in $\mathbf{U}$ in this manner, use the relevant relation (E1), and collect the products with respect to the right order (neglecting the quadratic and higher orders in curvature). For $U_{\mathcal{O}\mathcal{O}}$ we have

$$U_{\mathcal{O}\mathcal{O}}^{(0)} + U_{\mathcal{O}\mathcal{O}}^{(1)} = -\eta(W_{XL}^{-1\,(0)} + W_{XL}^{-1\,(1)})\cdot(W_{XX}^{(0)} + W_{XX}^{(1)})$$

or

$$U_{\mathcal{O}\mathcal{O}}^{(0)} + U_{\mathcal{O}\mathcal{O}}^{(1)} = \eta(-W_{XL}^{-1\,(0)} W_{XX}^{(0)} - W_{XL}^{-1\,(0)} W_{XX}^{(1)} - W_{XL}^{-1\,(1)} W_{XX}^{(0)} - W_{XL}^{-1\,(1)} W_{XX}^{(1)}).$$

The first term on the right-hand side is simply $U_{\mathcal{O}\mathcal{O}}^{(0)}$, while the last one is quadratic and can be neglected at first order. We then get

$$U_{\mathcal{O}\mathcal{O}}^{(1)} = \eta(-W_{XL}^{-1\,(0)} W_{XX}^{(1)} - W_{XL}^{-1\,(1)} W_{XX}^{(0)}).$$

Now, using (D3) and (D5) we may rewrite the above result in the following form:

$$U_{\mathcal{O}\mathcal{O}\bar\mu\bar\nu}^{(1)} = -\frac{1}{\Delta\lambda^2}\int_{\lambda_\mathcal{O}}^{\lambda_\mathcal{E}} R_{\bar\mu\bar\alpha\bar\beta\bar\nu} l^{\bar\alpha} l^{\bar\beta} (\lambda_\mathcal{E}-\lambda)^2 \mathrm{d}\lambda$$

(note the lowering of the first index due to η in front of the expressions).

We apply the same procedure to the other three blocks of $\mathbf{U}$ and obtain

$$U_{\mathcal{O}\mathcal{E}\bar\mu\bar\nu}^{(1)} = -\frac{1}{\Delta\lambda^2}\int_{\lambda_\mathcal{O}}^{\lambda_\mathcal{E}} (\lambda_\mathcal{E}-\lambda)(\lambda-\lambda_\mathcal{O}) R_{\bar\mu\bar\alpha\bar\beta\bar\nu} l^{\bar\alpha} l^{\bar\beta} \mathrm{d}\lambda,$$
$$U_{\mathcal{E}\mathcal{O}\bar\mu\bar\nu}^{(1)} = -\frac{1}{\Delta\lambda^2}\int_{\lambda_\mathcal{O}}^{\lambda_\mathcal{E}} (\lambda_\mathcal{E}-\lambda)(\lambda-\lambda_\mathcal{O}) R_{\bar\mu\bar\alpha\bar\beta\bar\nu} l^{\bar\alpha} l^{\bar\beta} \mathrm{d}\lambda,$$
$$U_{\mathcal{E}\mathcal{E}\bar\mu\bar\nu}^{(1)} = -\frac{1}{\Delta\lambda^2}\int_{\lambda_\mathcal{O}}^{\lambda_\mathcal{E}} (\lambda-\lambda_\mathcal{O})^2 R_{\bar\mu\bar\alpha\bar\beta\bar\nu} l^{\bar\alpha} l^{\bar\beta} \mathrm{d}\lambda.$$

The result is consistent with (10). As in the case of $\mathbf{W}$, we may rewrite $\mathbf{U}^{(0)}$ and $\mathbf{U}^{(1)}$ in more compact, matrix form

$$\mathbf{U}^{(0)} = \frac{1}{\Delta\lambda}\begin{pmatrix} -\eta_{\bar\mu\bar\nu} & \eta_{\bar\mu\bar\nu} \\ \eta_{\bar\mu\bar\nu} & -\eta_{\bar\mu\bar\nu} \end{pmatrix},$$
$$\mathbf{U}^{(1)} = -\int_{\lambda_\mathcal{O}}^{\lambda_\mathcal{E}} \left(\begin{array}{c|c} R_{\bar\mu\bar\alpha\bar\beta\bar\nu} l^{\bar\alpha} l^{\bar\beta} \frac{(\lambda_\mathcal{E}-\lambda)^2}{\Delta\lambda^2} & R_{\bar\mu\bar\alpha\bar\beta\bar\nu} l^{\bar\alpha} l^{\bar\beta} \frac{(\lambda_\mathcal{E}-\lambda)(\lambda-\lambda_\mathcal{O})}{\Delta\lambda^2} \\ \hline R_{\bar\mu\bar\alpha\bar\beta\bar\nu} l^{\bar\alpha} l^{\bar\beta} \frac{(\lambda_\mathcal{E}-\lambda)(\lambda-\lambda_\mathcal{O})}{\Delta\lambda^2} & R_{\bar\mu\bar\alpha\bar\beta\bar\nu} l^{\bar\alpha} l^{\bar\beta} \frac{(\lambda-\lambda_\mathcal{O})^2}{\Delta\lambda^2} \end{array}\right) \mathrm{d}\lambda.$$

APPENDIX F: PROOF OF THE INVARIANCE OF μ AND ν

We establish here the following Theorem:

Theorem F.1 Let $(u_\mathcal{O}, f_A, f_3)$ and $(u_\mathcal{E}, g_A, g_3)$ be a pair of ON, adapted and properly oriented tetrads at $\mathcal{O}$ and $\mathcal{E}$ respectively. Let $(\tilde{u}_\mathcal{O}, \tilde{f}_A, \tilde{f}_3)$ and $(\tilde{u}_\mathcal{E}, \tilde{g}_A, \tilde{g}_3)$ be another such pair. Then μ and ν given by (37) and (38) have the same values when calculated in both pairs of adapted tetrads.

Note that in this Appendix we are not using primes for internal tetrad indices at $\mathcal{O}$.

Proof.—We first need the following Lemma, closely related to the shadow theorem by Sachs [2,56]:

Lemma F.2. In this setting we have the following relation between the transverse vectors

$$\tilde{f}_A = R^B{}_A f_B + a_A l_\mathcal{O} \tag{F1}$$

$$\tilde{g}_A = S^B{}_A g_B + b_A l_\mathcal{E}, \tag{F2}$$

where both $R^A{}_B$ and $S^A{}_B$ are 2D rotation matrices, i.e., $R^T R = S^T S = I_2$, $\det R = \det S = 1$, and a_A, b_A are (irrelevant) four numbers.

Proof of Lemma F.2 The proof proceeds in two steps; we first prove that relations (F1)–(F2) indeed hold and that the matrices R and S need to be orthogonal. Then we show that their determinants must be positive as well.

Orthogonality of R and S: Let the dot denote the scalar product defined by the spacetime metric g. Since the $\tilde{f}_A$'s are orthogonal to both $\tilde{f}_3$ and $\tilde{u}_\mathcal{O}$ and the $\tilde{g}_A$'s are orthogonal to both $\tilde{g}_3$ and $\tilde{u}_\mathcal{E}$ we have $\tilde{f}_A \cdot l_\mathcal{O} = 0$ and $\tilde{g}_A \cdot l_\mathcal{E} = 0$, i.e., the transverse vectors are also orthogonal to the appropriate null tangents. Thus $\tilde{f}_A$'s and $\tilde{e}_A$'s lie in the subspaces orthogonal to the appropriate null tangent.

Consider now the decomposition of $\tilde{f}_A$ in the $(u_\mathcal{O}, f_A, f_3)$ frame, i.e., $\tilde{f}_A = C_A u_\mathcal{O} + R^B{}_A f_B + D_A f_3$, with undetermined so far coefficients $R^B{}_A$, C_A and D_A. Then the condition of orthogonality to $l_\mathcal{O} = Q(-u_\mathcal{O} + f_3)$ implies that $C_A = -D_A$, or equivalently $\tilde{f}_A = -D_A u_\mathcal{O} + R^B{}_A f_B + D_A f_3 = R^B{}_A f_B + \frac{D_A}{Q} l_\mathcal{O}$. Applying the same reasoning to g_A we prove the following relations:

$$\tilde{f}_A = R^B{}_A f_B + a_A l_\mathcal{O} \tag{F3}$$

$$\tilde{g}_A = S^B{}_A g_B + b_A l_\mathcal{E} \tag{F4}$$

with $R^B{}_A$, $S^B{}_A$, a_A and b_A arbitrary.

We now impose the orthogonality and normalization conditions between the transverse vectors, $\tilde{f}_A \cdot \tilde{f}_B = \delta_{AB}$, $\tilde{g}_A \cdot \tilde{g}_B = \delta_{AB}$, on relations (F3)–(F4). They imply then that $R^B{}_A R^D{}_C \delta_{BD} = \delta_{AC}$ and $S^B{}_A S^D{}_C \delta_{BD} = \delta_{AC}$, i.e., both $R^B{}_A$ and $S^B{}_A$ must be orthogonal 2×2 matrices. We now only need to prove that they are also special orthogonal, i.e., $\det S^B{}_A = \det R^B{}_A = 1$.

The determinants of R and S are equal to $+1$: Since both matrices are orthogonal, it suffices to show that $\det R^B{}_A > 0$ and $\det S^B{}_A > 0$. We will do it for $R^B{}_A$, because the reasoning for $S^B{}_A$ is identical.

Let κ denote the exterior product of all base vectors, i.e., $\kappa = u_\mathcal{O} \wedge f_1 \wedge f_2 \wedge f_3$. Since both tetrads $(u_\mathcal{O}, f_A, f_3)$ and $(\tilde{u}_\mathcal{O}, \tilde{f}_A, \tilde{f}_3)$ are assumed to be properly oriented we must also have $\kappa = \tilde{u}_\mathcal{O} \wedge \tilde{f}_1 \wedge \tilde{f}_2 \wedge \tilde{f}_3$ and an analogous relation for the other tetrad at $\mathcal{E}$. We now show that this implies $\det R^B{}_A > 0$.

At $\mathcal{O}$ we have $l_\mathcal{O} = \tilde{Q}(-\tilde{u}_\mathcal{O} + \tilde{f}_3)$, so

$$\kappa = \frac{1}{\tilde{Q}} \tilde{u}_\mathcal{O} \wedge \tilde{f}_1 \wedge \tilde{f}_2 \wedge l_\mathcal{O}.$$

The two four-velocities are related by

$$u_\mathcal{O} = \gamma \tilde{u}_\mathcal{O} + \gamma \beta^i \tilde{f}_i = \gamma \tilde{u}_\mathcal{O} + \gamma \beta^A \tilde{f}_A + \gamma \beta^3 \tilde{f}_3$$

where $\beta^i \beta^j \delta_{ij} < 1$ and $\gamma = (1 - \beta^i \beta^j \delta_{ij})^{-1/2}$. It follows that

$$u_\mathcal{O} = \gamma(1 + \beta^3) \tilde{u}_\mathcal{O} + \gamma \beta^A \tilde{f}_A + \frac{\gamma \beta^3}{\tilde{Q}} l_\mathcal{O}.$$

We can now substitute $\tilde{u}_\mathcal{O}$ by $u_\mathcal{O}$ in κ,

$$\kappa = \frac{\gamma(1 + \beta^3)}{\tilde{Q}} u_\mathcal{O} \wedge \tilde{f}_1 \wedge \tilde{f}_2 \wedge l_\mathcal{O}.$$

We can now make use of the relation (F3) between the two transverse vectors $\tilde{f}_A$ and f_A. Note that we have

$$\tilde{f}_1 \wedge \tilde{f}_2 = (\det R^B{}_A) f^1 \wedge f^2 + l_\mathcal{O} \wedge \alpha,$$

where α is an irrelevant one-form. Then

$$\kappa = \frac{\gamma(1 + \beta^3) \det R^B{}_A}{\tilde{Q}} u_\mathcal{O} \wedge f_1 \wedge f_2 \wedge l_\mathcal{O}.$$

In the last step we exchange $l_\mathcal{O}$ for f^3 using $l_\mathcal{O} = Q(-u_\mathcal{O} + f_3)$:

$$\kappa = \frac{Q\gamma(1 + \beta^3) \det R^B{}_A}{\tilde{Q}} u_\mathcal{O} \wedge f_1 \wedge f_2 \wedge f_3.$$

But we also have $\kappa = u_\mathcal{O} \wedge f_1 \wedge f_2 \wedge f_3$, so

$$\frac{Q\gamma(1 + \beta^3) \det R^B{}_A}{\tilde{Q}} = 1.$$

Now, since γ, $\tilde{Q}$, Q and $1 + \beta^3$ are all positive, it follows that $\det R^B{}_A > 0$ as well. The same argument can be applied to $\det S^B{}_A$.

End of proof of Lemma F.2. We now evaluate the transverse components of (lowered-index) $U_{\mathcal{O}\mathcal{O}}$ in the new frame

$$U_{\mathcal{O}\mathcal{O}}(\tilde{f}_A,\tilde{f}_B)=U_{\mathcal{O}\mathcal{O}}(f_C,f_D)R^C{}_A R^D{}_B+U_{\mathcal{O}\mathcal{O}}(l_{\mathcal{O}},f_D)a_A R^D{}_B +U_{\mathcal{O}\mathcal{O}}(f_C,l_{\mathcal{O}})R^C{}_A a_B+U_{\mathcal{O}\mathcal{O}}(l_{\mathcal{O}},l_{\mathcal{O}})a_A a_B. \tag{F5}$$

From (11) we know that for every $X\in T_{\mathcal{O}}M$ we have

$$U_{\mathcal{O}\mathcal{O}}(X,l_{\mathcal{O}})=U_{\mathcal{O}\mathcal{O}}(l_{\mathcal{O}},X)=-\frac{1}{\Delta\lambda}l_{\mathcal{O}}\cdot X,$$

where the dot again denotes the spacetime metric scalar product. Now, we have

$$l_{\mathcal{O}}\cdot f_A=l_{\mathcal{O}}\cdot\tilde{f}_A=l_{\mathcal{O}}\cdot l_{\mathcal{O}}=0$$

from the definition of an adapted base and from the null condition on $l_{\mathcal{O}}$. Thus the last three terms in (F5) simply vanish and we have the transformation rule in the form of

$$U_{\mathcal{O}\mathcal{O}}(\tilde{f}_A,\tilde{f}_B)=U_{\mathcal{O}\mathcal{O}}(f_C,f_D)R^C{}_A R^D{}_B.$$

The same reasoning gives then the following transformation rules:

$$U_{\mathcal{E}\mathcal{E}}(\tilde{g}_A,\tilde{g}_B)=U_{\mathcal{E}\mathcal{E}}(g_C,g_D)S^C{}_A S^D{}_B$$
$$U_{\mathcal{O}\mathcal{E}}(\tilde{f}_A,\tilde{g}_B)=U_{\mathcal{O}\mathcal{E}}(f_C,g_D)R^C{}_A S^D{}_B$$
$$U_{\mathcal{E}\mathcal{O}}(\tilde{g}_A,\tilde{f}_B)=U_{\mathcal{E}\mathcal{O}}(g_C,f_D)S^C{}_A R^D{}_B.$$

Since the rotation matrices S and R have a unit determinant, they have no impact on the value of the subdeterminants of $U_{\mathcal{O}\mathcal{O}}$ and others

$$\det U_{\mathcal{O}\mathcal{O}}(\tilde{f}_A,\tilde{f}_B)=\det U_{\mathcal{O}\mathcal{O}}(f_A,f_B)$$
$$\det U_{\mathcal{E}\mathcal{E}}(\tilde{g}_A,\tilde{g}_B)=\det U_{\mathcal{E}\mathcal{E}}(g_A,g_B)$$
$$\det U_{\mathcal{O}\mathcal{E}}(\tilde{f}_A,\tilde{g}_B)=\det U_{\mathcal{O}\mathcal{E}}(f_A,g_B)$$
$$\det U_{\mathcal{E}\mathcal{O}}(\tilde{g}_A,\tilde{f}_B)=\det U_{\mathcal{E}\mathcal{O}}(g_A,f_B).$$

Therefore the values of μ and ν defined by the expressions (37) and (38) are the same in any pair of adapted tetrads at $\mathcal{O}$ and $\mathcal{E}$.

End of proof of Theorem F.1. Thus μ and ν are independent of the choice of the adapted ON tetrad at $\mathcal{O}$ and $\mathcal{E}$, and thus $u_{\mathcal{O}}$- and $u_{\mathcal{E}}$-independent. Equation (37) can be used with any pair of adapted tetrads at $\mathcal{O}$ and $\mathcal{E}$.

APPENDIX G: μ, ν AND THE CROSS-SECTIONAL AREA OF INFINITESIMAL BUNDLES OF RAYS

For simplicity we derive only the expressions for μ, noting here that those for ν have exactly the same form, but with the role of $\mathcal{O}$ and $\mathcal{E}$ reversed. The problem of tracking the intersection of an infinitesimal bundle with a Sachs screen of an observer is an old one. It is well known that the area of this intersection is independent of the choice of the observer's frame [37].

We begin by picking an orthonormal, adapted tetrad (u,f_A,f_3) at $\mathcal{O}$ and parallel propagating it along γ_0. We consider an infinitesimal bundle of light rays intersecting the area spanned by f_1 and f_2, defined as $\mathcal{A}_{\mathcal{O}}=f_1\wedge f_2$, such that the null geodesics are parallel at $\mathcal{O}$. Its behavior is determined by the geodesic deviation equation along γ_0. From (17) we see that at $\mathcal{E}$ this bundle crosses the area element spanned by $W_{XX}(f_1)$ and $W_{XX}(f_2)$. The cross section of the bundle by the Sachs screen space f_1 and f_2 is given by the projection of these vectors to the Sachs screen. It can described by the products $f_B\cdot W_{XX}(f_A)$, with $\cdot$ defined by the spacetime metric.

In [1] the following definition of μ was given

$$\mu=1-\det w_{\perp}{}^A{}_B=1-\det(\delta^A{}_B+m_{\perp}{}^A{}_B), \tag{G1}$$

where $m_{\perp}:\mathcal{P}_{\mathcal{O}}\to\mathcal{P}_{\mathcal{E}}$ was the perpendicular part of the emitter-observer assymetry operator. It is easy to show that by construction, $w_{\perp}{}^A{}_B=W_{XX}{}^A{}_B$, i.e., it is a 2×2 submatrix of $W_{XX}{}^{\bar{\mu}}{}_{\bar{\nu}}$, corresponding to the projection onto the screen space spanned by f_1 and f_2. Namely, we have

$$w_{\perp}{}^A{}_B=[f_A]\cdot w_{\perp}([f_B]) \tag{G2}$$

where $[f_A]$ is the equivalence class defined by the equivalence relation $X\sim X+Cl$, where C is a constant. But, from the definition in [1] we also have $[f_A]\cdot w_{\perp}([f_B])=f_A\cdot W_{XX}(f_B)$, which proves the equality. Thus

$$\mu=1-\det W_{XX}{}^A{}_B. \tag{G3}$$

The determinant $\det W_{XX}{}^A{}_B$ plays the role of the coefficient defining how an area element of the screen space $\mathcal{O}$ appears rescaled on the screen space at $\mathcal{E}$ when carried by the beam. More precisely, it is equal to the ratio of the area element $W_{XX}(f_1)\wedge W_{XX}(f_2)$ projected to the screen space and $f_1\wedge f_2$ at $\mathcal{E}$. Since the latter defines the cross-sectional area of the infinitesimal bundle at $\mathcal{O}$, we can simply define μ as the ratio of (signed) cross-sectional areas of the bundle at $\mathcal{O}$ and $\mathcal{E}$,

$$\mu=1-\frac{\mathcal{A}_{\mathcal{E}}}{\mathcal{A}_{\mathcal{O}}}. \tag{G4}$$

This means that μ measures the focusing power of the spacetime along γ_0 by a simple comparison of the cross-sectional areas of an initially parallel bundle of rays sent backwards in time towards $\mathcal{E}$. Moreover, this formula leads immediately to a simple evolution equation for μ. Let $g_A=W_{XX}(\lambda)f_A$ be the solutions of the GDE corresponding to f_1 and f_2 at $\mathcal{O}$, defining the shape of the bundle. We start by differentiating $\mathcal{A}(\lambda)=g_1\wedge g_2$,

$$
\begin{aligned}
\frac{\mathrm{d}\mathcal{A}}{\mathrm{d}\lambda} &= \nabla_l g_1 \wedge g_2 + g_1 \wedge \nabla_l g_2 \\
&= (g_1^C \nabla_C l) \wedge g_2 + g_1 \wedge (g_2^C \nabla_C l) \\
&= (g_1 \wedge g_2)\nabla_C l^C = \mathcal{A}\theta,
\end{aligned} \tag{G5}
$$

where θ is the bundle expansion. We have used here the properties of wedge product and the commutation relation $\nabla_l g = \nabla_g l$. By differentiating (G4) we get

$$
\frac{\mathrm{d}\mu}{\mathrm{d}\lambda} = \theta(\mu - 1), \tag{G6}
$$

with the initial data of the form $\mu(\lambda_\mathcal{O}) = 0$.

Equation (G6) requires the expansion $\theta(\lambda)$ of the infinitesimal bundle along γ_0 as input. It can be obtained, together with shear $\sigma_{AB}(\lambda)$, using the null Raychaudhuri equation along γ_0 and the shear equation [37,57,58], also known as the Sachs equations

$$
\frac{\mathrm{d}\theta}{\mathrm{d}\lambda} = -\frac{\theta^2}{2} - \sigma_{AB}\sigma^{AB} - R_{\mu\nu} l^\mu l^\nu \tag{G7}
$$

$$
\frac{\mathrm{d}\sigma_{AB}}{\mathrm{d}\lambda} = -\theta\sigma_{AB} + C_{A\mu\nu B} l^\mu l^\nu. \tag{G8}
$$

As the initial data we take $\theta(\lambda_\mathcal{O}) = 0$ and $\sigma_{AB}(\lambda_\mathcal{O}) = 0$, corresponding to an initially parallel bundle. We do not include the twist, because it must vanish at $\mathcal{O}$ together with θ and σ, and thus also along the whole bundle.

[1] M. Grasso, M. Korzyński, and J. Serbenta, Geometric optics in general relativity using bilocal operators, Phys. Rev. D **99**, 064038 (2019).

[2] M. Korzyński and J. Kopiński, Optical drift effects in general relativity, J. Cosmol. Astropart. Phys. 03 (2018) 012.

[3] T. Damour, Binary pulsars as probes of relativistic gravity, Phil. Trans. Phys. Sci. Eng. **341**, 135 (1992).

[4] D. R. Lorimer, Binary and millisecond pulsar, Living Rev. Relativity **11**, 8 (2008).

[5] P. K. Dahal, Review of pulsar timing array for gravitational wave research, J. Astrophys. Astron. **41**, 8 (2020).

[6] S. Refsdal, On the possibility of determining Hubble's parameter and the masses of galaxies from the gravitational lens effect, Mon. Not. R. Astron. Soc. **128**, 307 (1964).

[7] S. H. Suyu, V. Bonvin, F. Courbin, C. D. Fassnacht, C. E. Rusu, D. Sluse, T. Treu, K. C. Wong, M. W. Auger, X. Ding, S. Hilbert, P. J. Marshall, N. Rumbaugh, A. Sonnenfeld, M. Tewes, O. Tihhonova, A. Agnello, R. D. Blandford, G. C. F. Chen, T. Collett, L. V. E. Koopmans, K. Liao, G. Meylan, and C. Spiniello, H0LiCOW I. H0 Lenses in COSMOGRAIL's Wellspring: Program overview, Mon. Not. R. Astron. Soc. **468**, 2590 (2017).

[8] A. Bauch, Time and frequency metrology in the context of relativistic geodesy, in *Relativistic Geodesy: Foundations and Applications*, edited by D. Puetzfeld and C. Lämmerzahl (Springer International Publishing, Cham, 2019), pp. 1–24.

[9] *Relativistic Geodesy: Foundations and Applications*, edited by D. Puetzfeld and C. Lämmerzahl (Springer International Publishing, Cham, 2019).

[10] T. B. Bahder, Relativity of GPS measurement, Phys. Rev. D **68**, 063005 (2003).

[11] N. Ashby, Relativity in the global positioning system, Living Rev. Relativity **6**, 1 (2003).

[12] I. I. Shapiro, Fourth test of general relativity, Phys. Rev. Lett. **13**, 789 (1964).

[13] J. L. Synge, *Relativity: The General Theory* (North-Holland Publishing Company, Amsterdam, 1960).

[14] P. Teyssandier, C. Le Poncin-Lafitte, and B. Linet, A universal tool for determining the time delay and the frequency shift of light: Synge's World function, in *Lasers, Clocks and Drag-Free Control: Exploration of Relativistic Gravity in Space*, Astrophysics and Space Science Library Vol. 349, edited by H. Dittus, C. Lammerzahl, and S. G. Turyshev (2008), p. 153.

[15] P. Teyssandier and C. Le Poncin-Lafitte, General post-Minkowskian expansion of time transfer functions, Classical Quantum Gravity **25**, 145020 (2008).

[16] B. Linet and P. Teyssandier, Time transfer and frequency shift to the order $1/c^4$ in the field of an axisymmetric rotating body, Phys. Rev. D **66**, 024045 (2002).

[17] This point is important, because in certain cases two or more signals may arrive almost at the same moment, leading to ambiguities in the data interpretation. Distinguishing of the incoming signals can be achieved, for example, by including a data stamp containing an identifier encoded in the signal (for example, see the method used to transmit the P-code in the Global Positioning System [10]), or by using different frequencies for each signal according to a prescribed sequence.

[18] G. Neumann, D. Puetzfeld, and G. F. Rubilar, Extended gravitational clock compass: New exact solutions and simulations, Phys. Rev. D **102**, 044027 (2020).

[19] D. Puetzfeld, Y. N. Obukhov, and C. Lämmerzahl, Gravitational clock compass in general relativity, Phys. Rev. D **98**, 024032 (2018).

[20] D. Puetzfeld and Y. N. Obukhov, Generalized deviation equation and determination of the curvature in general relativity, Phys. Rev. D **93**, 044073 (2016).

[21] P. Szekeres, The gravitational compass, J. Math. Phys. (N.Y.) **6**, 1387 (1965).

[22] I. Ciufolini and M. Demiański, How to measure the curvature of space-time, Phys. Rev. D **34**, 1018 (1986).

[23] S. L. Bażański, Kinematics of relative motion of test particles in general relativity, Ann. l'I. H. P. Phys. Théor. **27**, 115 (1977).

[24] S. L. Bażański, Dynamics of relative motion of test particles in general relativity, Ann. l'I. H. P. Phys. Théor. **27**, 145 (1977).

[25] F. A. E. Pirani, On the Physical significance of the Riemann tensor, Acta Phys. Pol. **15**, 389 (1956).

[26] M. Korzyński and E. Villa, Geometric optics in relativistic cosmology: New formulation and a new observable, Phys. Rev. D **101**, 063506 (2020).

[27] S. A. Klioner, A practical relativistic model for microarcsecond astrometry in space, Astron. J. **125**, 1580 (2003).

[28] A. G. Butkevich and L. Lindegren, Rigorous treatment of barycentric stellar motion: Perspective and light-time effects in astrometric and radial velocity data, Astron. Astrophys. **570**, A62 (2014).

[29] V. Červený, *Seismic Ray Theory* (Cambridge University Press, Cambridge, England, 2001).

[30] V. Farra, Computation of second-order traveltime perturbation by Hamiltonian ray theory, Geophys. J. Int. **136**, 205 (1999).

[31] V. Červený, E. Iversen, and I. Pšenčík, Two-point paraxial traveltimes in an inhomogeneous anisotropic medium, Geophys. J. Int. **189**, 1597 (2012).

[32] U. bin Waheed, I. Pšenčík, V. Červený, E. Iversen, and T. Alkhalifah, Two-point paraxial traveltime formula for inhomogeneous isotropic and anisotropic media: Tests of accuracy, Geophysics **78**, WC65 (2013).

[33] R. A. Isaacson, Gravitational radiation in the limit of high frequency. I. The linear approximation and geometrical optics, Phys. Rev. **166**, 1263 (1968).

[34] R. A. Isaacson, Gravitational radiation in the limit of high frequency. II. Nonlinear terms and the effective stress tensor, Phys. Rev. **166**, 1272 (1968).

[35] E. Poisson, A. Pound, and I. Vega, The motion of point particles in curved spacetime, Living Rev. Relativity **14**, 7 (2011).

[36] R. Low, Stable singularities of wave-fronts in general relativity, J. Math. Phys. (N.Y.) **39**, 3332 (1998).

[37] V. Perlick, Gravitational lensing from a spacetime perspective, Living Rev. Relativity **7**, 9 (2004).

[38] J. Vines, Geodesic deviation at higher orders via covariant bitensors, Gen. Relativ. Gravit. **47**, 59 (2015).

[39] T. B. Bahder, *Clock Synchronization and Navigation in the Vicinity of the Earth* (Nova Science Publishers, Inc., New York, 2009).

[40] Note that in the definitions of $M \times M$, $\mathbf{L}$ and $\mathbf{X}$ we have swapped the order of coordinates at $\mathcal{O}$ and $\mathcal{E}$ in comparison to the definition of the world function: we first take the four components related to the reception region $N_{\mathcal{O}}$, and then the four components related to the emission region $N_{\mathcal{E}}$, the opposite of the definition of the world function. Hopefully this should not lead to confusion.

[41] N. Uzun, Reduced phase space optics for general relativity: Symplectic ray bundle transfer, Classical Quantum Gravity **37**, 045002 (2020).

[42] B. S. DeWitt and R. W. Brehme, Radiation damping in a gravitational field, Ann. Phys. (N.Y.) **9**, 220 (1960).

[43] W. G. Dixon, Dynamics of extended bodies in general relativity. I. Momentum and angular momentum, Proc. R. Soc. A **314**, 499 (1970).

[44] E. Gallo and O. M. Moreschi, Gravitational lens optical scalars in terms of energy-momentum distributions, Phys. Rev. D **83**, 083007 (2011).

[45] G. Crisnejo and E. Gallo, Expressions for optical scalars and deflection angle at second order in terms of curvature scalars, Phys. Rev. D **97**, 084010 (2018).

[46] E. E. Flanagan, A. M. Grant, A. I. Harte, and D. A. Nichols, Persistent gravitational wave observables: General framework, Phys. Rev. D **99**, 084044 (2019).

[47] In practice the number of measurements can be made lower because the components of $\mathbf{L}$ and $\mathbf{U}$ are not independent, see Eqs. (11)–(14). However, we do not make any use of this possibility in this paper.

[48] On the other hand, note that this does not have to apply to the set of corresponding full 8-dimensional vectors, simply because the TOAs $\tau(\mathbf{H}_*^{\mathbf{a}})$, constituting the $\mathbf{0}$ component, will not obey the central symmetry in general.

[49] Y. N. Obukhov and D. Puetzfeld, Measuring the gravitational field in general relativity: From deviation equations and the gravitational compass to relativistic clock gradiometry, in *Relativistic Geodesy: Foundations and Applications*, edited by D. Puetzfeld and C. Lämmerzahl (Springer International Publishing, Cham, 2019), pp. 87–130.

[50] N. P. Pitjev and E. V. Pitjeva, Constraints on dark matter in the solar system, Astron. Lett. **39**, 141 (2013).

[51] R. Smits, S. J. Tingay, N. Wex, M. Kramer, and B. Stappers, Prospects for accurate distance measurements of pulsars with the Square Kilometre Array: Enabling fundamental physics, Astron. Astrophys. **528**, A108 (2011).

[52] T. Damour and J. H. Taylor, Strong-field tests of relativistic gravity and binary pulsars, Phys. Rev. D **45**, 1840 (1992).

[53] We do not distinguish the primed and unprimed indices in the Minkowski space since all tangent spaces in this case may be identified with each other.

[54] Since there is no free term in Eq. (A1), the signs can actually be flipped to (3,1,4) by multiplying both sides by -1, without affecting the normal form.

[55] E. Gallo and O. M. Moreschi, Explicit expressions for optical scalars in gravitational lensing from general matter sources, AIP Conf. Proc. **1471**, 82 (2012).

[56] R. Sachs, Gravitational waves in general relativity. VI. The out- going radiation condition, Proc. R. Soc. Ser. A **264**, 309 (1961).

[57] R. M. Wald, in *General Relativity* (Chicago University Press, Chicago, USA, 1984), Chap. 9, p. 222.

[58] E. Poisson, *A Relativist's Toolkit: The Mathematics of Black-Hole Mechanics* (Cambridge University Press, Cambridge, England, 2004).